Make Some Noise
Schiphol

A study on a parametric architectural strategy for the design of aircraft noise abatement landscape elements within cities.

AR4B025 Building Technology Graduation Studio

Main mentor: Dr. ir. M. J. Tenpierik (Building Physics chair)

Second mentor: Dr. MSc. Arch. M. Turrin (Design Informatics chair)

P5 Research report

Ioannis Tsionis

4873440

August 2020

Delft, Netherlands

Number of words: 21.412 (excluding figures, tables and references)

Focus and restrictions – This research focuses on aircraft noise exposed urban spaces around Amsterdam Schiphol airport. In particular, a case site in Rijsenhout is studied, where a representation of the noise wave propagation due to refraction is performed. Subsequently, a series of landscape configurations regarding geometry are gradually tested through acoustic simulation and noise maps are imported inside a parametric design environment. Finally, a conceptual design proposal is structured in order to explore the potential of such configurations in the urban environment.

Key words – aircraft noise, noise reduction, atmospheric refraction, landscape design, urban soundscape, Rijsenhout.

TU Delft

Table of contents

1 Introduction & Research framework

1.1 Introduction

1.1.1 Sound definition

It is known by Physics that sound is caused by the vibrations of a source that propagates through a transmission medium such as gas, liquid or solid as an acoustic wave. In the case of aircraft noise that this report attempts to examine, sources can be parts of the airplane, such as engines & propellers that vibrate and create disturbance to the surrounding air medium. The unit that we use to describe the frequency at which the particles of the transmitting medium are vibrating is Hertz (Hz), where 1 Hz describes 1 vibration over 1 second of time. As the first particles close to the source are vibrating, they transport this energy to the neighboring particles, resulting in their vibration and thus, the movement of sound through the medium. This is described as the speed of sound, which is determined by the inertia and elastic properties of the medium in which the sound wave travels. Under normal conditions (temperature of 20^{o}C) and atmospheric pressure, the speed of sound in air is approximately c=343m/s.

The human brain can perceive only part of the sound spectrum, the audio frequency range, which includes frequencies between 20 Hz up to 20 kHz. Soundwaves with frequencies above 20 kHz are called ultrasound, while frequencies lower than 20Hz are infrasound waves. These frequency ranges are inaudible for the human ear, but devices that produce such kind of sounds are often used in various science fields for diagnostics or detection of geological phenomena.

1.1.2 Perception of sound as noise

Noise is defined as any sound that is unwanted or unpleasant by the immediate or distant environment, and causes undesirable conditions such as discomfort, difficulty in communication, difficulty in work, loss of sleep, etc. and has direct or indirect effects on human health (Tsinikas, 2009). According to subjective factors, every sound stimulus that is perceived acquires a pleasant or unpleasant character. Based on this, the criteria for naming a stimulus as noise depends on the receiver's activity at the time of its transmission, its attitude and attention to it, that is, whether or not a sound receiver is prepared to process it and assimilate it (Bartels et al., 2015). Furthermore, factors like location, source type and the time of day can better describe the perception of a sound.

Noise sources are found everywhere, such as in the workplace, on the street and in our home. Commonly accepted sources of noise are motor vehicles, road construction and construction machinery, as well as the various electrical appliances available inside homes. Generally noises may come from the natural environment (natural phenomena, fauna), or the anthropogenic environment (machines, activities) (Mpiris et al., 2011), which can be classified into:

- *Urban noises (urban activities, leisure, home and commercial mechanical equipment)*
- *Traffic noises (suburban / urban, by private or public means of transport)*
- *Noise at workplaces (urban, industrial, agricultural, military facilities)*

This study focuses on the noise generated by air traffic, which is one of the loudest noise sources to be treated in modern days. However, aircraft noise tends to affect not only big cities where airports are usually located, but also residential regions around them during take-offs and landings or flyovers.

1.1.3 Urban noise and health

When the hearing is disturbed, it causes loss of ability to isolate an audio message from the ambient noise. In this case, the person feels exposed to a storm of auditory information, which is perceived distorted to some degree. Understanding the messages requires considerable effort, generating errors, increasing fatigue, irritability, and finally withdrawal (Tsinikas, 2009). Thus, the environment is experienced as problematic and attention and memory suffer. The most important acoustic effect is hearing loss, which is one of the most common diseases encountered in noisy urban environments.

However, non-acoustic factors (Bartels et al., 2015) are even more deceptive. They concern the nervous and various other bodily systems of the human body (circulatory, gastrointestinal, endocrine system) (Tsinikas, 2009). Long-term and / or high-intensity noise often concludes in headaches, nausea, hypertension, tachycardia, digestive and sleep disturbances, difficulties in erection and infertility, physical fatigue, irritability, tiredness, stress and anxiety (from wikipedia). For workers, trainees and mainly drivers, noise causes concentration loss, reaction time deceleration, increase in errors and accidents.

Nowadays, noise is one of the most important environmental problems and significantly deteriorates the quality of life of citizens. Its effects on health are related to its frequency, intensity, duration and repetition of noise. As a result, there can be observed from mere annoyance, to stress, difficulty concentrating, sleep disturbance and decreased productivity in the workplace (Kroesen, 2011). In many cases, urban planning practices are the cause of the economic downgrading of residential and commercial centers. Nevertheless, the adaption of urban design to the current problematic situation and the research on methods to improve the living conditions in noisy environments is proven to reduce the exposure amount of residents to harmful levels (Lugten, 2018).

1.2 Research framework

1.2.1 Problem statement

Aviation is a rising sector and so are the consequences of what this technology advancement contains. Special attention has to be paid to noise-sensitive areas, as the problems that air traffic creates, lead to residential areas being reported as unsafe and harmful for the exposed population. Legislation is applied to areas near airport facilities (Science Communication Unit, 2017), but there is still room for improvement to counter the expanding evolution of aircraft transportation. Apart from technological upgrades in the field of aircraft engineering, a promising perspective is that part of the solution may lie in urban design and building design. By adjusting what is already known from ground source sound reduction methods, we should be led to solutions for the aircraft noise exposure situation.

Flight routes located close to residential areas are now limited to paths away or around them. However, there is not enough awareness of what happens in cases of greater horizontal distances and urban areas are certainly not designed to minimize this exposure. Existing procedures on the topic of noise reduction focus mostly on street and railway traffic sources, but often for a non-refractive atmosphere. On the other hand, aircraft prediction models are reliable enough to produce macro-scale noise maps including atmospheric effects that illustrate where an exceedance of noise level limits occurs (see Figure 1.1 for the case of Rijsenhout), but only consider ground reflections (Lugten, 2018).

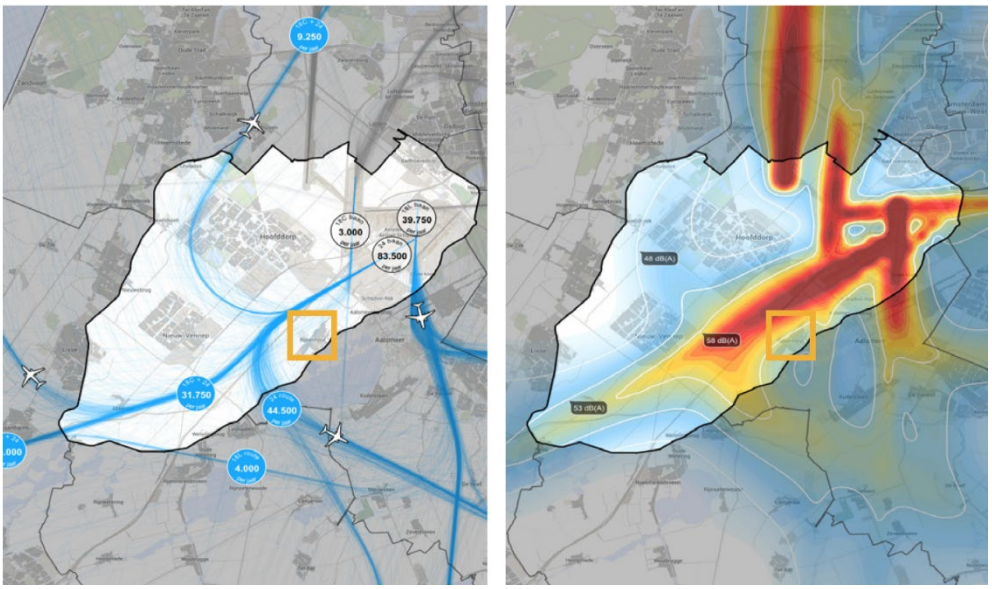

Fig. 1.1: Flight routes and noise contours map around Amsterdam Schiphol airport. The red areas illustrate where noise levels exceed 60dB. The yellow square shows the location of Rijsenhout. Source: podiumarchitectuur.nl [online] [Accessed 11 Nov. 2019]

A connecting link of these two scales is necessary to counter the issue of aircraft noise pollution. Cities grow and expand, similar to air transportation. Eventually, city borders and noise contours are met and measures have to be taken. Aircraft noise affects residential areas and a typology of architectural configurations within cities, such as noise barriers, building geometries and urban planning, is able to provide solutions. Finally, the integration of the conditions of each specific case in a parametric environment can offer dynamic solutions, so that varying locations can benefit from the scientific progress.

To sum up, the focus of this research according to the above should be mentioned as two main problem definitions, although their link is necessary to result in conclusions and recommendations:

1. Aircraft noise exposed residential area (Rijsenhout) near Amsterdam Schiphol airport and the constant exposure of inhabitants to harmful noise levels (>70dB).
2. Absence of a typology of landscape configurations that act as noise barriers and an understanding of their acoustical performance against aircraft sources within a city environment.

1.2.2 Research gaps

The following research gaps are linked numerically to the proposed objectives of this study:

1. The current methods of acoustic models mostly concern noise produced by sources at ground level. Computational simulation models concerning aircraft noise prediction in macro-scale omit the presence of buildings, but take ground surfaces impact into consideration for the purpose of noise mapping. In contrast, micro-scale urban acoustics models aim to solve street noise issues, or generally concern noise sources close to ground level (i.e. road, railway traffic, industrial facilities), while considering homogeneous atmospheres (Lugten, 2018). As a result, the case of abating aircraft noise is not fully embraced by simulation methods, since the issue of reducing noise levels inside residential areas has been recently explored by researchers, as noise reduction strategies so far have been focused on technological advancements of the source itself (i.e. engine, airframe).
2. Computational urban acoustics methods for sound propagation prediction such as wave-based methods are said to provide the highest accuracy, but at a limited time-efficiency ratio (Hornikx, 2016). In contrast, geometric acoustics methods are faster and simpler to handle and have been reliable for use over the years (i.e. Harmonoise, Nord2000, ISO 9613). Nevertheless, their analysis is committed to acoustics software that do not offer the ability of acoustical optimization in the same computational environment. CAD software is where such tasks are conducted, hence the integration of simulation results within a parametric environment for direct configurations would update the workflow of a designer for outdoor noise procedures.
3. Literature on aircraft noise abatement potential of buildings, due to design choices, geometry and urban density is unclear and limited so far (Lugten, 2018). A few studies have shown positive results on specific study locations and others predict the potential of urban planning on reducing noise annoyance. In the case of bigger horizontal than vertical distances of source and receiver, more air absorption and scattering occurs because of the ground surface and urban materialization in between. During aircraft flyover cases directly above urban areas, absorption is mostly important (on ground surfaces and building roofs), since low-heighted noise barriers cannot block direct soundwaves from above. Thus, new strategies or update of existing barrier methods should be explored towards the noise abatement of aircrafts.
4. Parameterization of acoustical surfaces and optimization through analysis is very common in room acoustics studies. However, the case is different for distant sound sources at a higher altitude. Similar processes can be applied but, different atmospheric effects alter the priority in which these should be considered along the sound travel distance (i.e. refraction & diffraction over absorption & reflection) for optimization tasks.

1.2.3 Research questions

The main research question, as the thesis topic and referenced doctoral suggests (Lugten, 2018), in combination with the goal to perform this research within a parametric environment, can be formed in the following way:

How can acoustic parametric landscape design and optimization tools contribute in the reduction of aircraft noise and to what extent can it improve the soundscape quality of areas near airports?

To specify this better, generated sub questions will guide the literature and research approach in order to reach a desired outcome. These are listed below:

1. To what extent can the structure of a computational acoustics study for outdoor environments be simplified and inserted into a design environment?
2. How can the propagation of aircraft sound rays affected by atmospheric refraction be represented inside a parametric design environment?
3. To what extent can landscape elements contribute in the dispersion and absorption of low frequencies of aircraft sources within noise exposed urban areas?
4. How can the design of landscape elements be parameterized and guide an acoustical performance-driven optimization process?

1.2.4 Research objectives

Based on the research gaps found so far and precedent methods found on literature, the primary goal of this research is the following:

To understand the extent to which acoustic parametric landscape design can be adopted as a strategy and provide solutions, regarding aircraft noise abatement on varying urban morphologies and flight paths.

This research objective aims at the following:

1. To understand how the structure of an outdoor environment computational acoustics simulation can be broken down in parts and to what extend can it be simplified.
2. To develop a representation of sound rays directionality of an aircraft source influenced by atmospheric refraction within a parametric design environment.
3. To verify the efficiency of landscape configurations on improving the soundscape of urban areas against aircraft noise.
4. To examine how the geometry of acoustic landscape configurations can be parameterized and guide to optimization processes.

1.2.5 Research hypothesis

The primary goal of this research is to investigate the potential of land configurations in achieving a better soundscape environment for the residential area of Rijsenhout. Prior to that, acoustic phenomena and atmospheric effects in outdoor environments have to be considered. In addition, the study of sound propagation within a design environment would prove beneficial for the further acoustic optimization of installations. Thus, in order to progress towards this target, literature on urban acoustics should be explored and broken down in equations that describe sound propagation of a distant source, before continuing on testing geometry cases on-site.

With reference to the design goal, and since no software was found to sufficiently tackle aircraft noise cases, the initial hypothesis was that a script can be developed with Python-coded components inside Grasshopper and Rhino design software that accurately predict propagation paths and noise levels of aircraft sources. However, during the study of urban acoustics, it was understood that the realization of such components is hard to be achieved within the thesis timeframe. Therefore, only a part of urban acoustics is further analyzed (atmospheric refraction), in order to initialize a study on scripted components. Subsequently, the addition of other atmospheric effects or developed scripts by other researchers will continue this approach.

Parallel to this, the design and testing of concepts is conducted with the use of acoustic simulation applications (iNoise, Pachyderm) and the continuous exchange of files between design and simulation software. While simulations guide towards noise mappings, a library of geometric suggestions is expected to emerge, regarding methods to mitigate noise. As a finishing step, urban grids are manually optimized, so that an efficient outdoor area of mitigated noise is achieved. Regarding that, the hypothesis is to handle the constraints of sustainable soil constructions that create shielded building areas underneath, in combination with shielded outdoor living spaces for residents. Consequently, a strategy on assorting the geometric aspects of ground barriers is assumed to conclude the research, as well as suggestions on ground coverage materials for landscape embankments with the purpose of noise reduction.

1.3 Research methodology

1.3.1 Research approach

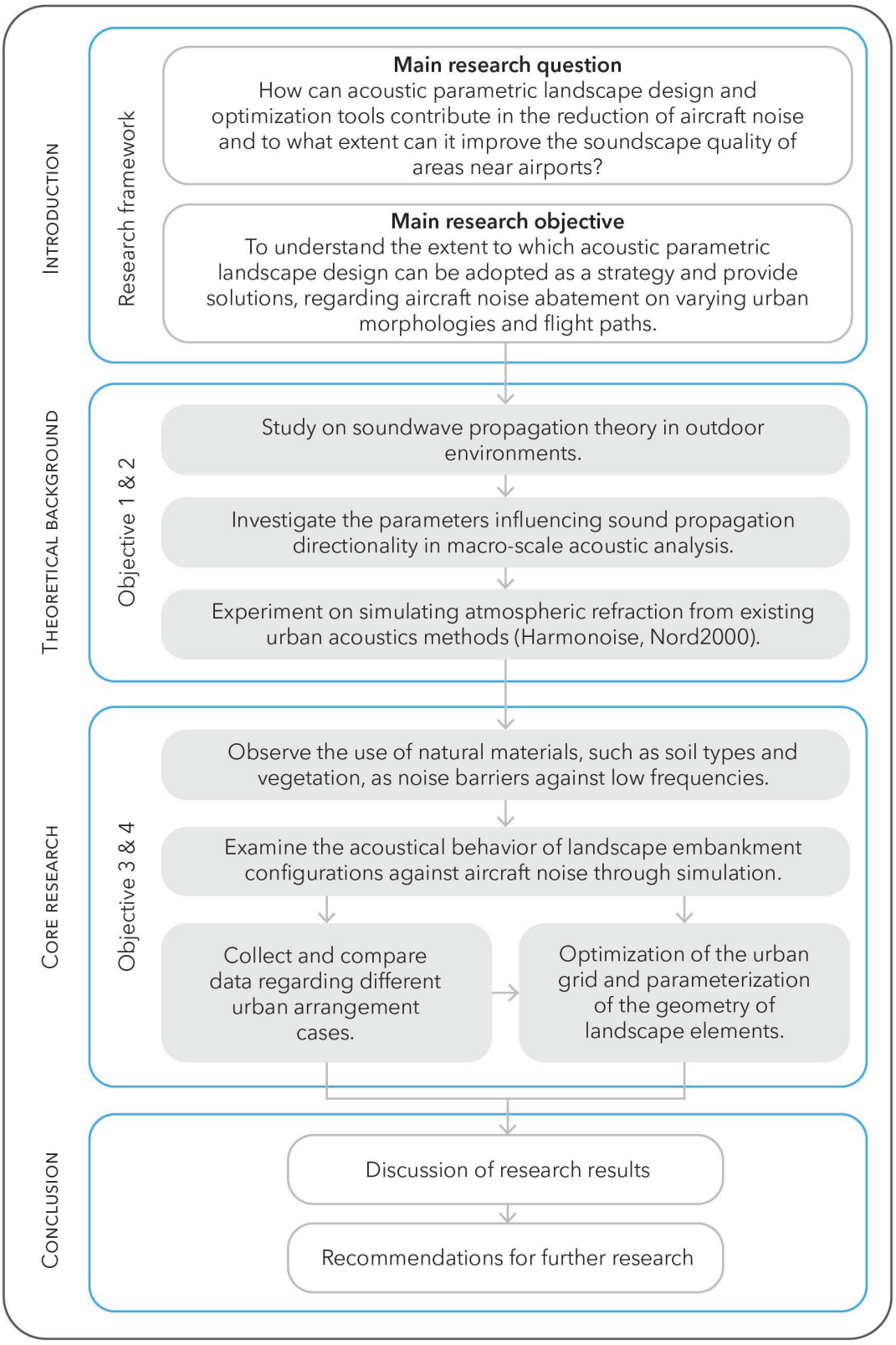

1.3.2 Research design

In accordance to the mentioned research objectives, the following method steps, tools & methods to be used are specifically described.

Objective 1

The first task is to analyze the behavior of sound propagation outdoors.

1. Study on sound propagation in outdoor environments through literature.
2. Comprehension of Nord2000 simulation method and its workflow.
3. Selection of an atmospheric effect (refraction) for further understanding and development into a script.
4. Forming of an acoustics equation sheet that describes the (refraction) effect.
5. Gathering of meteorological data, through Climate Consultant software and references, which are necessary for the equations.

Objective 2

Next is the formation of the script within a design software and representation of the effect graphically.

6. Development of the 3D urban context, within Rhino software.
7. Input of atmospheric parameters, within Grasshopper components.
8. Formation of a Python script that calculates the curvature of the path, which sound follows towards the study site due to atmospheric refraction.
9. Testing of the script to handle multiple cases in various locations.
10. Comparison of results for different locations and seasons.

Objective 3

The third objective concerns the acoustic response of geometry and materialization against the incoming aircraft noise.

11. Data acquisition from referenced experiments, regarding soil types and their acoustical properties.
12. Design of a principal landscape element as a sound barrier testing geometry within Rhino 3D environment.
13. Testing of different ground coverage materials on absorption of incoming noise, through iNoise simulation.
14. Investigation of geometric parameters of embankment configurations that influence diffraction, through iNoise simulation.
15. Testing of different urban grid arrangements, through iNoise simulation.
16. Addition of scattering surfaces, through Pachyderm acoustics software.

Objective 4

Finally, results of simulations are compared and combined into a design proposal.

17. Selection of the most effective testing cases regarding geometry and ground coverage and formation of an urban arrangement scenario.
18. Acoustic analysis of the proposal, through iNoise simulation.
19. Manual adjustment of the urban grid to compensate for unshielded areas.
20. Building configuration and materialization of surrounding outdoor areas.

1.3.3 Case study

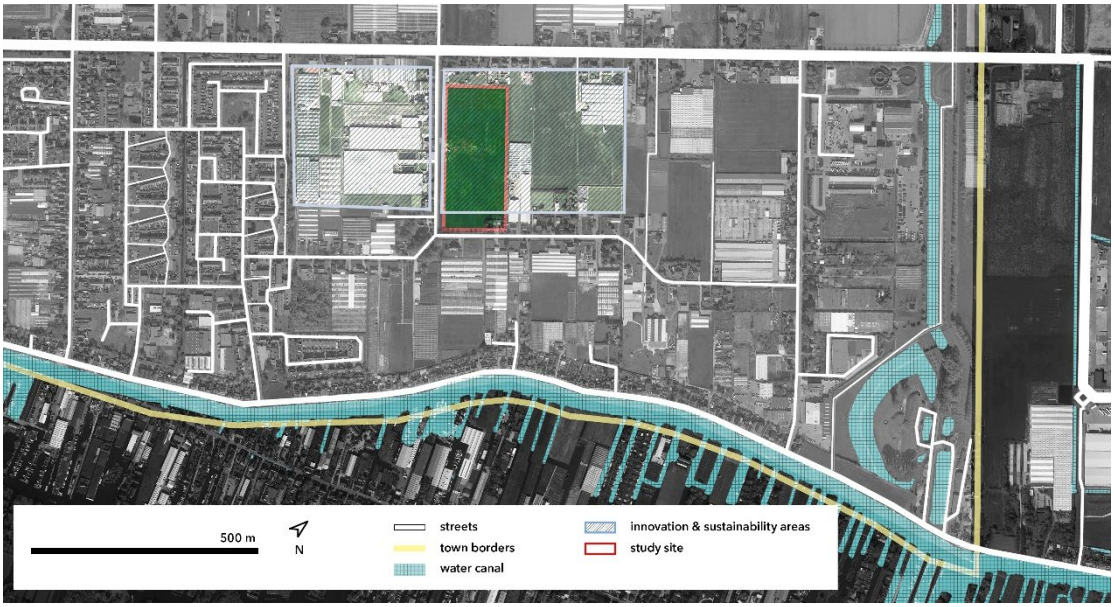

Fig. 1.2: Selected case study site (red outline) in Rijsenhout, Netherlands.
Background image source: Google maps
Illustration: Own work

Rijsenhout is a village located around 5 kilometers to the southwest of Schiphol airport. As a study area, an unbuilt rectangular site (500x200m) within Rijsenhout village is selected (Figure 1.2). The building block in which it is included has been declared as innovation & sustainability area by the municipality of Haarlemmermeer for further development.

The most significant routes that cause noise exceedance problems for this village come from a particular take-off runway. Kaagbaan (southwest) runway has a length of 3490 meters, it is mostly used for take-offs and is hardly preferred for use to and from the northeast. In principle, Kaagbaan is always in use at night in and from the southwest. The flight routes are limited to day and evening schedules according to legislation, but special nightly arrival and departure routes have been developed for Kaagbaan. In particular, it depends on the weather conditions and the preference order whether the runway is then used as a take-off or landing runway (Noiselab.casper.aero, 2020). The vertical distance of the routes taking off and surrounding Rijsenhout is 350m, before moving away and increase in altitude. These reasons generate a good opportunity to explore urban planning and larger landscape acoustical configurations in this urban area. Aircraft flyovers were noticed to reach, if not exceed the limit of 67dB set by the Federal Highway Administration (FHWA). Thus, the case recommends actions to ensure the reduction of noise levels and improvement of the urban soundscape. Finally, the greater horizontal than vertical distance describes the specific case parameters that will be tackled through this research.

Fig. 1.3: Flight routes of Kaagbaan runway (red line). Some of the paths (blue curves) circle around Rijsenhout area (yellow) before they increase in altitude and follow their route. The closest horizontal distance to the site is measured around 1,5 kilometers.
Source: Schiphol – Flight tracking (2020). [online] Flighttracking.casper.aero.

1.3.4 Tools & software

RHINOCEROS

Rhinoceros, or Rhino, is a 3D CAD modeling software package that enables accurate modelling of designs for rendering, animation, drafting, engineering, analysis, and manufacturing. It is a free-form NURBS surface modeler that supports a wide range of file formats and communication with other related software. It also supports the use of numerous plug-in components and programming languages. The latest version integrates Grasshopper that works in combination with Rhino software by "baking" the preview geometries within the modelling environment. Furthermore, Pachyderm acoustic simulation uses Rhino's environment for the set-up and visualization of its analysis. In this way, Rhinoceros' environment will be the basis where most of the design, optimization and analyses tasks will take place.

Available at:
https://www.rhino3d.com/

GRASSHOPPER

Grasshopper is an algorithmic modeling plugin for Rhino that uses a visual programming language, developed by David Rutten as an official plugin of Rhino. It is a parametric design tool that allows fast iterations and easy repetition of certain tasks comparing to a CAD design. Grasshopper allows the reference of Rhino geometry objects from it (points, curves, surfaces, etc.) and creates geometries that are "baked" back into Rhino. It provides foundation for many third-party components ranging from

environmental analysis to robotic control. Such components can be downloaded from *food4rhino.com*, which add new modules created by other users and expand the software's abilities through the use of programming languages, like Python and C#. Each module works as a function that gets inputs as variables and returns solutions or results which are called outputs. Thus, components of this plug-in will be extensively used, or developed for the particular study case, in order to set-up analyses, parameterization and other repetitive tasks.

Available at:
https://www.rhino3d.com/

PACHYDERM ACOUSTIC

Pachyderm Acoustical Simulation, by Arthur van der Harten, is an open source collection of acoustics simulation algorithms which can be used to predict noise, visualize sound propagation, and critically listen to designed spaces. The calculations for outdoor attenuation are based on the ISO 9613 method and are conducted through image-source and ray-tracing solutions. This software runs as a plug-in in Rhinoceros and provides professional grade tools for acoustical analysis and simulation. It also works as a plugin within Grasshopper, but features regarding materialization and other analysis components are missing. The calculations consider humidity and air temperature, but only for a homogeneous atmosphere without refraction effect. Absorption, scattering and transmission coefficients are inputs for materials, which are recognized through Rhinoceros as surfaces in different layers. Moreover, this software provides tools for scattering analysis of geometrical surfaces, an experimental yet implementation of edge diffraction, particle animation preview and other mapping methods. Finally, there is an option of assigning aircraft (ANCON) source as a line source input, nevertheless, it has been tested and does not seem to work for the distances that the selected case study refers to.

Available at:
http://www.perspectivesketch.com/pachyderm/

INOISE

iNoise is a quality assured software developed by "dGmR software" for industrial noise calculations in the environment. It mainly concerns noise prediction of industrial facilities and wind turbines sources and can be used for detailed calculations in addition to strategic noise maps. The calculations are based on the ISO 9613 method and the recommendations of the quality standard ISO 17534. However, the latest versions from 2019.1 and on implement the Harmonoise method for predicting street and railway noise, which is a more theoretical engineering method, such as Nord2000, and takes into account meteorological conditions. With Harmonoise the wind direction, wind speed and stability class can be defined, so that a much better validation of calculation models can be achieved. The software can also be licensed as a free version with Harmonoise in demo mode, limitations to the number of included objects and processor cores used for calculations.

Available at:
https://dgmrsoftware.com/products/inoise/

2 Literature chapters

2.1 Air traffic and noise

2.1.1 Aircraft noise

Efforts are continuously made in order to lessen the noise coming out of airplane parts. The main cause of noise emission while in flight is the air that is pushed through a fan into the engine and then the combustor, which burns jet fuel to eventually produce kinetic energy for flight. The way that this noise is reduced in modern aircrafts is by decreasing the required amount of air necessary for the engines or reducing the speed with which air exits the engine. Modern aircraft engines manage to reduce noise by limiting air intake of the combustor to lower than 10%. In the future, the levels of traffic noise are predicted to decrease with the use of electric and hybrid vehicles that utilize engines with significantly reduced noise. However, friction and vibrations of an airframe (parts of an aircraft apart from the engines) while moving on the ground surface is a major source of noise.

The sounds coming out of an aircraft vary during flyovers, take-offs and landings. Noise that reaches the ground level is influenced by factors like the distance and slant angle in relation to a ground receiver. In addition, during landings the landing gear and flaps are deployed, so that the aircraft becomes less aerodynamic and its noise increases (Aircraftnoise.com.au, 2020). The propellers and the fans also produce noise waves that are subsequently reverberated by the aircraft frame. During take-offs the noise levels reach their maximum, as well as when engines accelerate and generate turbulence of the air mass that cycles through the large fans.

Noise waves from an aircraft can travel as far as 10km (Aircraftnoise.com.au, 2020) and as they travel higher frequencies are absorbed by the atmosphere, making distant airplane sources feel like a low frequency rumble. The typical aircraft noise levels that reach the ground are between 65dB and 95dB. In Figure 2.1, a comparison is made between three types of traffic noise sources. Aircraft sound contains proportionally louder levels of low frequencies than street traffic sources (Lugten, 2018), although the distance of observation affects the air absorption of frequency ranges, depending also on humidity, air density and cloud cover.

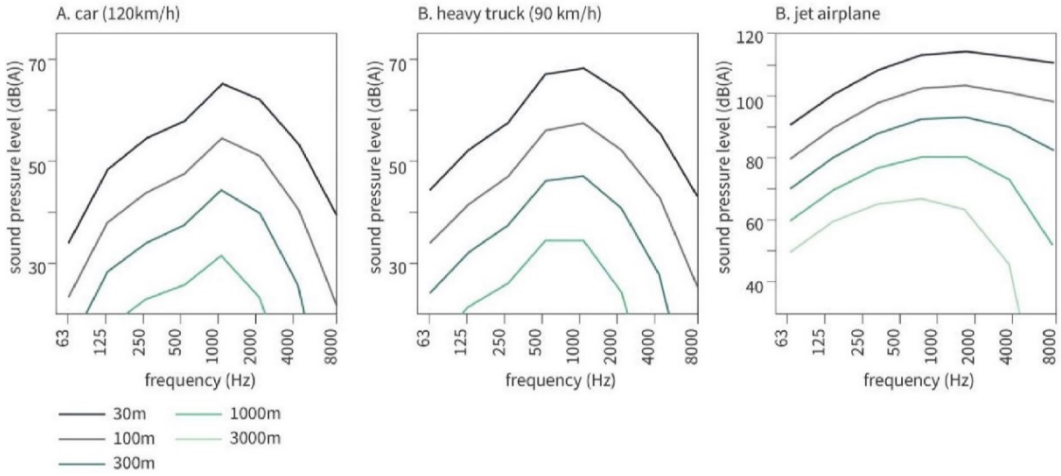

Fig. 2.1: Sound spectrums of three traffic sources with an indication of the decay with distance, based on atmospheric absorption and spread.
Source: Lugten, M. (2018). Tranquillity by design

Finally, it should be noticed that because of the location of an aircraft source, noise abatement procedures differ highly from street traffic sources and railways, since noise waves originate from the sky above and for longer distances buildings are not an easy task to protect against noise by constructing sound barriers.

To conclude, aircraft noise can be divided to the following types of noise emission operations through literature (Zaporozhets et al., 2011):

1. *"Starting engine operation*
2. *Pre-flight engine run*
3. *Taxiing to line up*
4. *Acceleration on the runway with full or reduced throttle*
5. *Take-off and roll-on*
6. *Flight path*
7. *Landing*
8. *Run-on operation and engine run-up for maintenance"*

2.1.2 Air traffic annoyance in Rijsenhout

The average value of ambient sound in natural environments is 40dB for a whole day and 30dB for the night. In order to avoid population annoyance and negative health effects, the World Health Organization has also defined a penalty factor at the limit of 30dB for sound exposure during night (Science Communication Unit, 2017). This time period refers to the hours between 23.00 and 07.00, which is the recommended sleep time period for adults and therefore every sound source emitting more than the limit may be considered a noise source. Despite the effort of authorities to cope with the growth of air traffic in the Netherlands, the number of complaints hasn't dropped accordingly (Lugten, 2018). The citizens living around Schiphol area are constantly exposed to noise levels above 70 dB, reaching up to 76dB in several cases, as shown in the figures below. Citizens around Schiphol area have been compensated over the years with better acoustic insulation (Netjasov, 2012), but the annoyance remains, as researchers showed that this depends on other non-acoustic factors as well, such as the public attitude towards air traffic, the number of flights and the location of people during flyovers (Bartels et al., 2015).

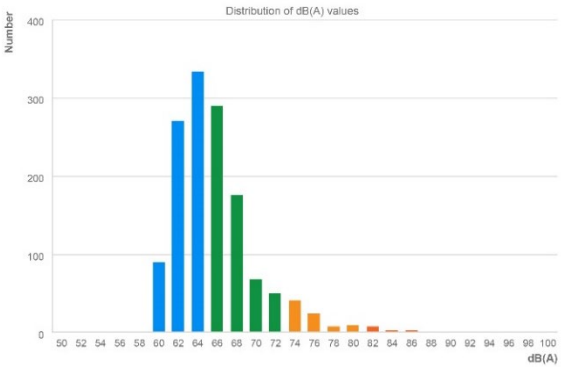

Fig. 2.2: Distribution of dB(A) values for flights recorded through the measuring station in Rijsenhout for a period of 5 random consecutive days.
Source: Noiselab.casper.aero, 2020

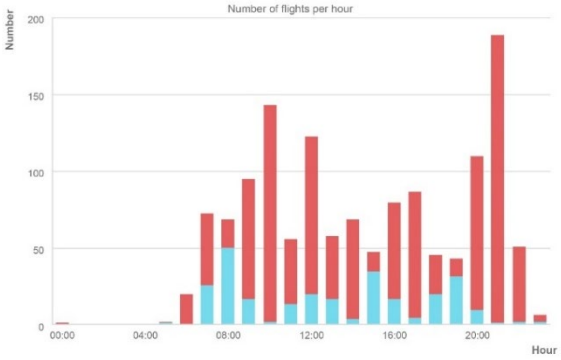

Fig. 2.3: Number of flights per hour for seven days of a random week for flights taking off or landing on Kaagbaan (southwest) airport runway.
Source: Noiselab.casper.aero, 2020

2.2 Sound propagation in outdoor environments

In this section, the description of the most influencing meteorological parameters are introduced, along with the atmospheric effects that these produce and the way of Nord2000 propagation prediction model to simulate the effect of refraction.

2.2.1 Meteorological factors

i. Temperature

In general, speed of sound depends on the type and the temperature of the medium it travels through. In order to find c0 for each encountered condition, equation [2.1] (Grc.nasa.gov, 2020) is used:

$$a = \text{sqrt}\ (g * R * T) \qquad [2.1]$$

where,

a	is the speed of sound (m/s)
g	ratio of specific heats (1.4 for air)
R	gas constant (286 $m^2/ s^2/ K$ for air)
T	temperature (K)

When simulating a ray path propagation of a sound from source-to-receiver points under stable weather conditions (homogeneous atmosphere), the path can be illustrated as a straight line. In real-life conditions, the speed of sound in air depends on the temperature of the air in which it travels. Across the atmosphere different temperature values are noticed in relation to the ground temperature and this causes sound speed gradients. Specifically, as temperature increases, the speed of sound increases and conversely, therefore in cases of unstable temperature values in the atmosphere between two points, the path of a sound ray is bent into a curved line and the effect of refraction is caused (Jónsson, 2007). In order to measure sound speed at a specific height z above ground the following formula is used, where c_0 = 331 m/s at T_0 = 0°C and T(z) is the absolute temperature at height z.:

$$c(z) = c_0\sqrt{\frac{T(z)}{T_0}} \qquad [2.2]$$

From this equation, it can be derived that a change of 1°C in temperature corresponds to 0.6m/s difference in the speed of sound (Jónsson, 2007). According to the positive or negative vertical temperature gradient, atmospheric refraction can take two forms, downward refraction or upward refraction.

During the day, the temperature of the ground is theoretically warmer than the air just above it, since it gets heated by solar radiation and then shortly transmits the heat to the air waves close to ground surface (Jónsson, 2007). This causes soundwaves to travel with higher speed close to ground level and bend the wave propagation path in an upward direction, resulting in upward refraction as seen in Figure 2.2. Then, a shadow region is created at a distance from the source, where sound cannot reach into (Acs.psu.edu, 2020). Thus, a receiver inside that zone might not be able to hear the sound even though he might see the source.

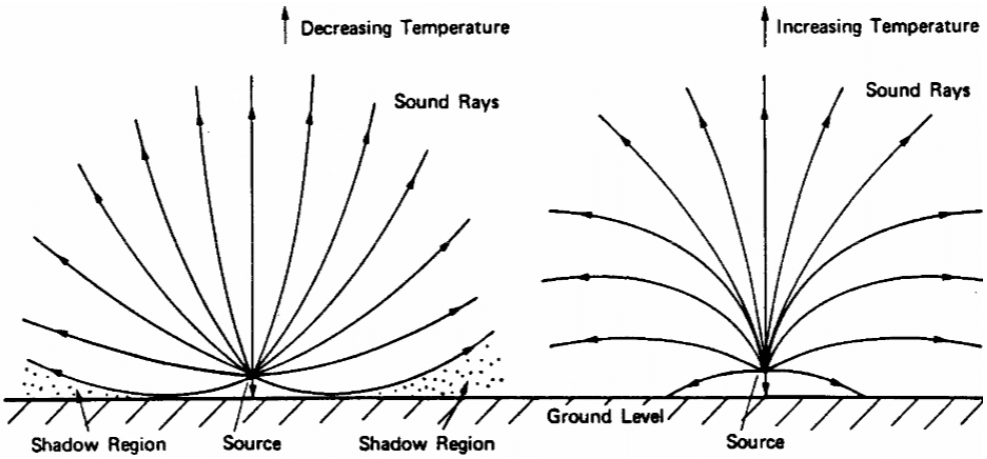

Fig. 2.4: Situations of refraction under the effect of temperature gradients and no wind. Upward refraction and the created shadow region is illustrated on the left, downward refraction on the right. Source: Simanek, D. (2015). [online] Available at: https://www.lockhaven.edu/~dsimanek/puzzles/soundreasons.htm [Accessed 19 Jan. 2020].

Downward refraction, as illustrated in Figure 2.4, can often occur during the shift from day to night, when the ground is not heated by solar radiation and cools off quicker than the air above it (Jónsson, 2007). The same temperature difference car occur close to large bodies of water or over snow covered ground. This effect results in some of the sound energy to be refracted back toward the ground and multiple reflections of a soundwave on the ground surface before reaching a receiver, explains why sometimes sounds can be heard louder over long distances around lakes than in environments of stable conditions.

ii. Wind

Wind is another meteorological factor that can cause refraction effect depending on the direction and speed of a soundwave. The speed of sound can be approximated as the sound speed in a non-moving atmosphere plus the wind speed in the direction of propagation (Jónsson, 2007). Naturally, vertical wind speed gradients exist, as wind speed is slower close to the ground due to friction of its surface. With increasing height, less friction occurs, so the wind speed increases and changes the speed of a sound. Depending on the directionality of wind, same as or against a soundwave, downward and upward refraction accordingly happens for spherical emitting sound sources (Figure 2.5). Similar to the temperature gradient result, there is again sound shadow zone created when wind bends waves upwards or sound energy that is refracted back towards the earth when wind pushes sound waves downwards.

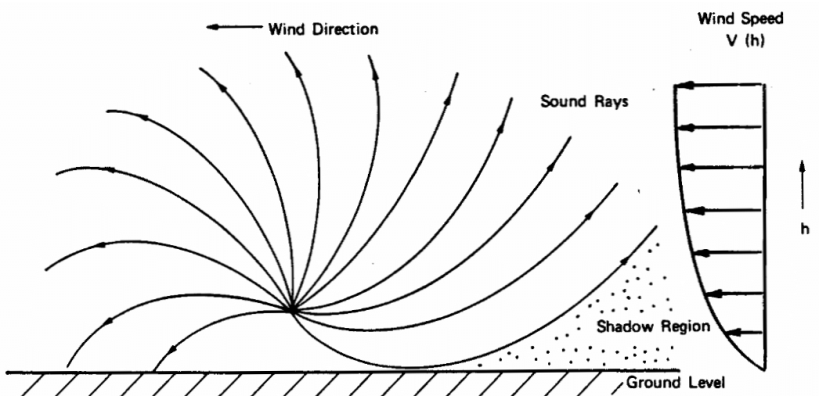

Fig. 2.5: The effect of wind speed gradient with increasing height to create bending of sound waves and thus, refraction. Here, there is the result of a wind direction from right to left. Source: Simanek, D. (2015). [online] Available at: https://www.lockhaven.edu/~dsimanek/puzzles/soundreasons.htm [Accessed 19 Jan. 2020].

iii. Humidity

The relative humidity plays an important role in the abatement of sound as it propagates through atmosphere and is used next to temperature values for air absorption calculations. In general, a dense medium absorbs more acoustical energy. As Attenborough states (2007), water vapor weighs less than air, thus a moist atmosphere attenuates less than a dry atmosphere. During a day, absolute humidity variates between the different time periods, especially in the summer. But it is usual to find humidity value peaks in the afternoon.

2.2.2 Atmospheric sound effects

In the specific case study, power levels and attenuation due to atmospheric effects is not considered. The reason is that the information of sound power levels is already known for the location of Rijsenhout, from the microphone recordings placed at the ground level of the residential area. Thus, the final outcome of the acoustics analysis for the potential configurations regarding the reduction of noise levels will be compared in relation to the statistics of these recordings (Noiselab.casper.aero, 2020). What is mostly of interest is the angle of incidence at specified locations, in order to have a more accurate estimation of the absorption and scattering coefficients of landscape acoustical elements. However, a brief description is made here to recognize some of the most significant effects, when sound travels in the atmosphere.

i. Air absorption

As a sound wave travels through the atmosphere, a proportion of sound energy is attenuated by the air itself. This energy loss occurs due to heat conduction, shear viscosity and molecular relaxation (Attenborough, 2007). As a result, atmospheric layers provide a primary absorption, especially for high frequencies above 2 kHz, when a sound wave covers long distances until it reaches a receiver. The attenuation coefficient α for air absorption may be calculated through formulas that introduce frequency,

humidity, temperature and pressure as variables and a prediction for the absorption of pure tones can be made with an accuracy of 10% (Attenborough, 2007). In addition, the time of day and year has a significant effect on these values, since variations in humidity and ground temperature along a given time period can alter the propagation path prediction. Thus, validated mean values of local climate statistics during a day of summer or winter through hourly averages should be compared in order to have more accurate estimations for air absorption.

ii. Atmospheric refraction

Across the atmosphere and as height above ground increases, varying temperatures and wind speeds exist, which can be grouped in different atmospheric layers. These meteorological properties influence the speed with which sound travels across the air and results in sound refraction (Salomons, 2001). As can be seen in Figure 2.6, sound speed gradients along the atmosphere of propagation change the angle at which sound waves travel across different mediums with varying properties. Subsequently, the directionality of waves affect the way that surfaces induce sound, since effects like edge diffraction, reflection and absorption depend on the angle of incidence (Lugten, 2018). It is common for some prediction models to omit temperature from calculations, since wind affects the refraction effect in a much more significant way (Attenborough, 2007).

The exact results and effect of meteorological factors for refraction are extensively described in later chapters. The representation of the curvature is the main focus at the stage of setting-up the study case and simulation methods will be studied as well.

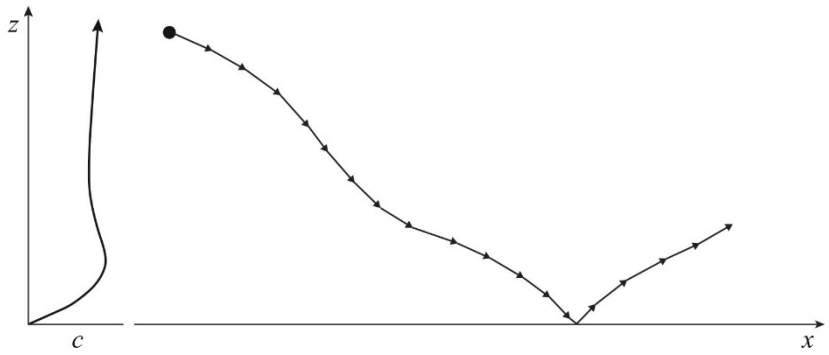

Fig. 2.6: A ray path is, due to a non-uniform effective sound speed, curved instead of straight.
Source: Arntzen, M. (2014). Aircraft noise calculation and synthesis in a non-standard atmosphere.

iii. Edge diffraction

When a sound wave meets an obstacle, it tends to bend its path around the edges of its geometry, in contrast to a straight normal line path. This effect is called diffraction and is more noticeable in low frequency sounds (Everest & Pohlmann, 2001). When the object is much smaller than the wavelength, sound penetrates the barrier and continues its path by curving the direction followed behind it. In cases of high frequency sounds, sound rays are more common to get reflected and a shadow zone is noticed behind the barrier. The diffraction effect then is limited to the space close and around the edges.

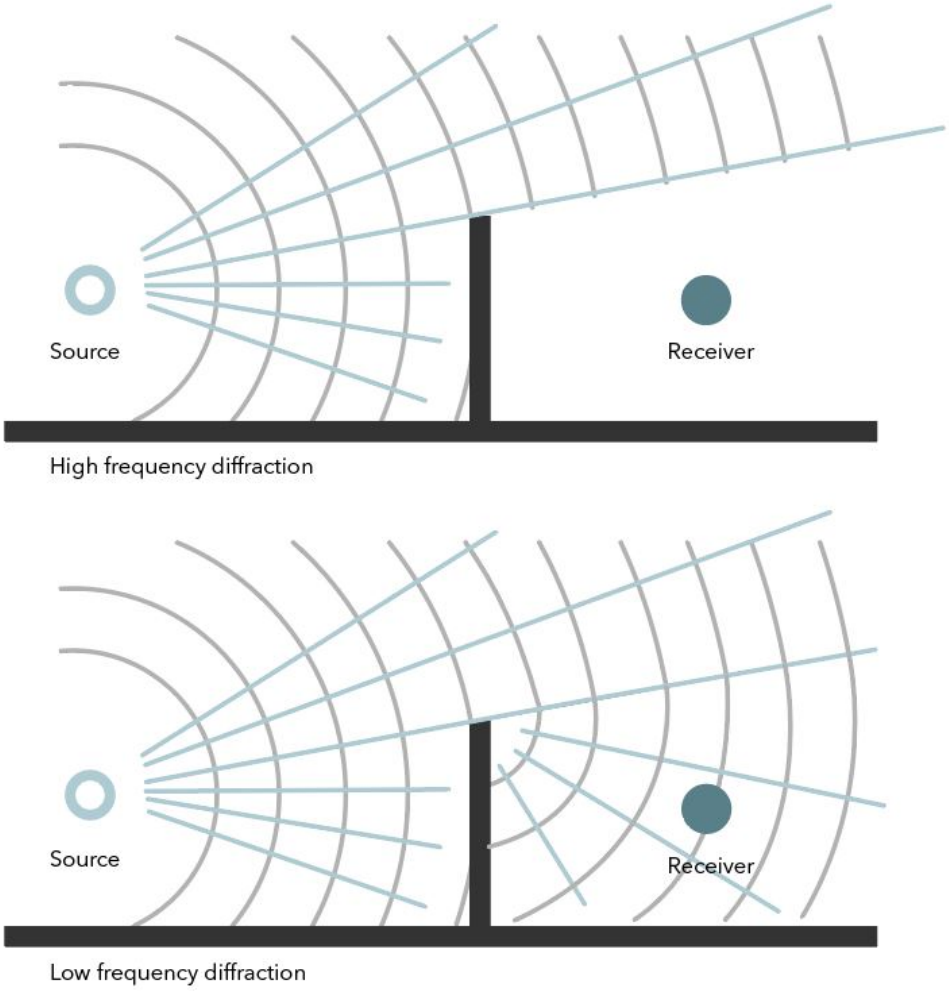

Fig. 2.7: The diffraction effect that occurs around the edges of an obstacle, more noticeable in low frequency sounds.

In complex spaces where more objects and walls obstruct the straight propagation of a sound, sound waves continue to get diffracted accordingly. This is a case of double or multiple diffraction and is usually studied as such. The amount of bending is determined by the position of the source and the angle that meets the barrier edges, but in general, more corners tend to multiply the effect and potential shadow zones are skipped.

iv. Ground reflection

When a sound wave travels through the atmosphere, it eventually makes contact with ground surfaces, especially in downward refraction effect, resulting in absorption or reflection of the sound. In case of a rough surface the reflected wave may be scattered in different directions, in which case the reflection is diffuse (Arntzen, 2014). Figure 2.8 shows an example of downward refraction, where soundwave rays hit the ground several times along a distance of propagation. At some spots more than one rays might reach the same spot, causing the power levels to fluctuate in relation to what a single ray would emit. In other spots, a shadow zone is noticed, although in real occasions this effect is underestimated, since sound scattering due to wind will fill this void and some smaller amount of sound energy can be heard.

When vegetation and roots exist on the ground, the surface becomes more porous. In order to have an effect on sound levels though, vegetation has to be relatively tall and dense (Attenborough, 2007). At ground surfaces where farm plots exist, the ground becomes more compacted and as a result more reflective, mainly due to frequent mowing. The amount of water that penetrates the ground surface also has an effect on absorption, with moist grounds limiting the absorption capabilities of soft grass-covered floors. In contrast, snow coverage renders ground significantly more porous than any other ordinary soil type material.

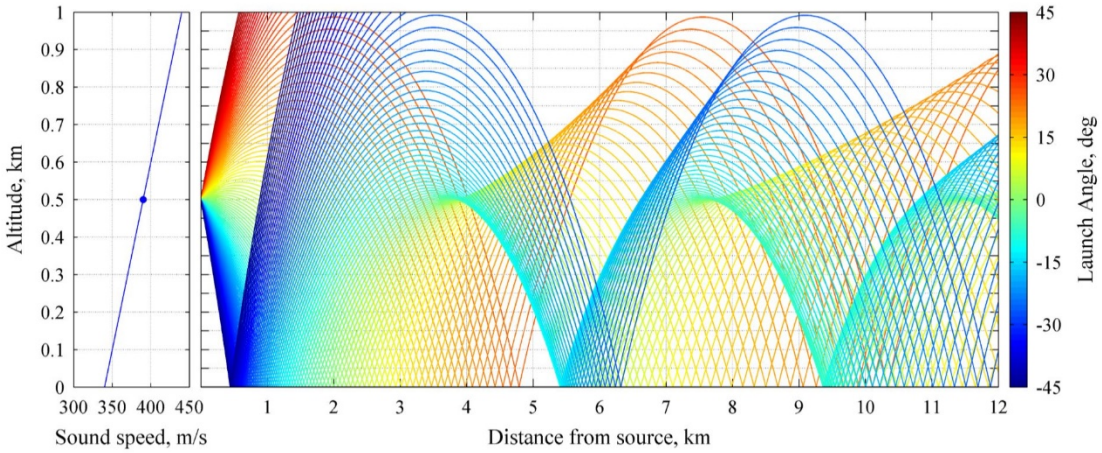

Fig. 2.8: Rays from a source at 500 m in an atmosphere with a linearly increasing (positive gradient) sound speed with altitude.
Source: Arntzen, M. (2014). Aircraft noise calculation and synthesis in a non-standard atmosphere.

v. Geometrical divergence

The geometrical divergence refers to the spreading of waves emitted from a source point spherically to the surrounding air (Nota et al., 2005). The attenuation due to a sound source radiating equally in all directions at any distance does not depend on frequency, but only travelling distance and is given by the equation:

$$A_{div} = 10 \log\left[4\pi\left(\frac{R}{R_0}\right)^2\right] \qquad [2.3]$$

where,
R is the distance from source to receiver (m)
R_0 is the reference distance (1m)

From equation [2.3] it can be derived that there is an increased attenuation of 6dB per distance doubling in all directions. It should be noted that this does not mean energy loss, but energy is progressively spread over larger surfaces and eventually its density is reduced, according to the inverse square law (Figure 2.9). Intensity I (W/m^2) at a distance r (m) from the source of power P (W) is given by equation [2.4] (Attenborough, 2007):

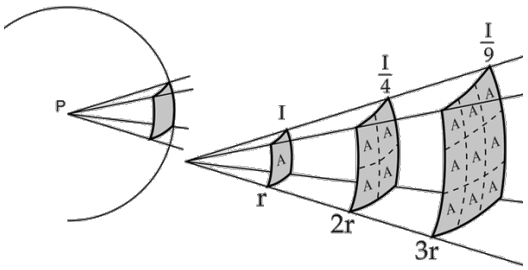

$$I = \frac{P}{4\pi r^2} \qquad [2.4]$$

Fig. 2.9: Spherical spreading of an omnidirectional sound source.
Adapted from: Inverse Square Law for Sound. [online] Available at: http://hyperphysics.phy-astr.gsu.edu/hbase/Acoustic/invsqs.html#c1 [Accessed 23 Jan. 2020].

2.2.3 Propagation prediction models

i. Urban acoustics methods

The prediction of noise propagation at an urban scale is influenced by a series of soundwave effects that occur due to the acoustics of the environment. The main methods used for urban acoustics prediction and soundwave propagation simulation at urban microscale (street scale) are three (Hornikx, 2016). There are:

- geometrical acoustics based methods, which can also be mentioned as engineering methods in literature and will be the focus on this research,
- diffuse field methods, specialized in interior acoustics, and
- wave-based methods, which provide a higher accuracy, but at a higher processing time cost for the higher range of frequencies

Wave-based methods provide the highest accuracy, as they consider all the effects of wave propagation in the atmosphere. These methods can be used to validate engineering methods in frequency ranges where those fail, a fact that inspires towards the development of hybrid models. Geometric acoustics methods consider mainly the effects that sound rays can present due to boundaries. These include reflections from ground or building geometries, diffraction that occurs when soundwaves encounter building edges and scattering from rough irregular surfaces (Hornikx, 2016). Geometric methods include meteorological conditions, but only as simplifications that could underestimate the realistic effect of the atmosphere.

Diffuse field methods are used for indoor acoustics, or generally when the environmental variables affecting sound waves are stable and can be predicted. In diffuse field methods sound energy is propagated inside a grid, instead of ray-tracing techniques that geometric models use (Hornikx, 2016).

Geometric methods, which will be the main focus for the simulation model in this research, are able to simulate noise maps much faster than wave-based methods. Two quite similar models to mention are *Harmonoise* and *Nord2000*, which are expected to produce noise maps with an accuracy of around 3dB (Jónsson and Jacobsen, 2008). Differences though, can be found in the way that each one simulates refraction and diffraction. Nord2000 predicts edge diffraction at low frequencies better than Harmonoise. In contrast, Harmonoise gives better results for diffraction in high frequencies and handles downward refraction more accurately, but both seem to fail in cases of upward refraction (Jónsson and Jacobsen, 2008).

Naturally, a lot more than the simulated effects on geometric methods happen because of the properties of the atmosphere between a source and a receiver. Refraction due to differences in temperature and wind speed is important in urban scales, as they bend the curvature of the soundwave propagation accordingly. The different layers in the atmosphere present differences in those parameters and should be taken into account at urban macroscale with the most possible accuracy allowed. The same applies for atmospheric turbulence and absorption by air itself. The most accurate engineering models take those into account with an acceptable accuracy, but topographical and ground conditions, as well as vegetation can influence sound propagation significantly. And these become even more important when it comes to sound sources like airplanes taking off and landing, which introduces the variable of larger height and length differences in relation to a ground receiver.

ii. Ray tracing model

Many of the current acoustics software use the ray tracing method mainly for room acoustics simulations. In this method, a large number of rays are casted from a source point in various directions. The rays are advanced over distances, while considering the medium of the propagation space for change in direction and solid objects that collide with the path of the rays. When boundaries are met, rays are subject to energy loss by absorption and will reflect or scatter (Vlaun, 2015: 33). Then, the ray-tracer recalculates the ray directivity until a full path is completed.

It is understood that the number of rays that is examined in a ray tracing simulation is important for the accuracy of the analysis. The analysis is repeated for a specified amount of rays, which depends on the processing power of the computer to achieve results in a reasonable time. This justifies its main use on interior acoustics, where the space and the analysis objective are much more limited in terms of propagation. In an outdoor environment simulation, reflections and scattering after object collision show a significant spreading of rays over large distances. Only the rays that meet a receiver point is of interest, the eigenray, thus maintaining a small number of rays makes it harder to come to reliable results. During this research, Pachyderm acoustics' ray tracing model was examined for its potential to perform an outdoor simulation. However, this software could not handle the large propagation distance of an aircraft noise source towards a point of interest and most of the simulation results were unreliable or completely misleading. An issue like this can be surpassed by increasing the amount of rays that are processed, thus increasing the demand in processing power, or by setting up a pseudo-simulation with shorter distances targeted to derive specific results. In any case, it is up to the user to define the interest and handle the level of result accuracy.

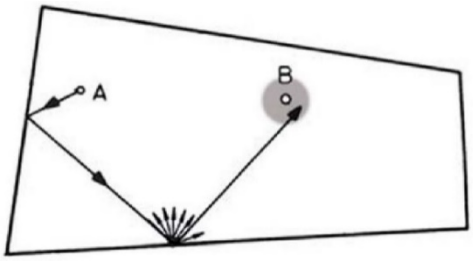

Fig. 2.10: The eigenray. Principle of ray tracing.
Source: Kuttruff, H. (2009). Room acoustics.

iii. Simulating atmospheric refraction

As already mentioned, the effect of atmospheric refraction is the bending of the line paths that a sound follows due to temperature and wind speed direction differences in a point-to-point propagation. At very short distances the refraction effect is unnoticeable, since the propagation distance reduces and accuracy can be achieved by simple models without considering atmospheric refraction. However, a simulation for the large distances up to an aircraft flyover cannot omit the presence of refraction and should be considered to retrieve the angle of incidence at a receiver point. In micro-scale studies the situation is simplified by considering a stable sound speed and rays travel linearly as shown in Figure 2.11. In reality, there is a non-uniform speed of sound gradient, in which sound speed increases almost logarithmically during the daytime (Lugten, 2018).

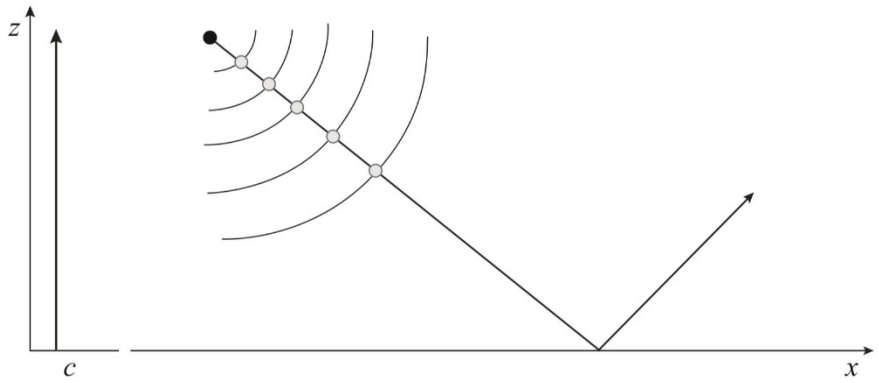

Fig. 2.11: A ray path is formed by a straight line, connecting the same initial point of an acoustic wave-front, if the speed of sound is uniform.
Source: Arntzen, M. (2014). Aircraft noise calculation and synthesis in a non-standard atmosphere.

For simulating the curvature of a sound wave, Nord2000 and Harmonoise were considered for their method, since these provide the most accurate model regarding existing engineering methods of sound propagation prediction. Both models take into account the effect of atmospheric refraction, but each method is fundamentally different in terms of handling. As Jónsson states (2007: 27), "*while Nord2000 replaces the straight rays in the model for a homogeneous atmosphere by curved rays, thereby simulating the actual phenomenon of refraction, Harmonoise uses straight rays but curves the ground using conformal mapping to simulate the same effect*".

A comparison between Harmonoise and Nord2000 on their accuracy for simulating the refraction effect showed some differences when compared to scaled experiments (Jónsson, 2008). Nord2000 does not accurately predicts sound pressure levels due to reflections of a downward refracted soundwave, as an increase in levels should be expected. As a result, Harmonoise seems to handle downward refraction better than Nord2000. Unfortunately, neither model can handle upward refraction satisfactorily. For the purpose of this research and because Nord2000 provides an extensive and much more descriptive report for handling the refraction effect (Delta, 2006), its method will be further explored and guide the refraction curvature simulation process. It should be added that the prediction model, firstly published in 2000, has been revised and informed to handle more accurately the effects from multiple ground reflections and effects in shadow zones.

iv. Nord2000 refraction model
[Delta, 2006]

Refraction angle and length of curved ray

The principle to predict the effect of atmospheric refraction is replacing the straight rays of a source-receiver path in a homogeneous atmosphere with curved rays. In this model, a linear sound speed profile is assumed, where sound speed is calculated depending on the height above ground surfaces, according to the equation:

$$c(z) = c(0) + \frac{\Delta c}{\Delta z} z \qquad [2.5]$$

where,
c(0) is the sound speed at the ground (m/s)
z is the height above ground (m)
Δc/Δz is the sound speed gradient (s^{-1})

A linear sound speed gradient is rarely encountered in real condition atmospheres, so an approximation of a non-linear profile based on an equivalent linear profile will be studied. The modification of rays due to refraction concerns the direct paths, but also the paths of reflected rays. The modified rays of downward and upward refraction are illustrated in Figures 2.12 and 2.13.

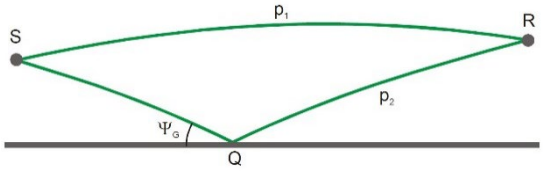

Fig. 2.12: Sound propagation over flat terrain in case of downward refraction.
Source: Delta (2006). Nord2000. Comprehensive Outdoor Sound Propagation Model.

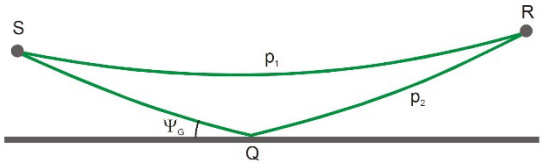

Fig. 2.13: Sound propagation over flat terrain in case of upward refraction.
Source: Delta (2006). Nord2000. Comprehensive Outdoor Sound Propagation Model.

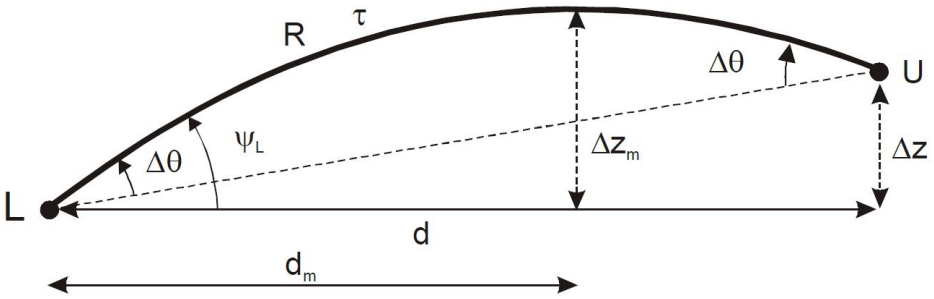

Fig. 2.14: Definition of geometrical parameters for a circular ray.
Source: Delta (2006). Nord2000. Comprehensive Outdoor Sound Propagation Model.

Figure 2.14 shows the point-to-point propagation geometrical parameters for a refracted direct ray path between source L and receiver U positions. For these parameters, the sound speed profile from equation [2.5] is rewritten in the following way:

$$c(z) = c_0\left(1 + \xi\left(z - z_L\right)\right) \quad [2.6]$$

$$\xi = \frac{\Delta c / \Delta z}{c_0} \quad [2.7]$$

$$\Delta z = z_U - z_L \quad [2.8]$$

where,

$c_0 = c(z_L)$	is the sound speed at lowest point L (m/s)
Δz	is the height difference between points L and U (m)
ξ	is the relative sound speed gradient (m^{-1})
$\Delta c/\Delta z$	is the linear sound speed gradient (s^{-1})
z_L, z_U	are the heights of points L and U above ground (m)

Following is the calculation of the angle ψ_L and horizontal distance d_m from point L to the projected position of the highest point of the circular ray as shown in Figure 16. Subsequently, R, τ, Δθ can be determined.

$$\tan \psi_L = \frac{\xi\, d}{2} + \frac{\Delta z\,(2 + \xi\, \Delta z)}{2d} \quad [2.9]$$

$$d_m = \frac{\tan \psi_L}{\xi} \quad [2.10]$$

If $\xi > 0$ and $d <= d_m$, R and τ are calculated by equations [2.11 – 2.14]:

$$R(\Delta z) = \frac{1}{\xi \cos(\psi_L)} \left(\arcsin\left((1 + \xi\, \Delta z) \cos(\psi_L)\right) - \frac{\pi}{2} + \psi_L\right) \quad [2.11]$$

$$\tau(\Delta z) = \frac{1}{2\,\xi\, c_0} \ln\left(\frac{f(0)}{f(\Delta z)}\right) \quad [2.12]$$

where,

$$f(0) = \frac{1 + \sin \psi_L}{1 - \sin \psi_L} \quad [2.13]$$

and

$$f(\Delta z) = \frac{1 + \sqrt{1 - (1 + \xi \Delta z)^2 \cos^2 \psi_L}}{1 - \sqrt{1 - (1 + \xi \Delta z)^2 \cos^2 \psi_L}} \quad [2.14]$$

If $d > d_m$, R and τ are instead calculated by equations [2.15, 16 and 17]:

$$\Delta z_m = \frac{1}{\xi}\left(\frac{1}{\cos(\psi_L)} - 1\right) \quad [2.15]$$

$$R = 2\,R(\Delta z_m) - R(\Delta z) \quad [2.16]$$

$$\tau = 2\,\tau(\Delta z_m) - \tau(\Delta z) \quad [2.17]$$

where,

Δz_m	is the height of the ray at the highest point of the circular ray (m)
$R(d\Delta z_m)$ & $R(d\Delta z)$	are calculated by equation [2.11] (m)
$\tau(\Delta z_m)$ & $\tau(\Delta z)$	are calculated by equation [2.12] (curvature parameter)

Finally, Δθ can determined by equation:

$$\Delta\theta = \psi_L - \arctan\left(\frac{\Delta z}{d}\right) \quad [2.18]$$

If ξ < 0, R, τ and Δθ are also determined by equations [2.9 – 2.18] using the absolute value of ξ (ξ = |ξ|), but the calculated value of Δθ is multiplied by (-1).

In order to avoid computer coding numerical problems, when Δz becomes less than 0.01, a value of 0.01 should be used instead. Finally, when ξ = 0, we have a homogeneous atmosphere. Therefore, when $|\xi|<10^{-10}$, $\xi = 10^{-10}$ is used instead.

Equivalent sound speed profile

The effective sound speed profile c(z) can be approximated by a simple combination of a logarithmic and a linear relationship as shown in equation [2.19].

$$c(z) = A \ln\left(\frac{z}{z_0} + 1\right) + B\,z + C \quad [2.19]$$

where,

z	is the height above ground (m)
z_0	is the roughness length (m)
A, B, C	are constants that describe meteo-classes

The logarithmic part of equation [2.19] is determined only by the wind speed component u in the direction of propagation and is calculated at a height z_u by [2.20]:

$$A = \frac{u(z_u)}{\ln\left(\frac{z_u}{z_0} + 1\right)} \quad [2.20]$$

The linear part of the profile is determined only by the temperature and is assumed to increase linearly with height (dt/dz is constant) and is calculated by [2.21]:

$$B = \frac{dt}{dz}\frac{10.025}{\sqrt{t + 273.15}} \quad [2.21]$$

According to research by Arntzen et al. (2014), there are occasions where refracting rays that account for atmospheric refraction in non-uniform atmospheres can have insignificant or no change in directivity compared to straight rays. In specific, this should happen when the incident angle between receiver point and the source position is higher than 15 degrees. For the study location and flight path in interest, the angle of incidence from straight rays was measured to be close, but always higher than 15^0.

2.3 Noise abatement strategies

Airplanes have become quieter over the last decades, but flight routes are increasing and new airport runways are demanded. The International Civil Aviation Organization (ICAO) Balanced Approach to Aircraft Noise Management was developed in 2004, which regulates procedures about noise issues at individual airports in an environmentally and economically responsible manner. Some of its approaches concern land-use planning and management, noise-preferential routes and new technologies to reduce the noise at its source. Other zoning policies for new airport runways also restricts planning at neighboring populated areas.

Technology, industry and related research studies are joining forces to counter the noise emission at its source by upgrading the mechanical parts of an aircraft. Noise and CO_2 emissions is the core problem to resolve, with forward steps being evaluated over the last decades. Optimization for low Environmental Noise Impact Aircraft (OPENAIR) focuses on new aeroacoustics technologies towards the reduction of engine and airframe noise. Despite the technological progress, populated areas are still reported to be affected by exceeding the limits for noise exposure, thus, new efforts are necessary to mitigate aircraft noise. The number of people exposed to noise from European airports is forecast to increase by 15% by 2035 (from 2014 levels) (Science Communication Unit 2017). To overcome this, urban management strategies combined with smart building arrangement methods, absorbing construction materials and macroscale noise barriers are able to limit the exposed public activities and bypass sensitive cases where flight routes cannot be altered.

2.3.1 Vertical noise barriers

An effective way of abating traffic noise close to residential areas from highways and railways has been the installation of wall barriers. Their effect depends on delicate dimensioning and positioning, in order to eliminate direct propagation, as well as materialization to get the maximum desired effect. A wide range of typical construction materials including concrete, aluminum and glass are used. Some of the usually favored types, as stated in the Noise abatement approaches by the Science Communication Unit (2017: 20), are:

- *''Absorbing barriers, which have absorbing materials on the side facing the noise, but tend to be relatively expensive.*
- *Angled barriers, which reflect sound away from the receiver.*
- *Capped barriers, which have a specially designed top section to attenuate sound waves.*

- *Covering barriers, which offer significant noise reduction. Examples include a grid set over a road or a complete cover over a road, such as a tunnel.''*

Larger-scaled configurations are likely to put limitations on procedures due to high application cost and alternatives should be researched on space and cost effectiveness. Since population is affected by urban installations, visually 'hiding' a noise source with natural material elements has been reported to reduce the annoyance (Science Communication Unit, 2017). A study with focus on the investigation of foliage and canopies of trees effect on noise pollution, examined the potential of tree belts to improve noise reduction effects in city environments (Maleki & Hosseini, 2011). In this study, it was concluded that urban green areas and particularly trees have a crucial role to reduce the noise pollution. Some of the results are shown in Table 2-1, including different types of Iranian-based tree species and their attenuation for distances up to 100 meters. As advised, mixed stands is the most efficient option and should be planted in belts with suitable width. Attention should be paid though at the types of plantations, in order to provide better growth conditions for a species depending on the ecological conditions of each region.

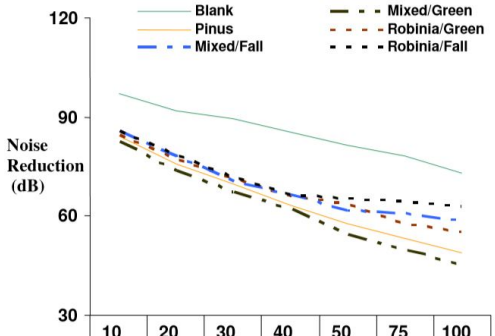

	10	20	30	40	50	75	100
Blank	97.1	91.8	89.5	85.3	81.3	78.3	72.9
Mixed/Green	82.5	73.7	67.3	62.3	54.6	50.2	45.4
Pinus	84.4	75.7	69.7	63.2	57.8	53.1	49.0
Robinia/Green	84.8	77.4	71.4	66.2	63.7	57.9	55.2
Mixed/Fall	85.8	78.2	70.5	66.5	61.8	60.9	58.6
Robinia/Fall	86	78.6	71.8	66.7	65.3	64.8	62.9

Table 2-1: Comparison of the effect of distances from noise source on noise attenuation in different tree types. Source: Maleki, K., & Hosseini, S.M. (2011). Investigation of the effects of leaves, branches and canopies of trees on noise pollution reduction.

2.3.2 Reduction through noise mitigation

An interesting approach to an aircraft noise reduction strategy around Schiphol airport should be mentioned here. Hoofdorp is a village located near one of the west flight paths of the airport, heavily influenced by aircraft noise. On the authority of Schiphol a multidisciplinary team worked on a world first project, Buitenschot Park, finished in 2013 (Figures 2.15, 2.16): ''*a park that exists by the grace of low frequency ground noise caused by aircraft taking off. Because of its design, the park landscape contributes to a considerable noise reduction by limiting the soundwaves that reach the village after ground reflections. Measurements and calculations have shown that the ground noise is distorted and dispersed, as it were, by oblique planes*'' (H+N+S Landscape architects, 2020). Nevertheless, it should be noticed that this case differs from the research's focus,

since it concerns sound travelling along the ground level, while aircraft is still on its track until take-off and is located between the flight path and the urban area. Despite that, this is still an innovative example in practice of landscape configurations that can reduce aircraft noise levels that propagate towards a residential area.

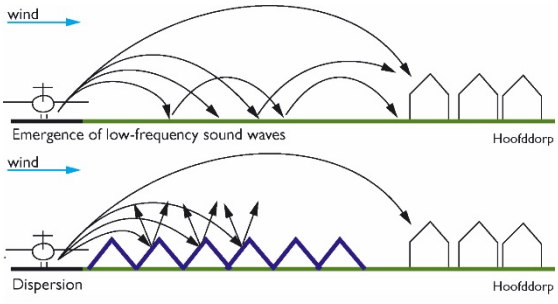

Fig. 2.15: Rays from the aircraft are dispersed because of the rough geometrical greenery and ground reflections that reach residential area are avoided.
Source: H+N+S Landscape architects (2020). [online] http://www.hnsland.nl/en/projects/land-art-park-buitenschot [Accessed 06 Nov. 2019].

Fig. 2.16: A site view of the Buitenschot land art park.
Source: H+N+S Landscape architects (2020). [online] http://www.hnsland.nl/en/projects/land-art-park-buitenschot [Accessed 06 Nov. 2019].

Another example where geometry is used to acoustically shield an urban space from street traffic noise is the Pavilion 21 MINI Opera space, designed by Coop Himmelblau. The shell of this project intends to secure the soundscape of the square in front of the building, which serves as the entrance to the opera space. To achieve this, the façade walls that face the street have been designed parametrically with prismatic elements that deflect noise away from the entrance. Then, these prismatic forms have been coated with reflective and absorptive materials accordingly in order to avoid problematic reflections towards the ground, but limiting reflections' directivity away from the street canyon. The method of shielding that this project utilizes demonstrates a case of deflecting traffic noise away from outdoor areas that are vital to the public. The proximity of the source does not compare to the distances of an aircraft flyover, but the materialization and geometry of such elements targeted directly to solve noise related issues is a step to consider when going over the detailed construction in a smaller scale.

Fig. 2.17: Pavilion 21 MINI Opera Space.
Source: Coop Himmelblau (2010). [online] Available at: http://www.coop-himmelblau.at/architecture/projects/pavilion-21-mini-opera-space/

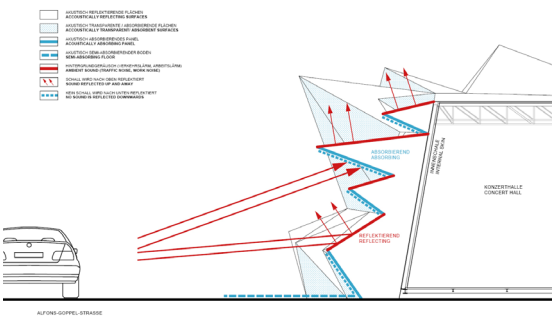

Fig. 2.18: Absorptive and reflective elements of the façade that deflect traffic noise.
Source: Coop Himmelblau (2010). [online] Available at: http://www.coop-himmelblau.at/architecture/projects/pavilion-21-mini-opera-space/

2.4 Acoustical properties of surfaces

2.4.1 Acoustic absorbers

Acoustic absorption accounts for the amount of sound energy that is captivated by a material when sound waves meet its surface. The properties of a material as well its surface area are responsible for the amount of energy that is converted into heat due to deformation and movement of the molecules within it. The absorption coefficients are measured in different frequency bands and the sound energy that is not absorbed is reflected or scattered away. As Peters states (2009): *"there are generally three types of acoustic absorbers: porous absorbers, diaphragm absorbers, and volume absorbers. The absorbing capabilities of the porous absorber depends on the complex inner structure of the constituent material. The other two absorbers are types of acoustic resonators. Acoustic resonators, either a resonating diaphragm or a resonating volume of air, are primarily used to absorb low frequency sounds"*. Since materials with different density and size are responsible for the absorption of part of the frequency spectrum, it is commonly recommended to combine a variety of acoustic absorbers, when the objective is to eliminate the across all frequency bands.

2.4.2 Acoustic diffusers

When sound reaches a surface, sound energy that is not absorbed or transmitted through the material can be either reflected or scattered. Reflection concerns the specular direction, whereas scattering refers to reflection in many different directions. When a larger amount of acoustic energy is reflected elsewhere than the specular direction, the effect is known as diffuse reflection and the surface that produces this effect as diffuser (Cox, 2009). The diffusion coefficient characterizes the spatial uniformity of reflections in terms of resulting reflection angles produced by a surface (Cox et al., 2006). With this effect in mind, different combinations of acoustical properties are proven to achieve additional reduction in sound levels through diffusing sound frequencies. For instance, diffusing elements can scatter rays towards absorptive materials and multiply the surfaces they encounter for a more efficient absorption (Peters, 2009).

Regarding geometrical surface irregularities, the dimensions of an acoustical element influence the response effect according to the frequency of sound (Figure 2.19). In specific (Hornikx, 2016: 413): "*i) for frequencies with wavelength much larger than the dimension of the irregularities, surfaces reflect the wave as it would be flat, ii) for wavelengths in the order of the irregularity scales, the sound wave is diffusely reflected, iii) for wavelengths smaller than the irregularities, the reflection is specular again*".

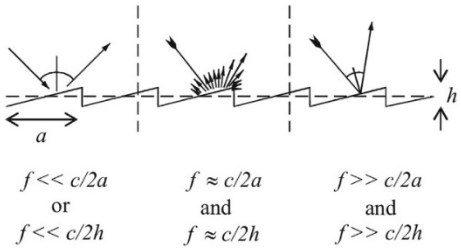

Fig. 2.19: Frequency ranges for scattering from a periodic surface of repetition distance a, and roughness depth h.
Source: Cox et al. (2006), A tutorial on scattering and diffusion coefficients for room acoustic surfaces.

Diffusers can have a variety of irregularities and type of array onto a surface, in order to be effective. But as mentioned, the result is not the same for different sounds. One of the most common diffusers developed and still used (Figure 2.20) is the Schroeder diffuser discovered in the 1970s. It consists of rectangular forms arrayed on a surface with constant well width and random well depth depending on the frequency of interest. The rule of its depth configuration is based on mathematical sequences that increase the predictability of its diffusing properties. Other sequences and configurations can be followed as well, such as pyramids, hexagons, well depth variations, in order to also overcome the shape factor of materials used for a component. For instance, the fractal technique to divide surface shapes might be used to include multiple frequency ranges in diffusion. However, variation of geometries and arrays can be considered effective, as long as their acoustical properties are verified by testing (Peters, 2009).

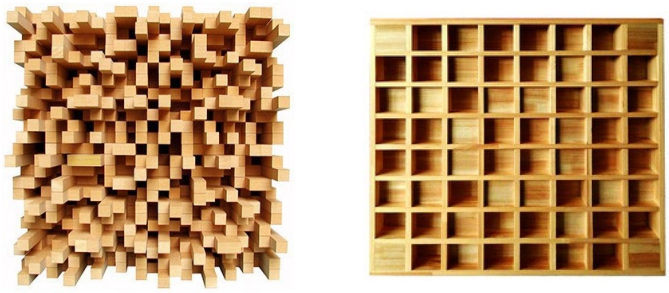

Fig. 2.20: Examples of diffusing element arrays based on the Schroeder diffuser.

2.4.3 Acoustic reflectors

In contrast to the scattering effect, reflectors are called the surfaces responsible for the sound reflected in a mirrored direction. Reflection is usually encountered when sound bounces off a smooth and hard surface with no irregularities, same as light being reflected by a mirror. The angle of incidence is equal to the angle of reflection in this case (Vlaun, 2015). Similar to the scattering parameters, reflection coefficient depends on the wavelength of the sound, in addition to the shape, roughness and materialization of the surface. Reflectors are commonly used in music halls for strengthening the acoustical energy that meets the audience position, or in noise barriers in an attempt to reflect traffic noise away from habitable areas.

2.4.4 Ground Impedance

The acoustic impedance of non-porous materials is given by the one-parameter model of Delany and Bazley (1970):

$$Z = 1 + 9.08\left(\frac{f}{\sigma}\right)^{-0.75} + j\,11.9\left(\frac{f}{\sigma}\right)^{-0.73} \qquad [2.22]$$

where,

f is the 1/3 octave band center frequency [Hz]

σ is the effective flow resistivity [kNsm^{-4}]

2.4.5 Vegetation & ground surfaces

In the modern years of sustainability-guided design, urban planning and construction in general are heading towards the development of green spaces inside the built environment. With the will to preserve and enhance the existence of the natural element inside cities, various sectors of construction design aim to use circular materials concerning the emission reduction within urban environments and methods to achieve this are widely preferred. Similarly, since urban acoustics configurations have a significant impact in shaping the built environment, they should also be inspired by this philosophy. To materialize this, acoustical treatments with vegetation and green noise barriers have been studied over the years as substitutes to the conventional free-standing barrier.

Green materials exist naturally over ground surfaces and contribute to the soundscape environment of a city in their own way. Nevertheless, the knowledge of their acoustical properties is a great opportunity to battle more environmental issues than only what an acoustical treatment necessitates, since their use on construction is desired to generate microclimate effects, increase urban green spaces and improve cityscapes. A paper investigating the acoustical properties of vegetation and soil (Kim et al., 2011) presents some interesting results for different types and densities of those alternatives. According to real-scale laboratory measurements, they resulted in variations in the acoustical properties of soil and leaf molds. In particular, absorption coefficients of sandy soil and leaf mod increase with increased soil depth, but sound abatement decreases because of heavier weights and density change. Furthermore, water content ratio was tested and resulted in worse scenarios regarding high frequencies, with no water inclusion proven to be the best scenario. Other organic mixtures showed complex coefficients, whereas compressed soil decreased the absorption significantly, since the porosity of the mixture is reduced and mostly reflects sound waves.

Another study explores normal and random incident absorption coefficients of vegetated roofs. In this report (Connelly & Hodgson, 2015), moisture content was proven again to decrease the absorption ability of soil, while increased substrate depth and organic matter improved absorption as it was added. A collection of data and quantified noise reduction coefficient is gathered, as can be seen in Table 2-2, aiming to be used in design environments for multi-layered building partitions. The best results of the experiment were found to be above 1000 kHz, reaching values around 0.90 for absorption coefficient.

	Octave band (Hz)				
Oven dried	250	500	1000	2000	AVG.
Mean	0.62	0.76	0.68	0.79	0.71
Min	0.28	0.63	0.53	0.70	
Max	0.77	0.91	0.80	0.91	
Wilting capacity					
Mean	0.28	0.71	0.58	0.75	0.58
Min	0.15	0.36	0.41	0.52	
Max	0.52	0.87	0.81	0.89	
Wilting capacity – compacted					
Mean	0.35	0.50	0.49	0.58	0.48
Min	0.18	0.22	0.32	0.39	
Max	0.53	0.70	0.68	0.79	
Field capacity					
Mean	0.17	0.28	0.42	0.54	0.35
Min	0.13	0.09	0.07	0.08	
Max	0.22	0.70	0.71	0.85	
Field capacity – compacted					
Mean	0.12	0.13	0.23	0.40	0.22
Min	0.03	0.04	0.04	0.06	
Max	0.30	0.34	0.58	0.49	

Table 2-2: Average normal incidence absorption coefficients of test substrates. Source: Connelly, M., & Hodgson, M. (2015). Experimental investigation of the sound absorption characteristics of vegetated roofs.

2.5 Constructability of soil embankments

The construction of embankments is intended to be materialized exclusively by ground materials. Further addition of reinforcing materials is considered, but only up to a limited amount of necessary support structures. This option will lead to much more sustainable and economically favorable configurations, since it has less installation requirements and environmental impact compared to technologically advanced noise reduction methods, such as concrete or glass-based sound barriers. Moreover, the use of natural materials and vegetation for blocking and absorbing noise contributes to the creation of greenery zones within urban areas, which are pleasant to the inhabitants and is shown by researchers to add value with the positive psychoacoustics and masking effect (Hao, 2014) of natural environment areas at noise affected residential spaces.

In order to achieve this, prior to testing design concepts is the study on constructability, limitations and usability of the embankments. After all, dealing with the low frequencies and lengthy paths of aircraft flyovers involves large configurations and extended ground coverage that make it difficult to develop property. Search around the soil reinforcement industry showed that the construction of soil embankments is handled differently among various companies and technical details are dependent on the site, existing soil types and custom requirements. Nevertheless, a specific company named Strata Systems (Geogrid, 2020) explores the limits of reinforced slopes and supplies free of charge some of the technical solutions on their website. This information is not required to be followed precisely, nor to be trusted for varying site cases, but give a useful impression on how to tackle geometry and stabilization.

2.5.1 Soil stabilization

One of the first questions encountered regarding soil slopes was the feasibility of steep angles, alongside top geometry and erosion control. Strata categorizes slopes in 45^0 tilt from the horizontal and flatter or steeper than 45^0 (Figure 2.21). Cases where the slope angle is steeper than 70^0 are considered to be solved as retaining walls. Embankments are preferred when weak soils exist underneath and a foundation fill is required to form a structural base to build over.

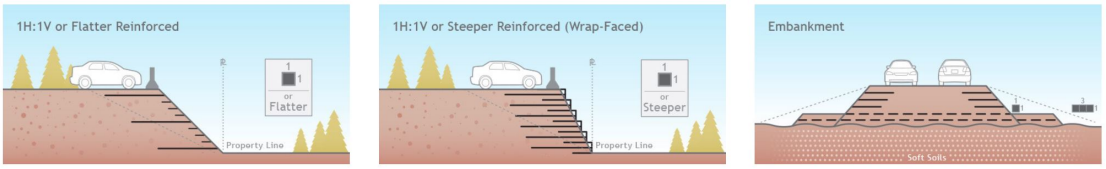

Fig. 2.21: Types of slopes, categorized by Strata.
From left to right: 1:1 or flatter, 1:1 or steeper, embankment.
Source: Derived from Geogrid.com. (2020). Reinforced Steep Slopes. [online] Available at: <https://www.geogrid.com/en-us/applications/reinforced-steep-slopes> [Accessed 18 May 2020].

In order to evaluate the stability of slopes, computer software is available to determine the safety factor of soil constructions. This geological software is used to calculate the forces within the whole volume, as well as several failures types of its surfaces. Subsequently, a reinforcement structure consisting of primary and secondary geogrids is optimized for safety and economics by analyzing the tensile strength of the structure. Each part has to be analyzed for failures individually and improved until the necessary stability factor is achieved. According to Strata systems (Geogrid, 2020), the slope stability is defined by three main failure rules, as shown in the Figure below. The internal failure refers to surfaces existing within the reinforced soil zone. The second, compound failure, happens outside the reinforced zone, but affect the foundation or outer face of construction and third is the global failure, which concerns deep surfaces that are not reinforced and pass through the core foundation soils.

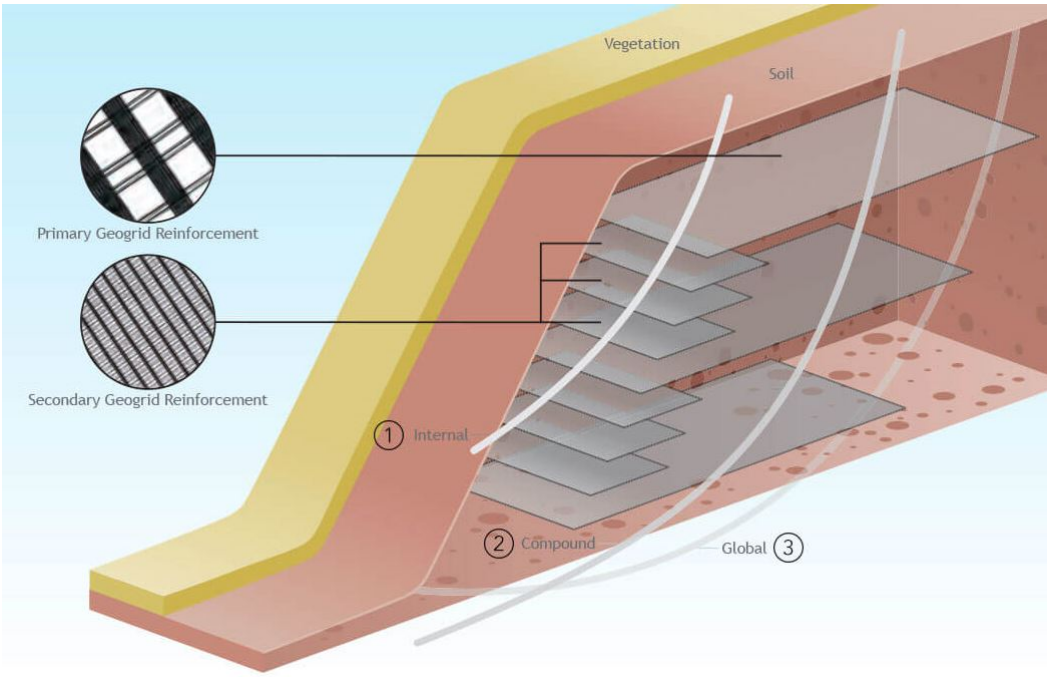

Fig. 2.22: Three failure regimes that are commonly examined in a soil stability analysis.
Source: Derived from Geogrid.com. (2020). Reinforced Steep Slopes. [online] Available at: <https://www.geogrid.com/en-us/applications/reinforced-steep-slopes> [Accessed 18 May 2020].

After installing the main structure and reinforcement grids, surface erosion becomes the main stability issue of the outer surface. This is commonly controlled by covering the surface with temporary erosion control blankets, which can be 100% bio-degradable and their main function is to prevent soil erosion in steep surfaces due to rainwater or wind. In addition, blankets help in sowing seeds on the surface until vegetation grows and roots are established. Straw and coconut are mainly used as fibers to construct nets in rolls forms that are easily laid down on slopes and can be functional for up to 36 months (Titan Environmental Containment Ltd., 2020) depending on environmental conditions. After they slowly degrade into the soil construction, it is checked whether new blankets should be added or the slope has reached the expected stability with the help of plant growth. The placement of blankets help as well in anchoring the top of slopes by extending their reach and creating a flat cap on top.

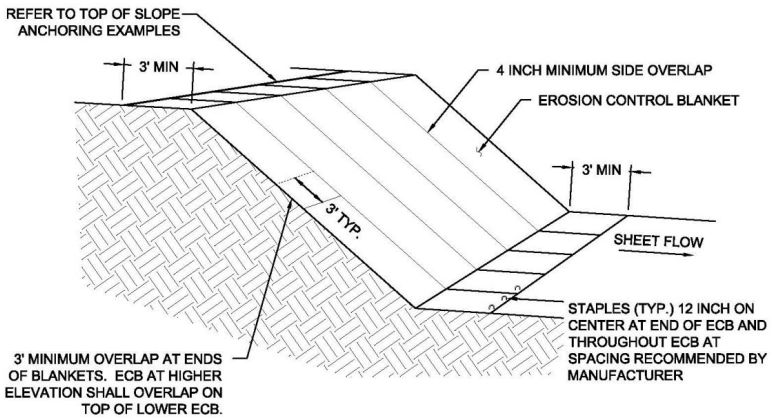

Fig. 2.23: Isometric view of erosion control blankets installation.
Source: Derived from Erosion Control Blankets - Titan Environmental Containment Ltd. (2020).

2.5.2 Facing options

i. Vegetation

Depending on the location of slope installation, it is possible to take advantage of rainfall or irrigation to create vegetation. Apart from providing the most economical facing solution, addition of vegetation contributes to the further stabilization of surface soil, when the roots of plants are established in the ground. The greenery sloped view also adds to the pleasant aesthetics of the construction, which is essential to the inhabitants around it. But most importantly, low vegetation provides a sound engineered solution that further improves the absorption performance of the outer surface by a small amount (Maleki et al., 2011). Naturally, adding of vegetation can be achieved in close to vertical surfaces. However, the steeper the structure, the less plant species are appropriate for cultivation and irrigation becomes more critical.

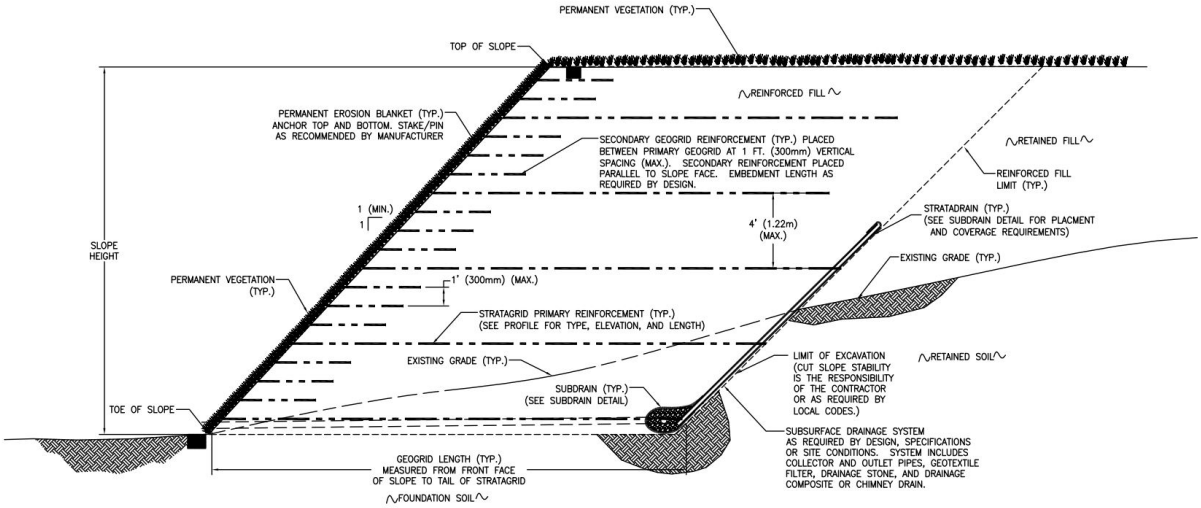

Fig. 2.24: Reinforced soil slope – Typical cross section – 1:1 or flatter.
Source: Designed and drawn by RLC (2010). Geogrid.com. (2020). CAD Drawings-Sheet 8 - Geogrid. [online] Available at: <https://www.geogrid.com/en-us/cad-drawings> [Accessed 18 May 2020].

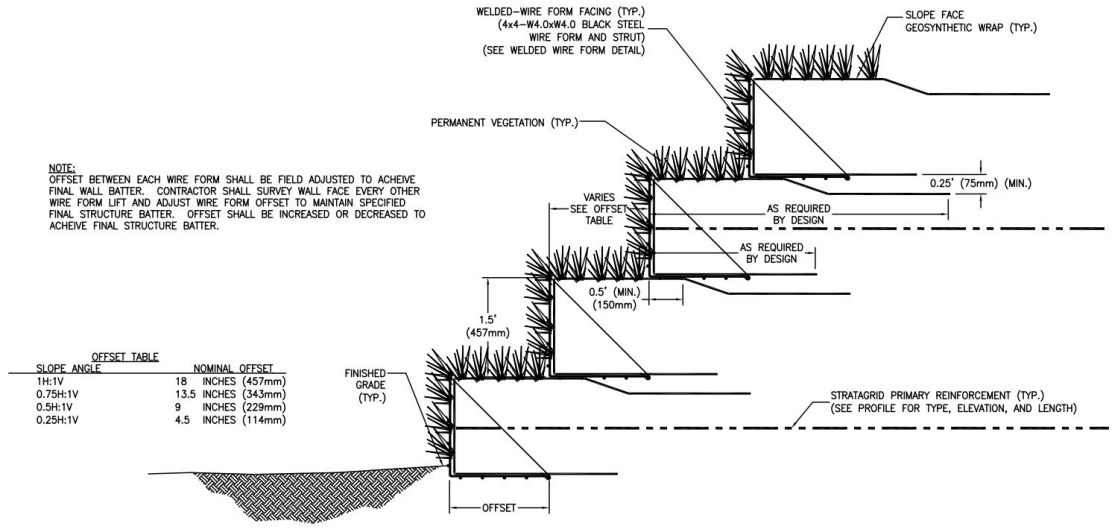

Fig. 2.25: Reinforced soil slope – Vegetated facing detail – 1:1 or steeper.
Source: Designed and drawn by RLC (2010). Geogrid.com. (2020). CAD Drawings-Sheet 7 - Geogrid. [online] Available at: <https://www.geogrid.com/en-us/cad-drawings> [Accessed 18 May 2020].

ii. Rock fill

In steeper than 45 degrees slopes and in situations where vegetation is not recommended, it is possible to achieve slope stability by stone-facing methods. This utilizes the addition of black steel welded-wire forms and crushed stone filling. Nevertheless, this option is excluded from the design selection, since rocks provide a very hard surface for shielding and compose a reflective component against aircraft noise, when the intention of embankment barriers installation in this research aims to absorb part of the noise that reaches the surroundings.

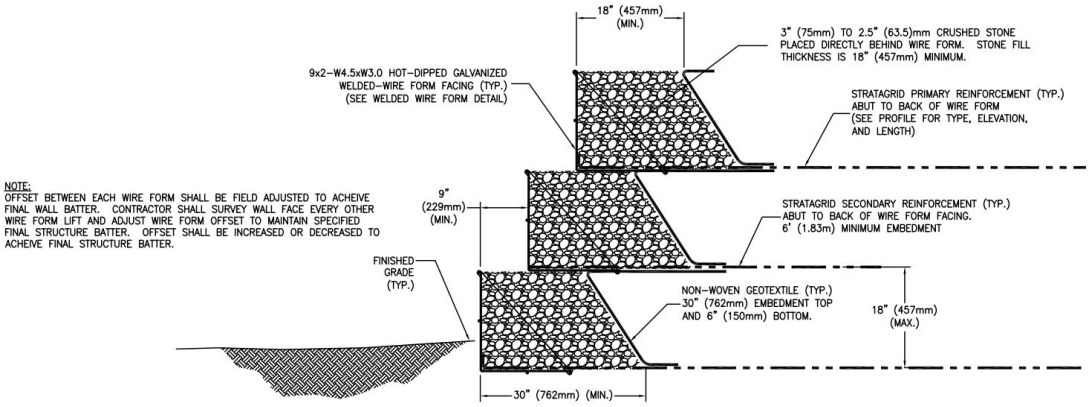

Fig. 2.26: Reinforced soil slope – Rock filled facing detail – 1:1 or steeper.
Source: Designed and drawn by RLC (2010). Geogrid.com. (2020). CAD Drawings-Sheet 7 - Geogrid. [online] Available at: <https://www.geogrid.com/en-us/cad-drawings> [Accessed 18 May 2020].

2.5.3 Advantages & constraints

According to Strata (2020), "*the construction of reinforced slopes with these methods has the following advantages:*

- *Significant cost savings compared to steel-reinforced concrete structures*
- *Tolerant of total or differential settlement*
- *Multiple facing solutions including vegetation and rock fill*
- *Fast Installation (1,000 to 1,500 sf/day)*
- *Environmentally friendly*
- *Minimal impact on environmental areas (i.e. wetlands, natural habitats)*
- *Excellent structural capacity (i.e. 70º reinforced slopes exceeding 25m vertical height)*
- *Utilize on-site fill or minimize borrow requirements."*

3 Research chapters

3.1 Research workflow

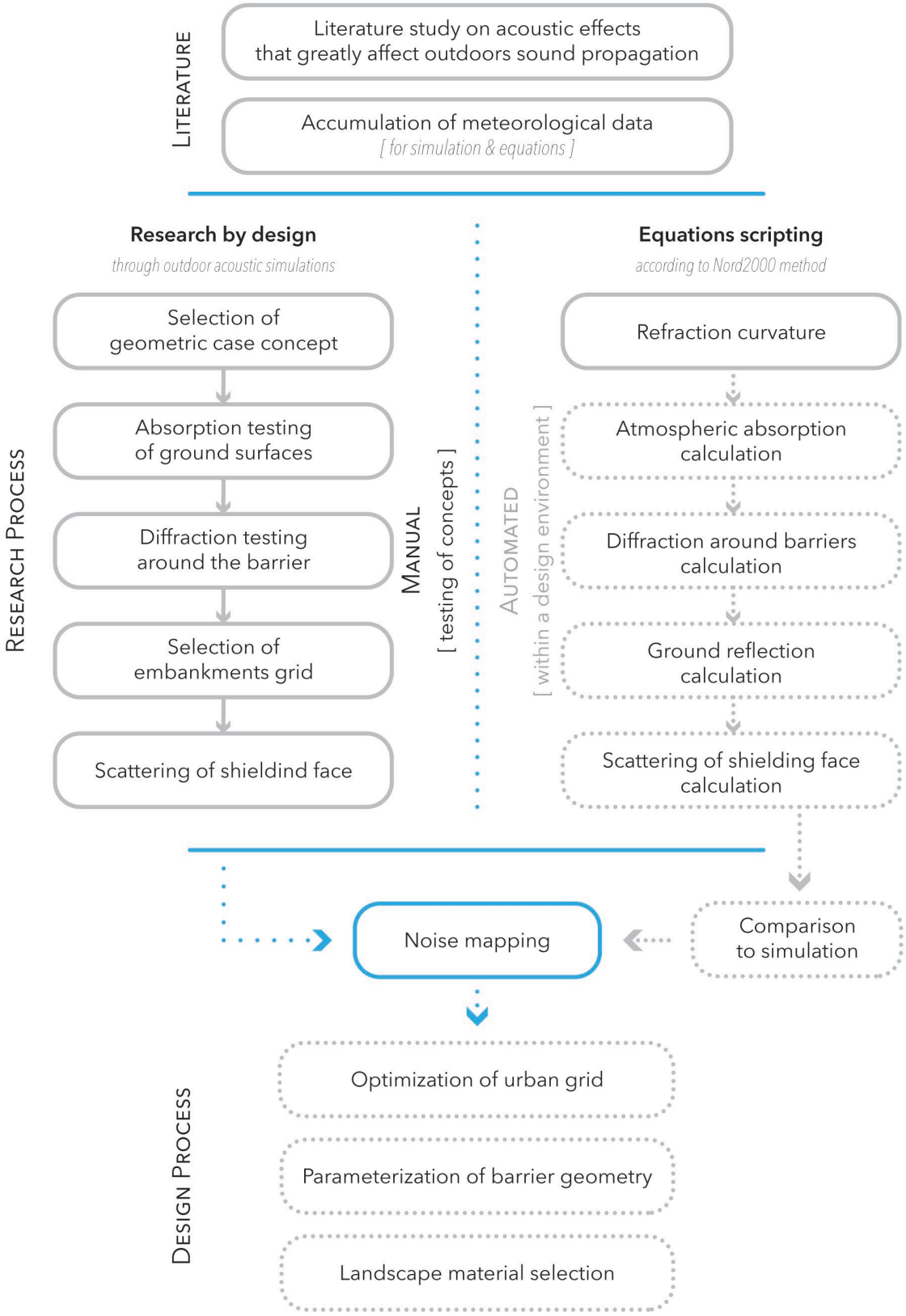

This chapter includes the research process steps followed during the urban acoustics study. The initial concept was to conclude to an automated process that can handle various geometries of embankment barriers and later optimize their acoustical performance in order to generate shielded outdoor areas against aircraft noise. Unfortunately, it was realized that the existing analysis software embedded within the parametric design environment of Rhino 3D could not yet manage to succeed in air traffic cases, so that a fully integrated process within design software was not achievable with the selected tools. Therefore, an alternative way was chosen as more appropriate to come to a workflow that resembles an acoustic analysis.

First of all, this alternative option requires a study on the most important factors that affect sound propagation over large distances of sources much higher above ground than usually studied in street traffic cases, as found in the literature chapters. In addition, meteorological data of the study location are gathered, as they compose the input of the acoustic equations. Afterwards, it is possible to include the equations that describe these phenomena with the use of a scripting language and Grasshopper components. Effects like atmospheric refraction, absorption, diffraction and ground reflection greatly affect aircraft noise propagation and should be part of this urban acoustics study. When the whole process is properly simulated this way, the designer can utilize parametric tools to generate varying concepts that meet the acoustical requirements and have a better estimation of the design's performance, as complex as it can be. Nevertheless, the precision of the script has to be evaluated beforehand with comparisons to simulation software, so that the expected level of accuracy is known.

During this research, it was proven that an informed script was difficult to be completed over the given time period, since each specific atmospheric effect requires further attention and testing on its own. The study of refraction curvature became the focus of the equation scripting process in an attempt to initiate an acoustic analysis script and predict the curvature of soundwaves motion until reaching the study site. The Nord2000 way of simulating the refraction effect is presented later in the chapter, along with the transfer of its equations into a Python script. The script is then used to analyze different results for winter and summer periods and determine the importance of the effect for the specified location. However, the predictions depend on the accuracy of Nord2000 simulation, so other effects should be gradually included until a comparison to noise maps from other acoustics software can be realized.

In parallel to the scripting process, a second manual process is conducted with more focus on the study of landscape elements and the behavior of primary geometric parameters. Although limited to the design ideas that are put into testing, iNoise software, which utilizes the Harmonoise method, was used to export noise maps of the area with the addition of embankment configuration against the flight path. The inclination, height and array of elements are examined and discussed on their potential to provide efficient solutions. Lastly, an addition of scattering geometries against the lower frequency range to the shielding façades is explored and tested through Pachyderm acoustics software. Although the scattering concept concerns a more detailed approach, it is recommended to research on methods to further mitigate the reflected noise that is not fully absorbed by atmosphere and the material coverage of the landscape configurations. After noise mapping is complete, the designer can choose between concepts, optimize the urban grid and finalize the construction according to the predictions.

3.2 Meteorological data

3.2.1 Accumulation & sources

As it is understood from the equations [2.18, 2.19], in order to find the incidence angle Δθ and vertical sound speed profile c(z), source and receiver positions, temperature and wind component values are necessary to perform the calculations. The position and height of source and receiver can already be described through the flight tracking website of Schiphol that provides data regarding flight route, height and speed of each aircraft (Flighttracking.casper.aero, 2020). Thus, the meteorological data on ground level (receiver position) and at source height (aircraft flight path) should consequently be gathered.

Climate Consultant (Figure 3.1) is an application that provides various information including temperature, humidity, wind speed and direction through daily/monthly mean values for a specified location at 10m above ground. In this case, weather data file around Amsterdam Schiphol airport was selected.

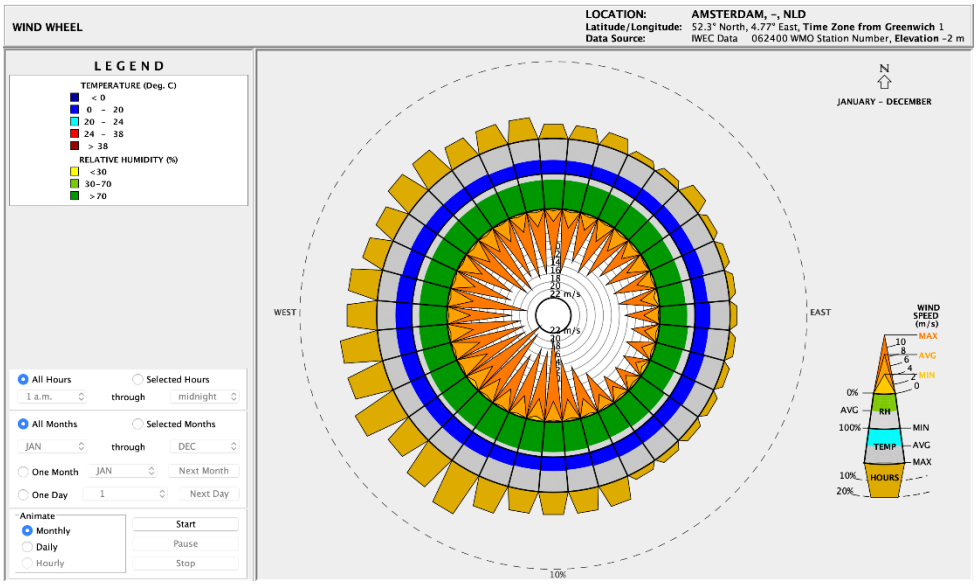

Fig. 3.1: Weather data for Amsterdam location from Climate Consultant 6.0. Temperature, humidity and wind profiles on ground level are illustrated in a wind wheel.

In order to describe temperature as a gradient, values at an altitude have to be found. In the troposphere, which runs from the ground surface until 11.000 meters height, the temperature decreases linearly and the pressure decreases exponentially (Grc.nasa.gov, 2020). The rate of temperature decrease is called the lapse rate. For the different temperature T_h (^{0}C) at a height h (m), the value within the troposphere during day is calculated by:

$$T_h = T - 0.00649*h \qquad [3.1]$$

There are more complicated ways to calculate this difference, but the mentioned equation is developed from atmospheric measurements that were averaged to provide an approximation curve. Since temperature gradients have less significance in influencing sound speed as wind does, this method is preferred when temperature data at an altitude is missing.

As for wind gradients, the most reliable way to gather data is real-time measurements along the height. Fluctuations due to turbulence and direction changes in the atmosphere make prediction through simplified linear equations unreliable. Such measurements are accessible through a University of Wyoming website for half-day time periods (Weather.uwyo.edu, 2020). However, measurements for various locations are limited to country data or have to be obtained from earlier years. For the Netherlands in specific, the weather station at De Bilt (06260), which is located outside of Utrecht at around 35km away from Rijsenhout, is used for observations, but no data are present for years back until 2015. Earlier than that, information is incomplete for various days and cannot be extracted reliably to collect averages. Fortunately, 2012 weather recordings are fully described for De Bilt station and these were extracted as the input for the calculation of refraction. Since weather changes cycle through each year, averaged and peak values would provide reliable information, even if it is collected from past years. Finally, values of atmospheric pressure, temperature, humidity and wind component can be acquired from this source (Table 3-1).

PRES	HGHT	TEMP	DWPT	RELH	MIXR	DRCT	SKNT	THTA	THTE	THTV
hPa	m	C	C	%	g/kg	deg	knot	K	K	K
1008.0	4	10.6	9.3	92	7.34	230	10	283.1	303.5	284.4
1000.0	71	10.0	8.9	93	7.20	230	12	283.1	303.2	284.4
967.0	350	8.2	8.1	99	7.05	241	24	284.1	303.8	285.3
940.0	584	7.3	6.8	96	6.62	250	34	285.5	304.1	286.6
925.0	717	6.8	6.0	95	6.38	255	29	286.3	304.3	287.4
882.0	1107	4.6	4.6	100	6.06	261	26	287.9	305.2	288.9
850.0	1409	4.6	2.1	84	5.27	265	23	290.9	306.3	291.9
836.0	1545	5.0	0.1	71	4.63	256	27	292.8	306.5	293.6
834.0	1564	5.5	-4.1	50	3.41	255	27	293.5	303.8	294.1
830.0	1604	6.6	-12.4	24	1.79	257	27	295.1	300.7	295.4
829.0	1614	6.8	-11.2	26	1.97	257	27	295.4	301.5	295.7

Table 3-1: 06260 EHDB De Bilt Observations at 00Z 01 Jan 2012.
Source: Weather.uwyo.edu. (2020). Atmospheric Soundings. [online] Available at: http://weather.uwyo.edu/upperair/sounding.html [Accessed 21 Jan. 2020].

3.2.2 Meteorological data input

Climate data is obtained from the weather recordings made at De Bilt weather station in 2012 (Weather.uwyo.edu, 2020). The interest of this study is on the situation during daylight, as nighttime flights are much more limited and restricted to a minimum by Schiphol's flight schedule regulations. For this reason, only the tables at 12Z (midday) were collected. In order to represent two opposite conditions, a winter and a summer month are examined. Subsequently, values are to be averaged for a winter and summer day, so that two tables are constructed and imported in the scripting workflow.

The measurements start from 4m height and reach up to 20km observations. Apart from the ground level, the rest of the height positions differ for each day, so prior to making a monthly average, each day's measurements are translated to values at distinct positions (Table 3-2). These positions were picked at the same heights at which the flight path was observed and constructed for consistency.

	Measured values					Mean values			
2012 / JAN / 12Z	HGHT [m]	TEMP [C]	W DRCT [deg]	W SPD [m/s]		HGHT [m]	TEMP [C]	W DRCT [deg]	W SPD [m/s]
1st	**4**	11,6	230	5,1		**4**	11,6	230	5,1
	71	11	230	6,2		**500**	8,7	238	10,4
	700	7,6	241	12,3		**625**	8,0	240	11,6
	718	7,6	250	17,5		**750**	7,4	251	17,0
	897	6,7	255	14,9		**875**	6,8	254	15,2
	1411	4	261	13,4		**1000**	6,2	256	14,6

Table 3-2: Table of translated values for De Bilt observations at 12Z (midday) 01 January 2012.

Following to that, the mean values for a whole month can be estimated in order to represent a typical day condition. The final tables were constructed until 1km altitude in relation to the segment of the flight path that mostly influences the specified study site. If it is required, more height data can be added, so that the refraction script can properly adapt to varying cases. Finally, conditions for a January and a July midday were exported to Table 3-3 and will then be inputted in the parametric environment, as text panels connected to the Python script component.

	January					July			
2012 / 12Z	HGHT [m]	TEMP [C]	W DRCT [deg]	W SPD [m/s]		HGHT [m]	TEMP [C]	W DRCT [deg]	W SPD [m/s]
	4	6,0	219	5,1		**4**	19,6	212	4,1
	500	2,8	238	12,3		**500**	14,1	218	6,8
	625	2,2	241	13,2		**625**	13,0	224	7,1
	750	1,4	238	14,0		**750**	12,1	232	7,3
	875	0,7	232	14,2		**875**	11,2	234	7,6
	1000	0,0	232	14,5		**1000**	10,2	231	7,8

Table 3-3: Mean values for De Bilt observations at 12Z for January and July.

3.3 Refraction curvature analysis

3.3.1 Flight path import

The first information that must be imported as input in the scripting process is the flight case that is the closest and most dominant above a study site. Many airports around the world provide the necessary flight tracking information and should be easy to access online. Specifically, live location and height position is extracted in this case to form the flight curvature.

In order to predict the aircraft positioning around Rijsenhout while on flight, take-offs from Kaagbaan runway heading southwest were observed. The live flight tracking website provided by Schiphol (Flighttracking.casper.aero, 2020) reveals the paths that each aircraft is following, along with their speed at specific height positions (Figure 3.2). The information panel updates every rise of 125m in altitude. A random aircraft taking-off during afternoon was followed and the extracted data were then assigned upon the mean path of this route.

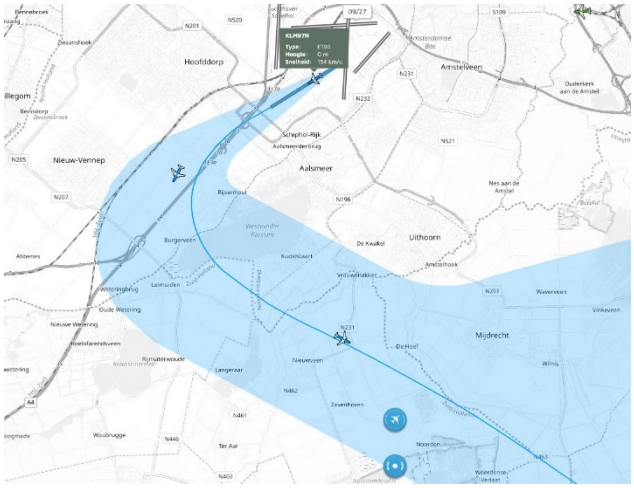

Fig. 3.2: Deviation of flight routes from main guide path. Source: Schiphol – Flight tracking (2020). [online] Flighttracking.casper.aero.

This way, the construction of the curvature in the 3D environment was easy to maintain through the construction of points at the observed locations. In Figure 3.3, the aircraft is illustrated taking-off at point 0, making its turn at points 5 to 8, and continuing southwest. The constructed curved path can subsequently be used to observe the most dominant noise source positions for varying cases at the analysis stage.

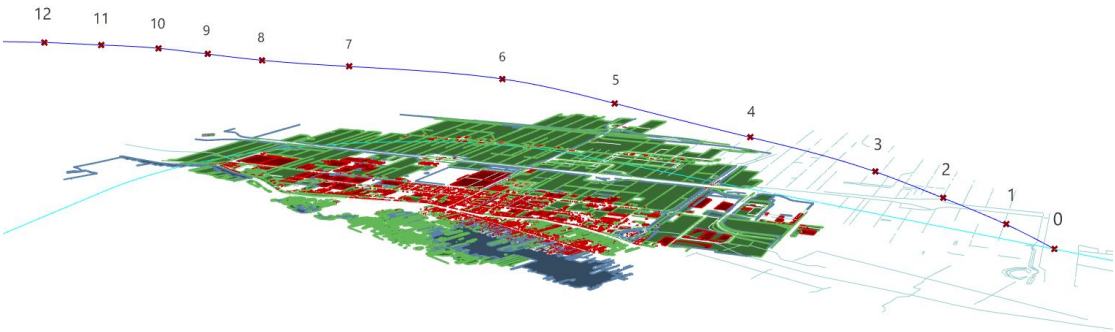

Fig. 3.3: Perspective view of Rijsenhout area from east and the constructed flight path (blue line) within Rhino software.

3.3.2 Refraction equations scripting

The process of determining the vertical angle Δθ in relation to a straight propagation path begins with the assignment of a receiver point, which is picked as a point on the study site. This point will later be the center of construction for reflecting barriers. Following this, Grasshopper components extract the necessary data for the equations, such as the closest source point on flight path, horizontal distance (d) and source height. In addition, temperature (tS, tR) and wind speed at the direction of propagation (uS, uR) are averaged to find the values at source (zS) and receiver height (zR). Subsequently, the python scripting is able to calculate the vertical speed of sound gradient ξ and finally Δθ. The equations used are listed below (Figure 3.4):

** [**m** .] is used in the script to recall a function from a syntax of mathematical modules*

Eq. [2.1]

Eq. [4.16]
Roughness length [z0] = 0.1 for low crops

Eq. [4.17]

Speed of sound at ground level

Eq. [4.15]

Eq. [4.4]

Eq. [4.3]
Eq. [4.5]
Eq. [4.6]

Eq. [4.14]

Δθ sign correction when ξ is negative

```
# Speed of sound at the ground surface
# for temperature at ground level
g = 1.4
R = 286
T = 273.15 + tS
c0 = m.sqrt(g*R*T)

# logarithmic part A
A = uS / m.log((zS/z0) + 1)

# linear part B
dz = zS - zR
dt = tS - tR
B = (dt*10.025)/(dz*m.sqrt(tS + 273.15))

# part C
C = c0

## Equivalent sound speed profile
cS = A*m.log((zS/z0) + 1) + B*zS + C

# ξ , ψR, dm
cR = c0 + uR
Δc = cS - cR
Δz = zS - zR

ξ = (Δc/Δz)/c0
tanψR = (ξ*d)/2 + (Δz*(2 + ξ*Δz))/(2*d)
ψR = m.degrees(m.atan(tanψR))
dm = tanψR/ξ

# Δθ
Δθ = ψR - m.degrees(m.atan(Δz/d))

# Δθ sign correction
if cR < cS:
    Δθ = gh.Absolute(Δθ)
if cR > cS:
    Δθ = (-1)*gh.Absolute(Δθ)
```

Fig. 3.4: Python script developed to import refraction equations.

3.3.3 Results

i. On study site

At first, the calculations were performed to analyze the difference in incident angle for various locations of the study site. Comparison between the resulted Δθ values would suggest whether it would be reasonable to repeat the calculations for multiple points of the same site. In addition, winter and summer Δθ values are compared and the refraction effect is described as downward (+) or upward (-) due to climate data. It should be noted that the site has an area of 42.000 m² and a diagonal distance of 330m.

Position	Distance to source [m]	Incident angle (straight path) [deg]	Winter	Summer
			Δθ [deg]	
1	**1800**	17,9	-0,2	-1,1
2	**1644**	19,6	-0,2	-1,0
3	**1694**	19,4	-0,1	-1,0
4	**1953**	16,5	-0,2	-1,2
5	**1909**	16,6	-0,2	-1,2

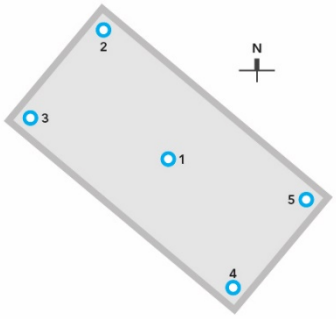

Table 3-4: Difference in angle Δθ due to refraction for winter and summer days at different positions on site.

As can be derived from Table 3.4, both for summer and winter day the effect is upward refraction. This can be justified by the fact that wind has a large effect on refraction and the wind speed component moving opposite to the direction of sound propagation. The difference in winter values is limited to 0.1 with an average Δθ of -0.2° at the center point. Similar is the range of 0.2 for summer and an average of -1.1°. The variation of less than half a degree in the resulting angles even for the maximum distance of this area should be stated as insignificant. In that case, computing only the refraction effect for the centroid of an area is accurate enough. On the other hand, wind speed against the propagation direction was observed higher for summer, thus creating an increase of 1° to the refraction curvature. This variation is again considered minimal for the purpose of designing acoustical elements, but an investigation is suggested for different cases, since propagation path and wind direction may not match similarly for other sites. In conclusion, it can be said that the specified site is slightly influenced on the incident angle of the most dominant (closest) aircraft noise position. The fact is that wind direction is almost perpendicular to the examined propagation path, so effects of sideways curvature on propagation should be investigated in a future research.

ii. On multiple sites

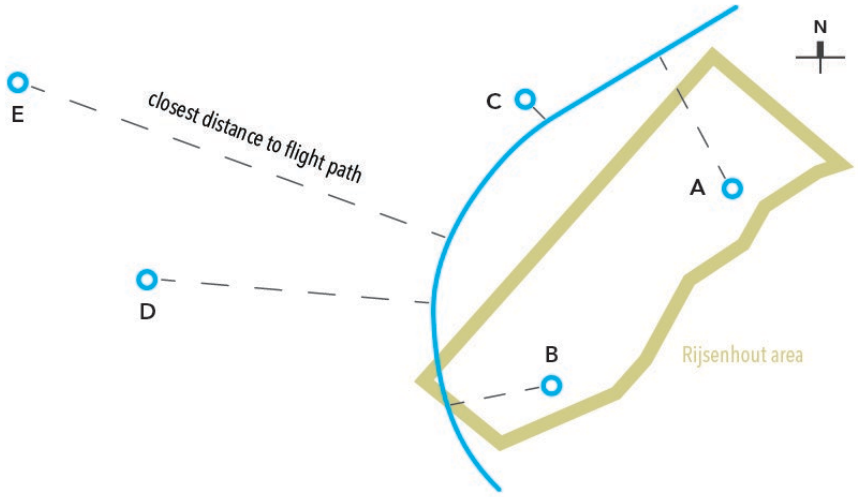

Fig. 3.5: Site position of 5 random locations in relation to Rijsenhout area.

In order to have a better understanding of distance and heights, more cases were added to the calculation (Table 3-5). Five sites were picked inside or outside the residential areas. A is the case study site of this research, B is closer to the flight turn, C almost below, D and E further away from the flight path.

Site	Distance to source [m]	Source height [m]	Incident angle (straight path) [deg]	Winter	Summer
				Δθ [deg]	
A	**1800**	**559**	17,9	-0,2	-1,1
B	**1670**	**995**	36,3	0,6	-0,2
C	**759**	**677**	62	-0,2	-0,2
D	**3346**	**860**	14,8	-3,6	-3,0
E	**5202**	**806**	8,8	-5,3	-4,5

Table 3-5: Difference in angle Δθ due to refraction for winter and summer days at five different site locations around Rijsenhout.

It is observed that in most cases wind component moves from southwest, opposite to propagation paths, thus causing downward refraction effect. Wind direction is more aligned for case B, where an upward refraction is noted for winter. However, due to higher summer temperature on ground and larger height difference from source, speed of sound at receiver was computed higher than at source, leading to a downward refraction. In general terms, it can be said that the values are insignificant for sites A, B and C. On the other hand, sites D and E have more noticeable results up to 5° difference downwards. This justifies the fact that as the distance between aircraft and receiver increases, atmospheric effects become more pronounced (Lugten, 2018). Nevertheless, the results disagree with what is found by Arntzen and Simons (2014), who show that refraction becomes important when the angle of incidence is greater than 15°. This does not entirely disapproves the results, as in most cases wind direction and propagation path do not align and results may be underestimated in the specific study location.

3.4 Acoustic analysis of ground barrier cases

In the following sections, the acoustic analysis of several testing parameters regarding the inclination, materialization and volume of shielding elements in iNoise software is described. Since an automated approach to examine geometry parametrically is not yet accomplished with the selected tools and software, a manual testing of variables becomes the first stage towards understanding the behavior of shielding elements. What this method attempts to achieve is a gradual confirmation of ground coverage materials and volumetric parameters, regarding the sound effects encountered during noise propagation close to the configurations. Effects such as absorption, reflection, scattering and diffraction are tested through changes in the geometry of embankments, in order to conclude to a volume that provides better results.

At first, the surface of the volume and then the ground surrounding it are tested for their absorption capabilities. Later, the angle and height of the shielding face are examined for the noise shadow output they generate at the outdoor spaces behind. The angle of the back façade and top corner are also tested as they contribute to the diffraction effect. Subsequently, a number of principal urban grids are observed for the amount of shielded spaces they provide, when the embankments are placed within them. Lastly, a concept of scattering the reflected low frequency noise is added to the front shield and scattering coefficients are presented.

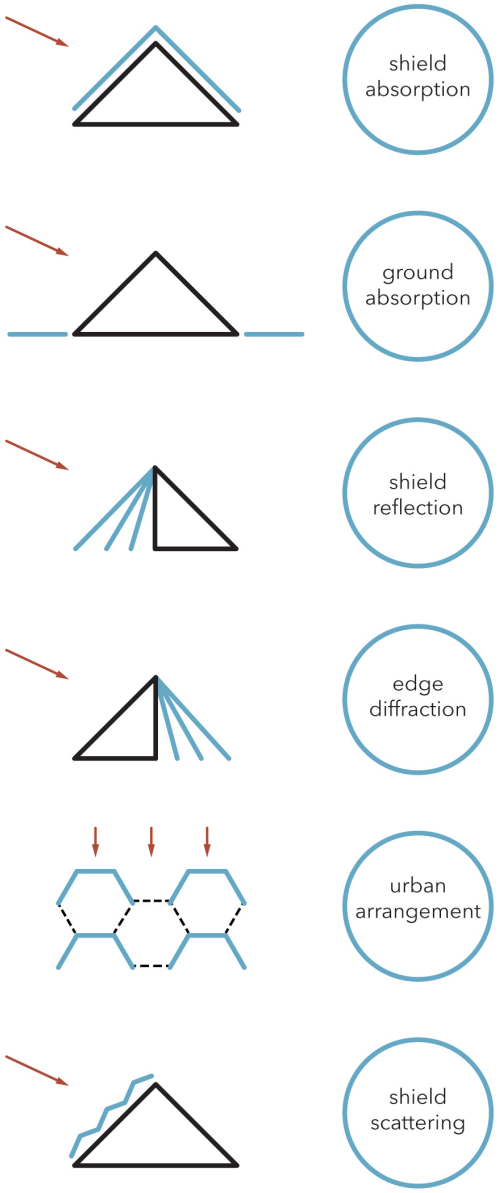

Fig. 3.6: Steps followed for examining the acoustic behavior of the shielding configurations.

3.4.1 Simulation set-up

The acoustic simulations that follow were performed in the free version of iNoise software. This software provides three calculation methods that form noise maps, ISO-9613 ½, ISO-9613 ½ (1/3 octave) or Harmonoise method. The last one was selected for all simulations as it is more informed of the effect of atmospheric parameters and works similarly to the Nord2000 method, as explained in the literature chapters. However, it does not provide results for the individual frequency ranges or the level at which each different effect, such as ground reflection and atmospheric absorption contributes to calculated sound levels, in contrast to the ISO method. Following calculation, it provides noise maps with the total sound attenuation for a specified grid of points that are presented through a top view, a cross section cut or a 3D view.

Regarding the calculation settings, the average meteorological values of winter found in literature (Table 3-3) were the input as follows in the Figure below. The software only asks for ground level measurements, while wind speed and cloud coverage are determined by simplified classes that can be found in the Harmonoise technical report appendices (Nota et al., 2005).

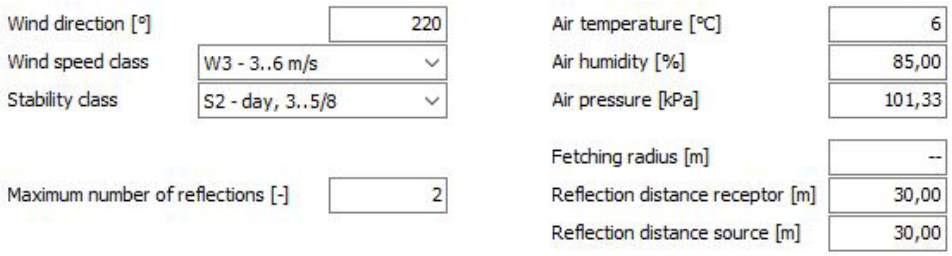

Fig. 3.7: iNoise calculation settings used for simulations.

Furthermore, the user has to specify the default ground properties of the calculation grid area that is not specified individually through objects from the design input of the analysis. Various impedance classes are provided by the method as defaults (Table 3-6). Based on a global description of the ground surface properties:

Class	Description	Representative flow resistivity σ [kNsm^{-4}]
A	Very soft (snow or moss-like)	12,5
B	Soft forest floor ground (short, dense heather-like or thick moss)	31,5
C	Uncompacted, loose ground (turf, grass, loose soil)	80
D	Normal uncompacted ground (forest floors, pasture fields)	200
E	Compacted field and gravel (compacted lawns, park area)	500
F	Compacted dense ground (gravel road, parking lot)	2000
G	Hard ground	20000
H	Hard surface (dense asphalt, concrete, water)	200000

Table 3-6: Flow resistivity of ground surfaces, as described by the Harmonoise method (Delta, 2006).

By analyzing the field of the studied case and due to the research focus on unbuilt city environments, class E that describes compacted field and gravel was preferred as a general description of the analysis area. Each class comes with certain impedance values

for frequencies between 63 and 8000 Hz and are shown in Table 3-7. If it was for a denser part of Rijsenhout or a more populated built environment, classes that refer to compacted dense ground or asphalt would be a better choice.

Impedance classes	E - Compacted field and gravel(compacted lawns	[KNs/m4]	500,00

Z (real)	63	125	250	500	1000	2000	4000	8000
Low	52,36	31,54	19,16	11,80	7,42	4,82	3,27	2,35
Medium	44,19	26,68	16,27	10,08	6,40	4,21	2,91	2,14
High	37,32	22,60	13,84	8,64	5,54	3,70	2,61	1,95

Z (imaginary)	63	125	250	500	1000	2000	4000	8000
Low	64,28	38,75	23,36	14,09	8,49	5,12	3,09	1,86
Medium	54,30	32,74	19,74	11,90	7,17	4,33	2,61	1,57
High	45,87	27,66	16,67	10,05	6,06	3,65	2,20	1,33

Table 3-7: Default ground properties selected in iNoise calculation settings.

Finally, the location of the flight path is imported as a corresponding line in iNoise. Then, the segment of the path that is closer than 2km away from the center of the study site is selected as the most dominant aircraft noise source path for analysis. Within the acoustics software, the source can be defined as moving, although the maximum allowable velocity of 150 km/h doesn't reach the true aircraft source speed of 250 km/h that was noticed at the particular position. Subsequently, the power levels of the source are set in a way so that the produced noise level in front of the study area is close to 75 dB, according to the average peak levels recorded within the Rijsenhout area.

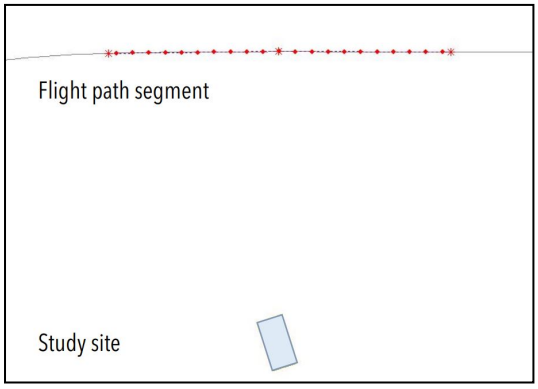

Fig. 3.8: Moving source position in relation to the study site. Top view of case study in iNoise.

Average velocity [km/h]	150	Length route segment [m]	2014,36
Distance between sources [m]	100,00	Number of point sources	21

Period	From	To	Flow	Cb [dB]
Day	07:00	19:00	500	15,74
Evening	19:00	23:00	500	10,97
Night	23:00	07:00	--	--
--	--	--	--	--

Table 3-9: Moving source properties, as imported in iNoise.

	63	125	250	500	1000	2000	4000	8000
Low	138,70	138,70	138,70	138,70	138,70	138,70	138,70	138,70
Medium	138,70	138,70	138,70	138,70	138,70	138,70	138,70	138,70
High	138,70	138,70	138,70	138,70	138,70	138,70	138,70	138,70
							Lw [dB(A)]	152,50

Table 3-8: Noise source emission levels, as imported in iNoise.

3.4.2 Soil types

The ground impedance of the overall configuration element was selected as a first case for examination. The flow resistivity σ of the different ground impedance classes comes with certain absorption coefficients, with soft uncompacted surfaces showing better results on the low frequency range. Four soil types of different compactness (B, C, D and E) and a hard concrete surface (H) provided by the Harmonoise method as presets (*see Table 3-6 above for class names, description and flow resistivity values) were compared and analyzed. The user is also able to define custom properties and simulate other types of soil with enhanced absorption coefficients.

3.4.3 Embankment configuration

The initial hypothesis for the geometry of ground embankments was that it should imitate the noise mitigation method of street traffic barriers. This means that a vertical wall volume would reflect noise back to the source it counters. However, within a living space environment, the vertical wall option would generate negative results due to the reflection of soundwaves close to ground and towards residential spaces in front. In addition, diffraction around the top edge should be taken into account, since an inclined sound barrier or a double edge capped volume, like a building, is found by literature to strengthen noise propagation behind barriers. Thus, an inclined shielding surface that reflects noise upwards and away from ground cover, but does not allow flow beyond the barrier would prove beneficial.

Several model cases were imported to iNoise software, in order to perform comparisons on the acoustical behavior of geometrical variations. These variations are selected in ways that urban acoustics are expected to improve or have significant results. As a rule, constructability tolerances for soil slope constructions are considered, so that a more feasible geometry is reached and verified within the urban acoustics software.

In accordance to how ground surfaces behave due to gravity, a low-polygonal pyramidal volume is designed to imitate a slope by soil constructions. The noise source-facing surface has a minimum size of 12m, according to the wavelength of the lowest frequency of interest, which is 30Hz with a wavelength of 11,3m. The 12 by 12 surface dimensions provide the necessary size for including scattering options of this frequency to the landscape element later, in addition to the sufficient specular reflection of the lower frequency range, which soil types cannot effectively absorb.

The initial volume was firstly oriented perpendicular to the most dominant source position to examine the maximum effect of the slopes in creating noise shadows at the flat ground beyond them. For the calculation settings, the default ground properties of the environment are set to impedance class E (compacted field and gravel) for compacted lawns or park area that is assumed to exist within an occupied urban block.

3.5 Absorption of ground surfaces

3.5.1 On shield barrier

The first simulation performed concerns the type of ground coverage of the soil embankments. Five typical ground cases were tested on a primitive pyramidal volume, in order to observe the changes to the shadow created beyond the barrier, as well as the peak sound levels of the waves reflected on the front of the shield.

It is noticed that the softer the ground coverage is, the better it performs as absorption. While the total area of mitigated noise remains the same for all cases, Ground B (forest floor) shows significant difference compared to ground H and E (concrete and compacted field) with more than 2dB additional reduction at the protected area close to the barrier. In addition, only surface B is able to prevent higher peak levels on the shielding face, thus, avoiding problematic specular reflections.

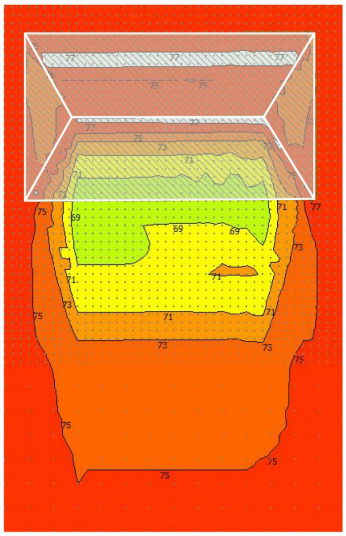

Ground surface H

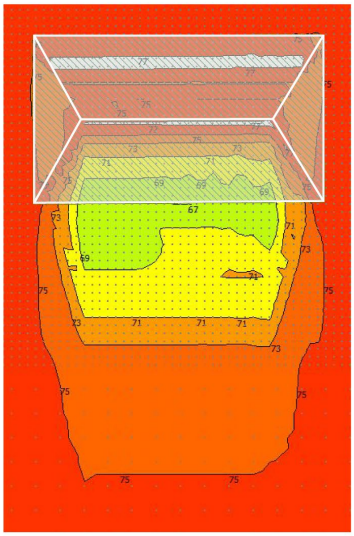

Ground surface E

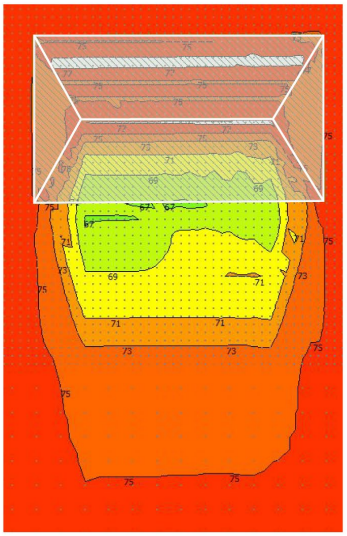

Ground surface D

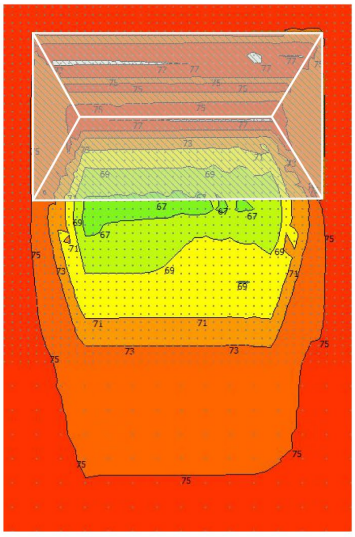

Ground surface C

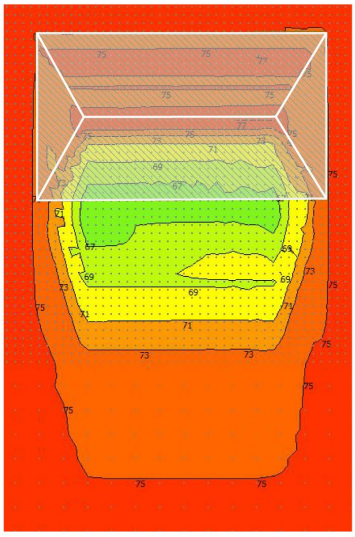

Ground surface B

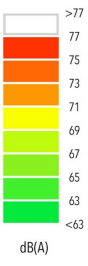

3.5.2 Beyond barrier

As a second test regarding ground coverage materials, the same five ground types were examined on how well they enhance the absorption of diffracted sound waves and ground reflections at the protected area behind the barrier (dashed area). The coverage of the pyramidal volume was selected as ground C (uncompacted loose soil) for all cases, since it is harder to assume a soft forest floor ground stabilized on inclined surfaces without the addition of support structures.

Similarly, the softer and more uncompacted the ground is, the more it improves the issue. It appears to slightly extend the area of absorbed noise by less than 2dB at areas where sound rays reach the flat ground. Nevertheless, the variation of soil at the ground beyond does not show as significant differences as before.

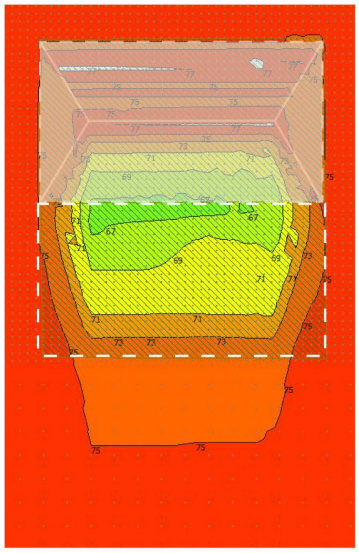

Ground surface H

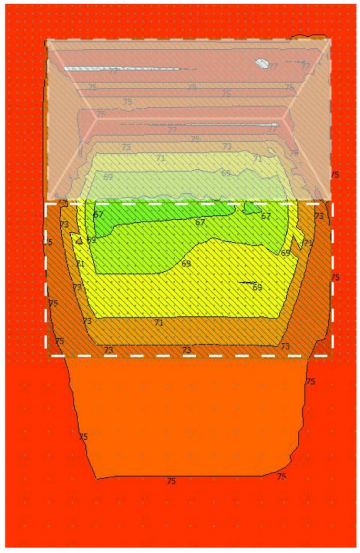

Ground surface E

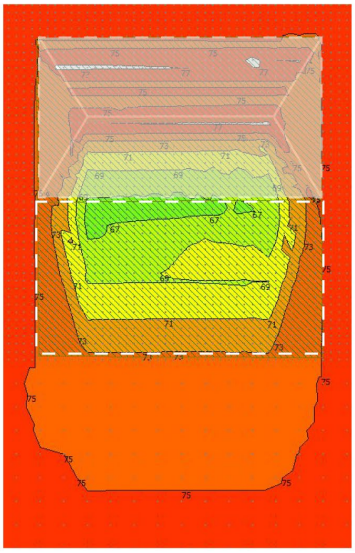

Ground surface D

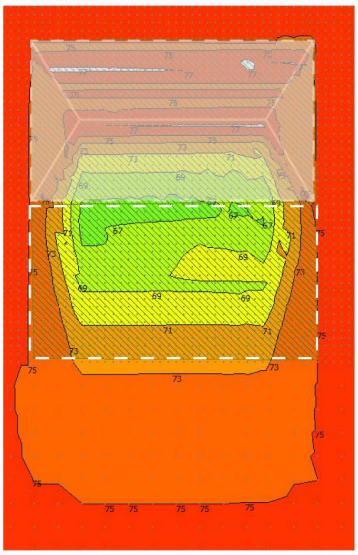

Ground surface C

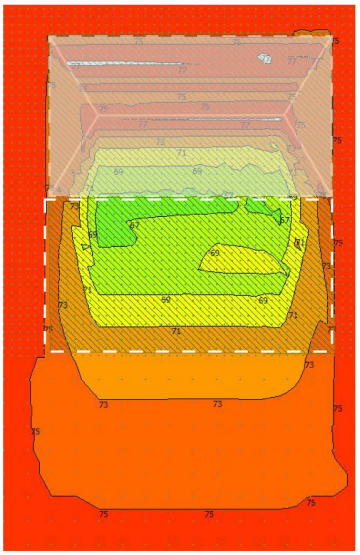

Ground surface B

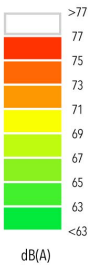

3.6 Diffraction around the barrier

3.6.1 Shielding façade

Alongside the concept of embankments as sound barriers comes the examination of how sound is diffracted and shielded due to the slope introduced. To perform this test, a surface of 12m width was rotated every 12 degrees. The height of embankments certainly affects the diffraction and shielding result, but it is reasonable to look at both parameters together, since a 12*12m surface is the period element necessary, as already mentioned, to later examine the scattering of frequencies down to 30Hz. The shielded face is considered vertical at this stage, in order to properly observe the effect of the front shield.

As illustrated below, slopes steeper than 45^0 show similar potential at achieving more than 10dB reduction. On the other hand, the steeper barrier generates a larger protected area as expected, but at the cost of height and a much less feasible soil construction. According to literature, slopes steeper than 70^0 should be solved as retaining walls and steeper than 45^0 need additional support elements. For constructability reasons, the case of 45^0 slope is considered effective enough for the time being.

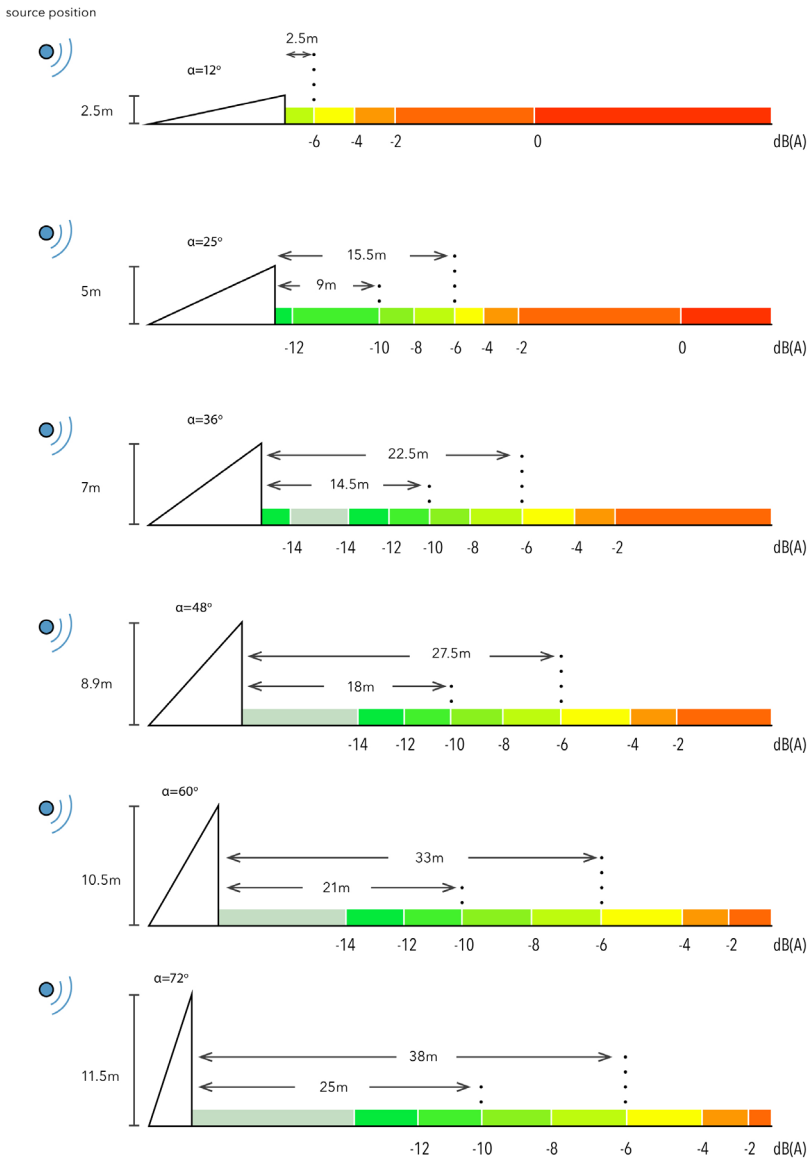

3.6.2 Shielded façade

From the previous stage of simulations, the test volumes of 36^0 and 48^0 slopes were further examined regarding the slope of their back façade, as more feasible concepts. Three options were tested, which correspond to three different scenarios. The vertical façade symbolizes a green wall volume, which potentially covers a semi-outdoor area beneath. The second option (0.5*width) symbolizes an inclined building façade and the mirrored slope (1*width) represents a soil constructed embankment within a park.

The particular test was conducted so that any changes presented by edge diffraction during design would be observed beforehand and taken into account. As can be seen below, nothing changes significantly apart from the total unbuilt protected area close to the barrier volume. However, depending on the application and desired function and since the back wall does not contribute to noise reduction as much as the front, a steeper back façade would maximize the total outdoor area for residents, while limiting their indoor areas.

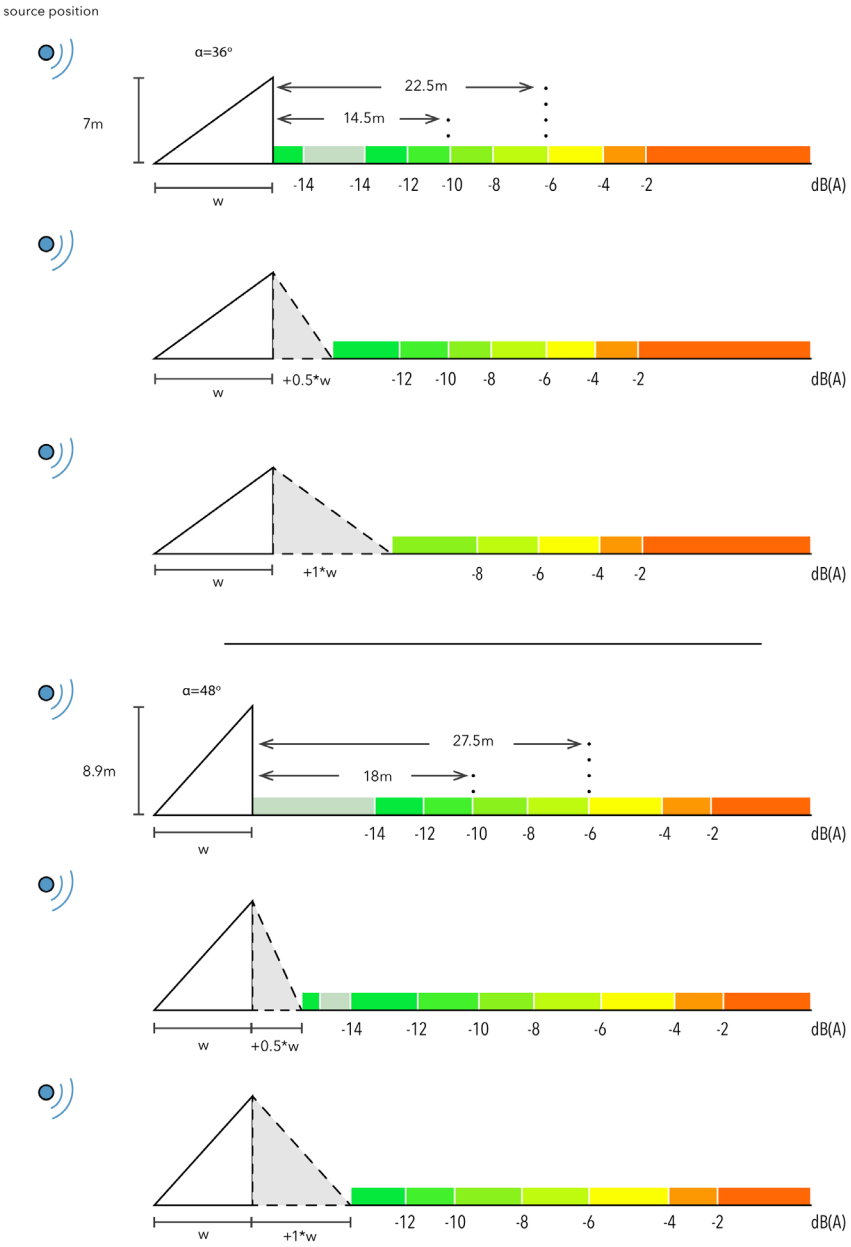

3.6.3 Top geometry correction

Another constructability constraint that should be observed beforehand is the feasibility of a sharp top edge by ground materials. According to technical drawings concerning the stabilization of reinforced slopes by Strata (2020), the secondary reinforcement grid placed vertically in order to stabilize each soil layer should have a specific length as required by the design. With this in mind, a correction of 2m extension is introduced to the top of the embankment.

The observation is made for the cases of 36^0 and 48^0 and a steeper protected façade. As seen in the sections below, the diffraction effect becomes more obvious for a flat top. Nevertheless, the change is more substantial for the flatter case, where noise reduction is limited to 2dB less at the majority of calculation points at ear height, thus eliminating this inclination as an efficient option. The 48^0 slope presents a slight change on how sound diffracts, although with no significant effect at the height of interest.

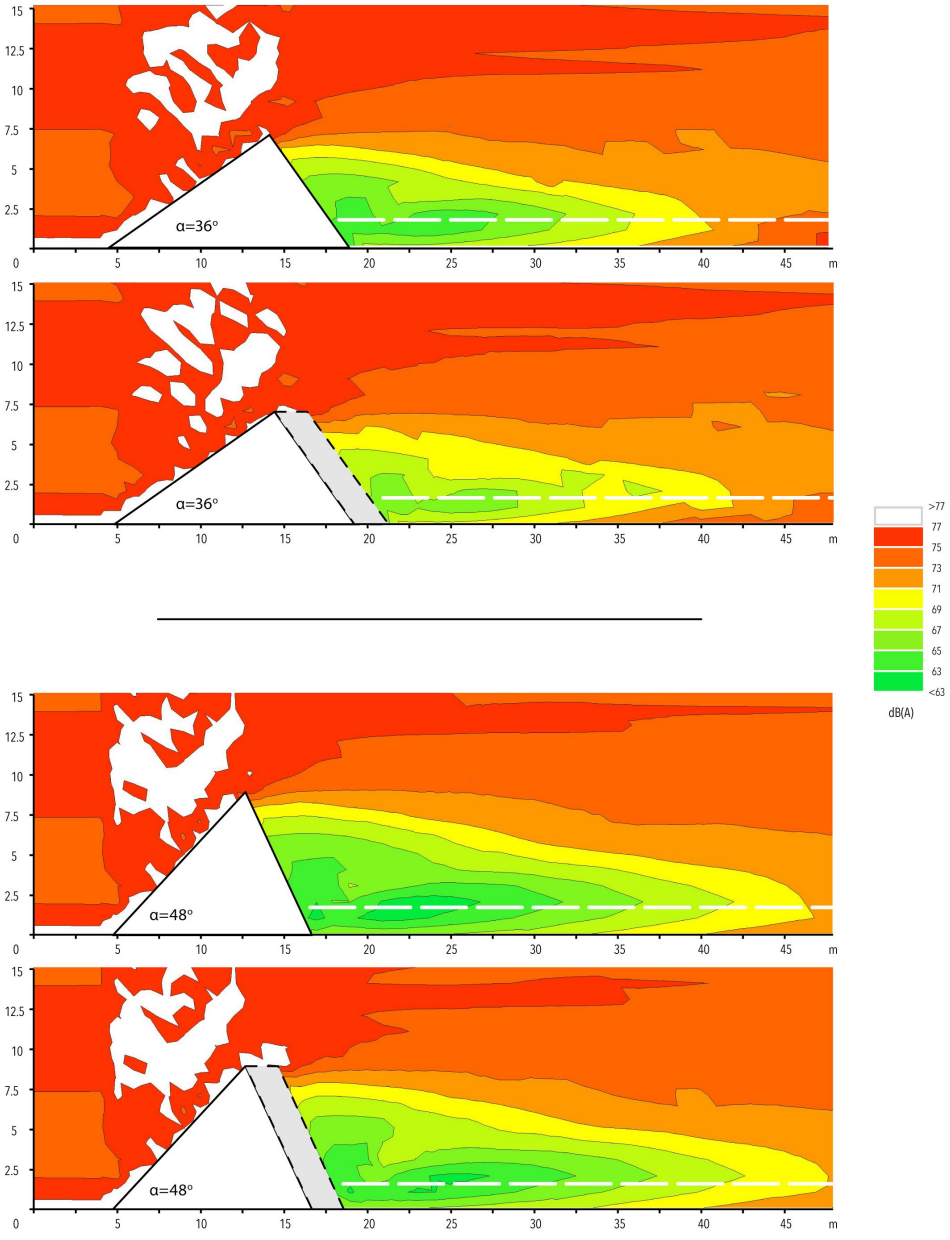

3.7 Shielding arrangement grid

**In all cases, source is moving on a linear segment of the flight path (the most dominant) at the top of the noise map images and at the left of the sections.*

3.7.1 Linear

i. Solid

Solid linear element

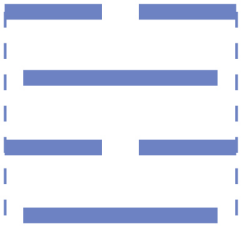

Potential urban grid arrangement

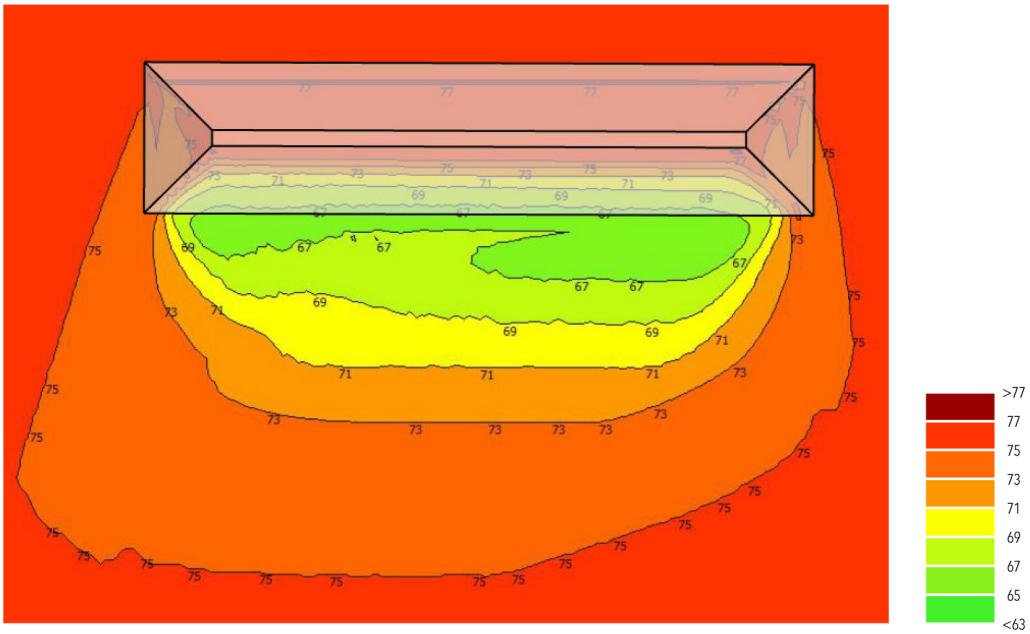

Noise mapping

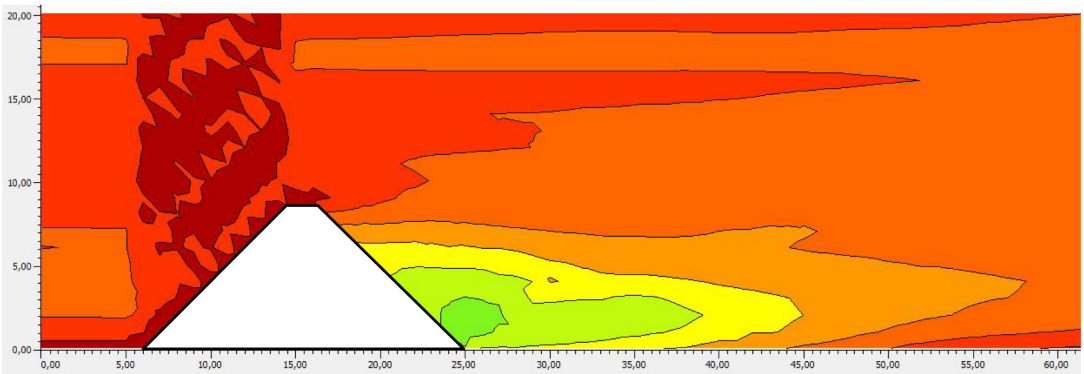

Section

ii. Multiples

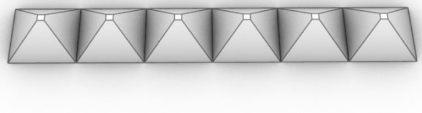

Multiple pyramidic elements

Potential urban grid arrangement

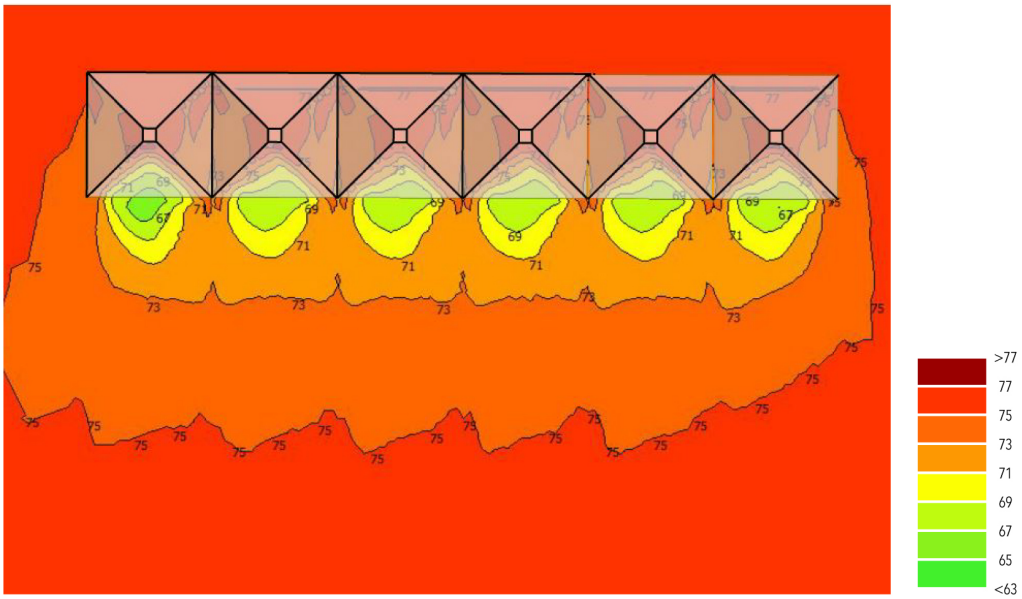

Noise mapping

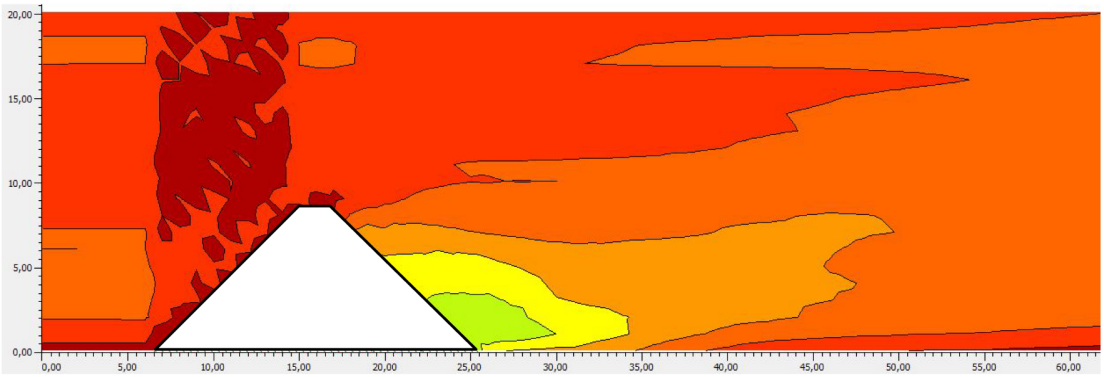

Section

3.7.2 Concentric

i. Rectangular

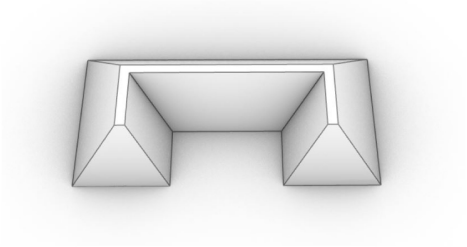

Rectangular element

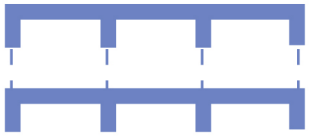

Potential urban grid arrangement

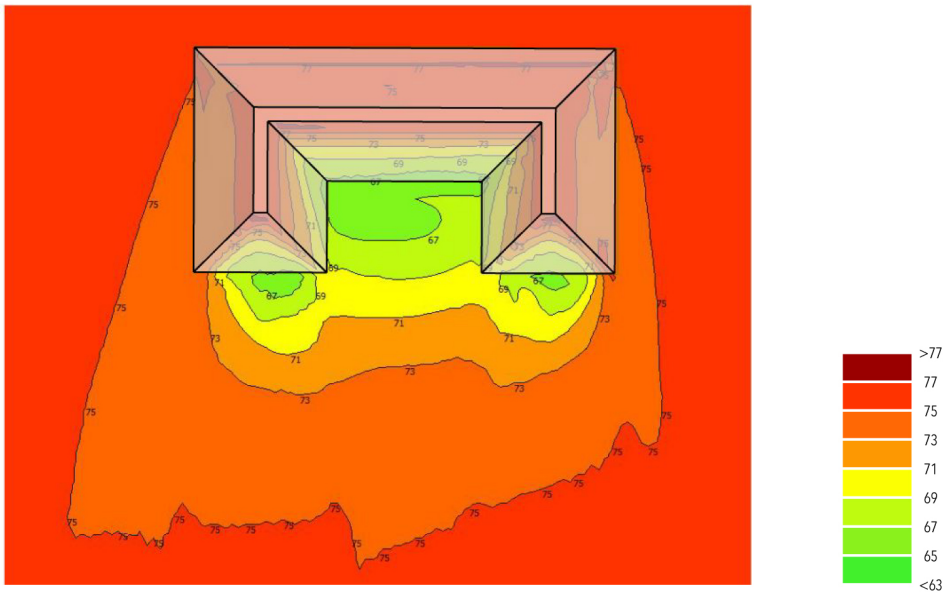

Noise mapping

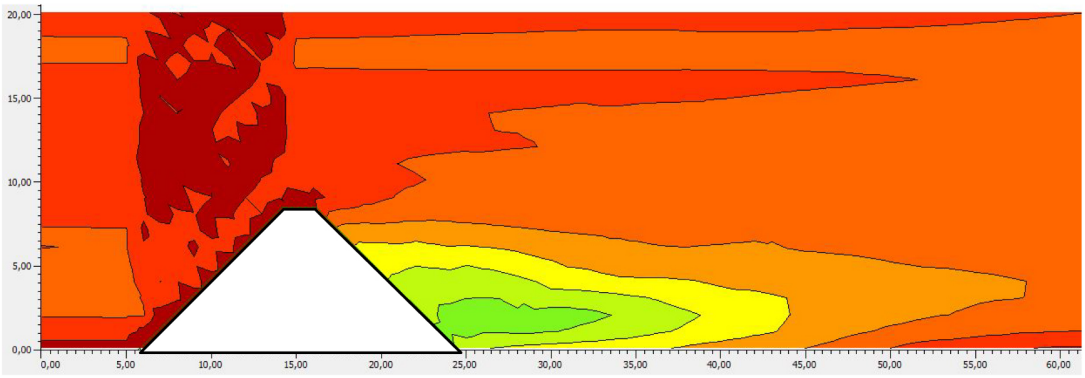

Section

ii. Hexagonal

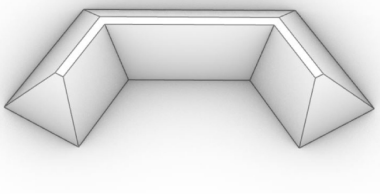

Hexagonal
outer edge shielding

Potential urban grid
arrangement

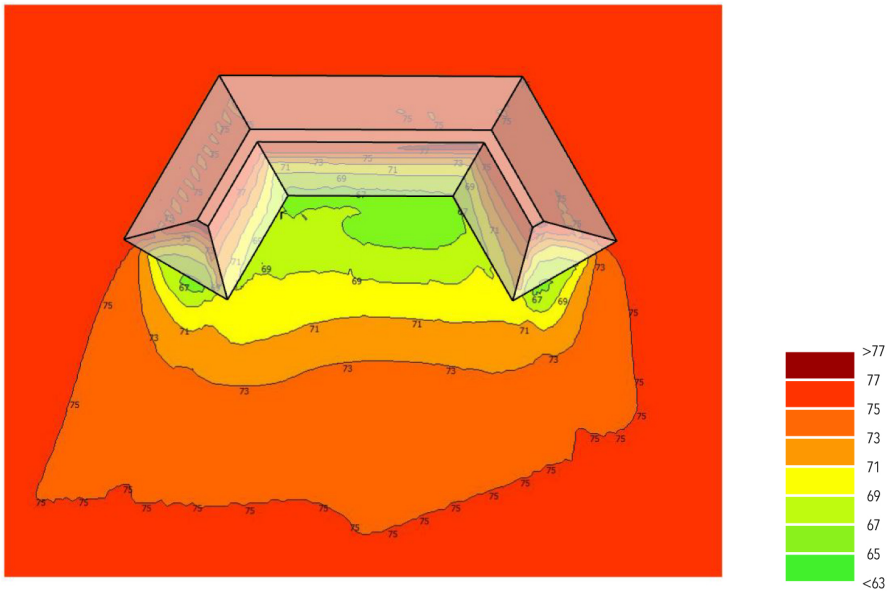

Noise mapping

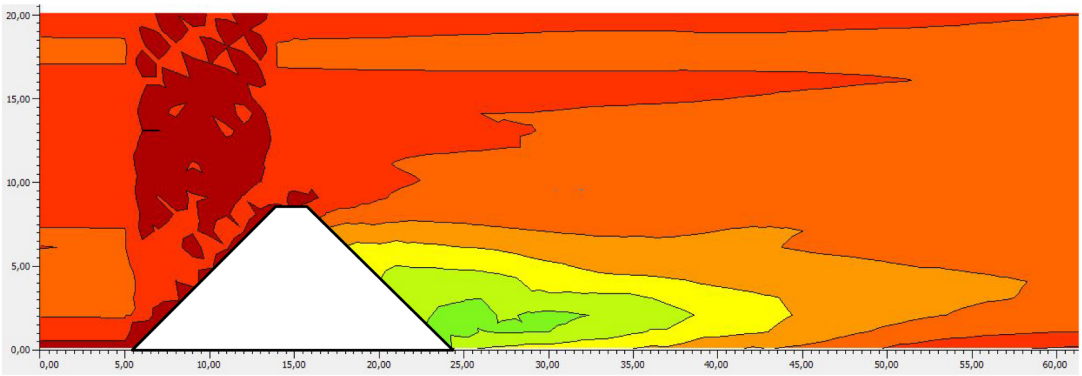

Section

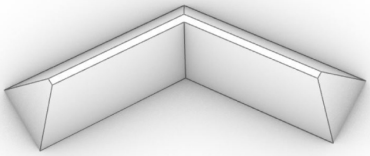

Hexagonal
outer corner shielding

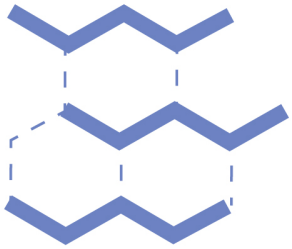

Potential urban grid
arrangement

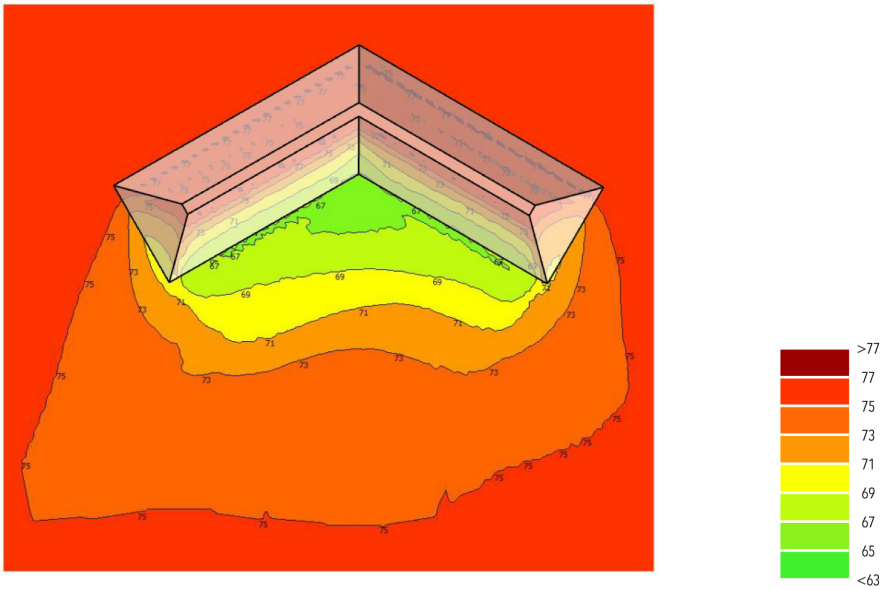

Noise mapping

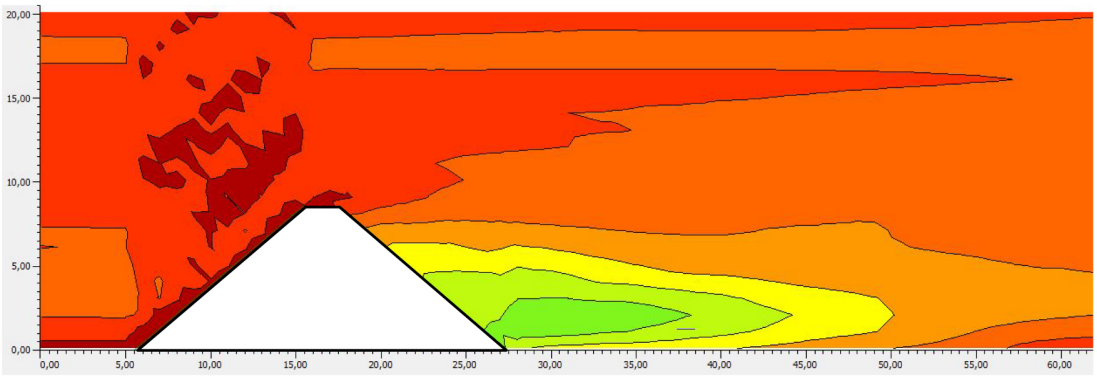

Section

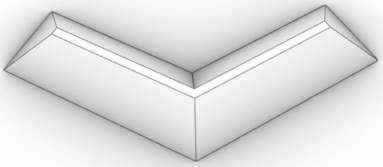

Hexagonal
inner corner shielding

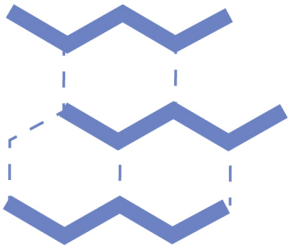

Potential urban grid
arrangement

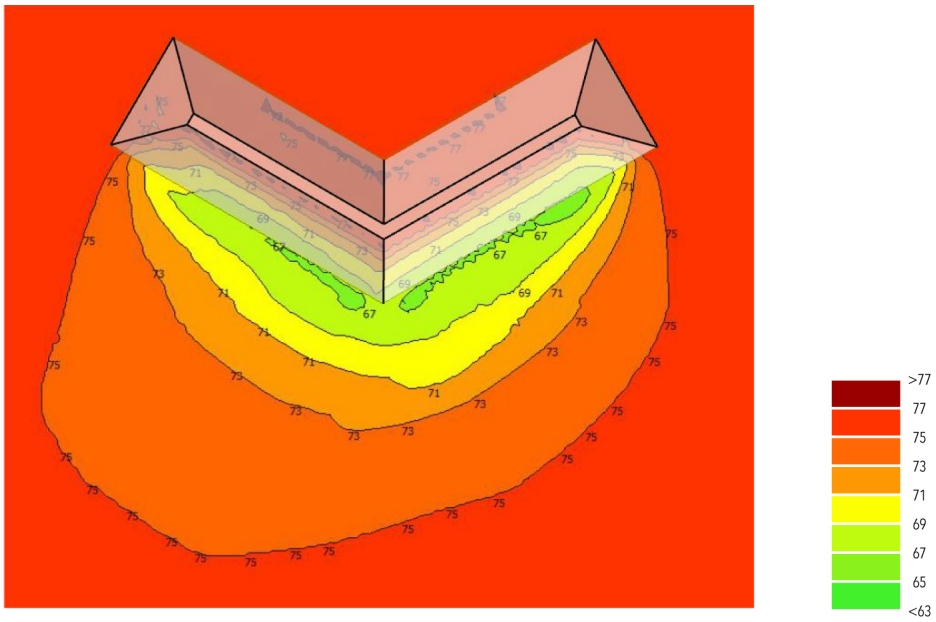

Noise mapping

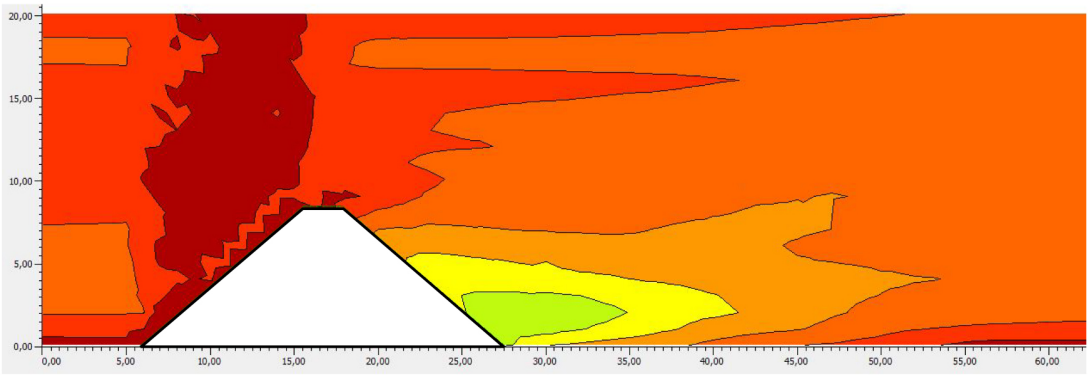

Section

iii. Octagonal

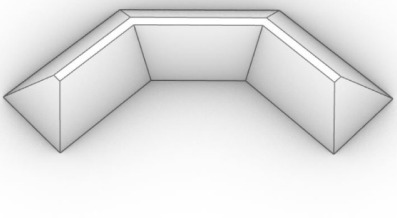

Octagonal element

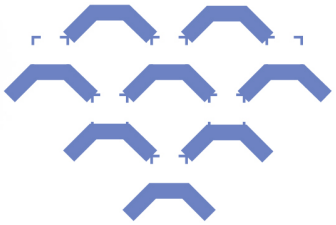

Potential urban grid arrangement

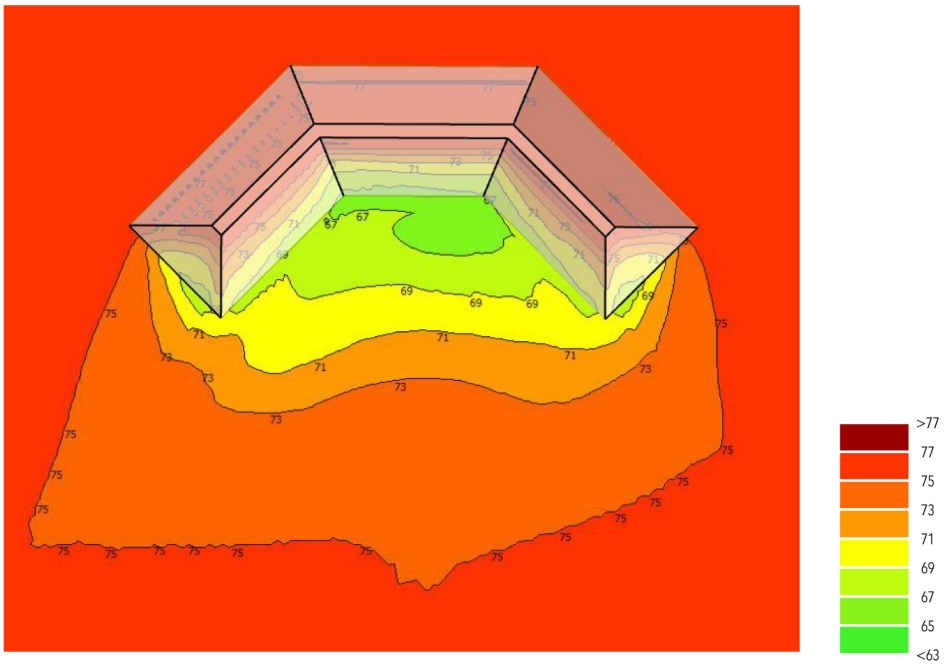

Noise mapping

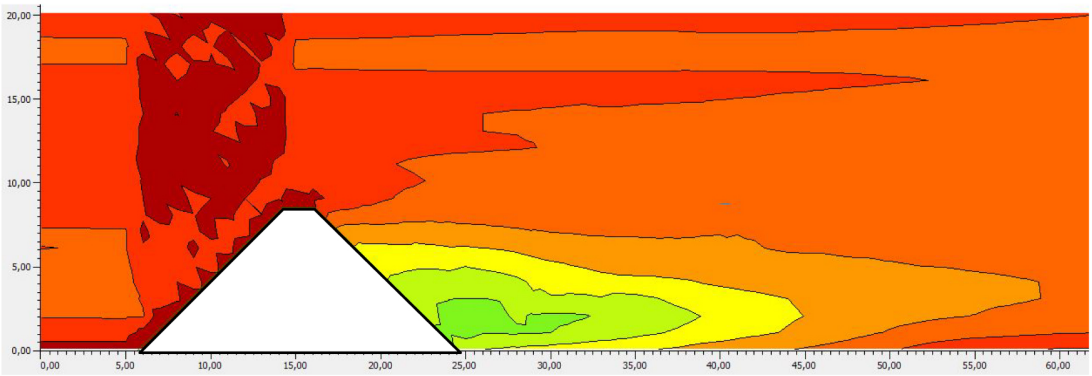

Section

iv. Dodecagonal

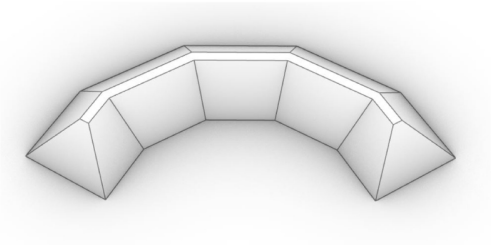

Dodecagonal element

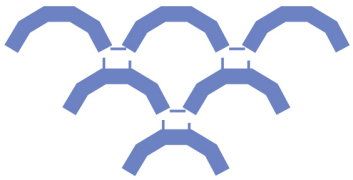

Potential urban grid arrangement

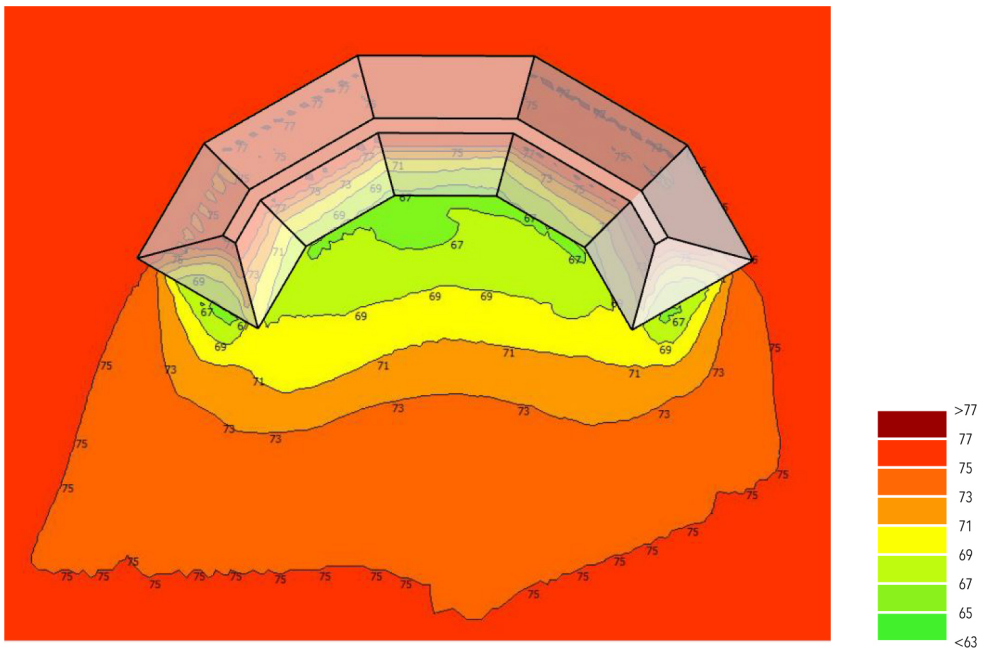

Noise mapping

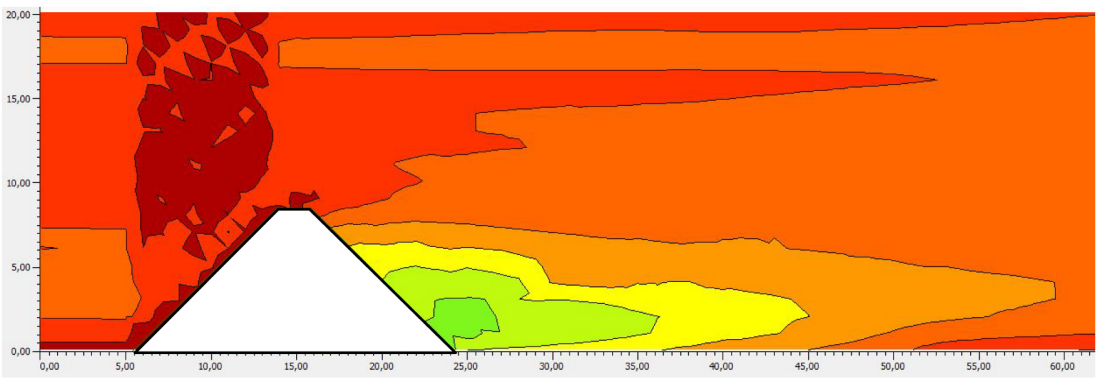

Section

3.7.3 Results comparison

The table below shows the measured outdoor areas of mitigated noise from the simulation results, regarding the selected urban grid cases. Apart from the total area where mitigated noise is noticed, three more columns of measurements are introduced and compared for better conclusions. The first refers to the area in which a reduction of 2 to 6 dB is noticed, which describes the area of a more significant reduction. The second is the area where more than 6dB reduction is noticed and it is the space which can be considered as protected due to the existence of the embankment barriers. Lastly, the maximum reduction that was measured over the whole grid of calculation points is added, in order to avoid seemingly better cases that cannot reach the peak potential of these urban configurations. Within green boxes are the better performing cases, while in red boxes are the worst results among them.

Arrangement			**Area of mitigated noise [m²]**			Max Reduction [dB(A)]
Case		Volume [m³]	Total area	2 < Rd < 6	6 < Rd	
Linear	Solid	6.922	4.169	994	834	10
	Multiple	6.819	4.466	1.398	216	8
Rectangular		7.105	3.275	684	397	10
Hexagonal	Edge	7.109	3.482	935	488	10
	Outer Corner	7.015	4.374	992	583	10
	Inner Corner	7.015	3.838	1.039	494	8
Octagonal		7.125	3.898	1.026	494	10
Dodecagonal		7.249	3.876	1.027	563	10

As can be seen in the table, all cases were designed in a way to have close to equal volume, so that the same amount of soil used for the construction is compared. The linear cases show the best results, but the case of multiple solids does not have consistency. Apparently, in order to reach the same construction volume, a longer installation is necessary and a larger area of effect is achieved. However, the gaps between the individual hills do not allow for concentrated protected spaces to be formed, in addition to the peak reduction not being able to reach more than 8dB. The rectangular grid shows the worst results, thus excluding it as a good solution against the linear flight path in interest. The very limited protected space would be a suitable choice when multiple flight paths surround a site, or a site located underneath the turning point of a flight. On the other hand, the hexagonal grid shows interesting results for the specific site. The outer corner case in particular behaves similarly to the solid linear case, where a larger total area is noticed, but a smaller area with reduction more than

6dB is measured. Finally, the octagonal and dodecagonal cases that resemble curved embankments did not perform any better than the linear case, although the measured areas of mitigated noise are close to the hexagonal outer corner volume.

These results are close to the expectation that in order to block efficiently the noise reaching out from a source moving linearly, a corresponding linear urban grid would maximize the shielded outdoor space behind the configuration. Furthermore, volumes that shield concentrically against flight paths are able to form more concentrated protected spaces, but are not good enough to perform effectively against longer flight paths. In any case, it should depend on the design needs, the function that these configurations might have and the connection type of the shielded façades and their outdoor space. This refers to the priority of the design to protect either bigger indoor spaces, or larger outdoor shielded areas. For this study, the focus is on the potential shielded outdoor urban area, so the linear grid with less construction volume and larger significant reduction space is preferred. Nevertheless, a variation with the addition of the hexagonal outer corner should be examined, since it generates an important concentrated space at its center, which can later form usable public spaces.

3.8 Scattering of reflected noise

As a further step to decrease the level of the reflected soundwaves, an additional treatment of the walls facing the noise source is introduced. This step can be considered optional for a landscape configuration aimed for park environments, since it requires in-detail configuration of the facing surfaces that change significantly their geometry, affecting their potential residential use and their urban footprint for the level reduction of soundwaves reflected upwards. However, it is shown later in the chapter that a slight additional reduction can be achieved concerning the level and direction of reflections exclusively.

Different methods of scattering performance can be considered at this stage, such as Helmholtz resonator cavities, Schroeder-based quadratic diffusers (1- or 2-dimensional diffuser) as shown in literature or other researched geometrical elements commonly used in room acoustics. Due to the nature of the research objective, which focuses on the constructability of such elements by soil types, the examination of a 1-dimensonal diffuser based on the Schroeder's mathematical sequences promises a less demanding construction for sloped landscape configurations. Furthermore, the axis of the arrayed wells plays an important role on the main directivity of scattered rays. A horizontal array guides reflections upwards and downwards, reinforcing problematic reflections towards the ground and therefore should be avoided, whereas vertical arrays scatter rays sideways (Figure 3.9).

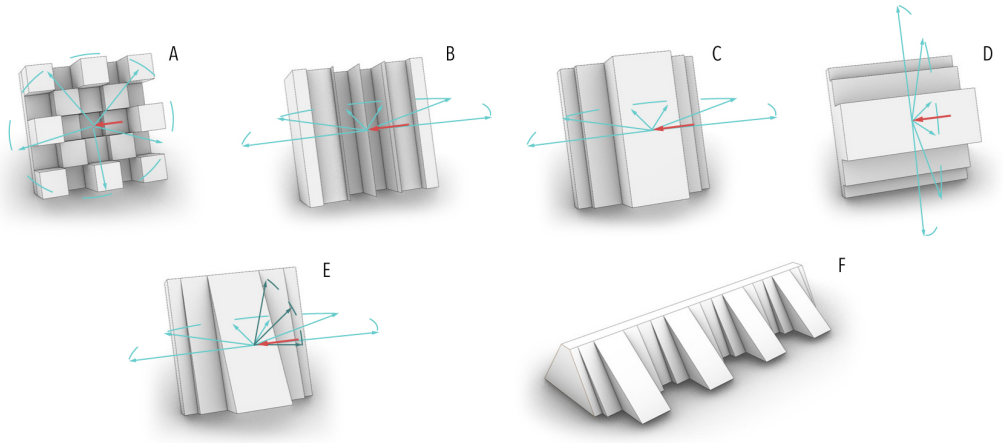

Fig. 3.9: Quadratic residue diffuser panels - A: 2-dimensional, B: Standard, C: Vertical inverse, D: Horizontal inverse. E: Inclined vertical inverse, F: Potential installation of (E) on slope's shielding façade.
The red lines show the incoming rays. The blue lines show an estimation for the main directivity of diffused frequencies.

In order to recreate the mentioned 1-dimensional vertical diffuser for the scattering of soundwaves with a design frequency as low as 30 Hz (which cannot be absorbed efficiently by common unmixed soil), a Quadratic Residue Diffuser calculator software is used, called QRDude, which can be downloaded for free (Subwoofer-builder.com, 2020). In this calculator, by increasing the number of wells in the arrangement, a wider range of diffusion frequencies with a higher frequency cutoff is achieved, depending on the acoustical needs of the installation. In addition, the user can choose between a 2D block arrangement of different heights, a standard panel that functions with the placement of fins between its wells or an inverse panel that deducts the fins. The inverse panel option is chosen as optimal for further investigation, because it is a 1-D diffuser and reduces the fins that construction-wise require more supportive material. Lastly, an inclination of the vertical blocks is explored, in order to simplify the design of the volume overall, while strengthening the upward-guided diffusion.

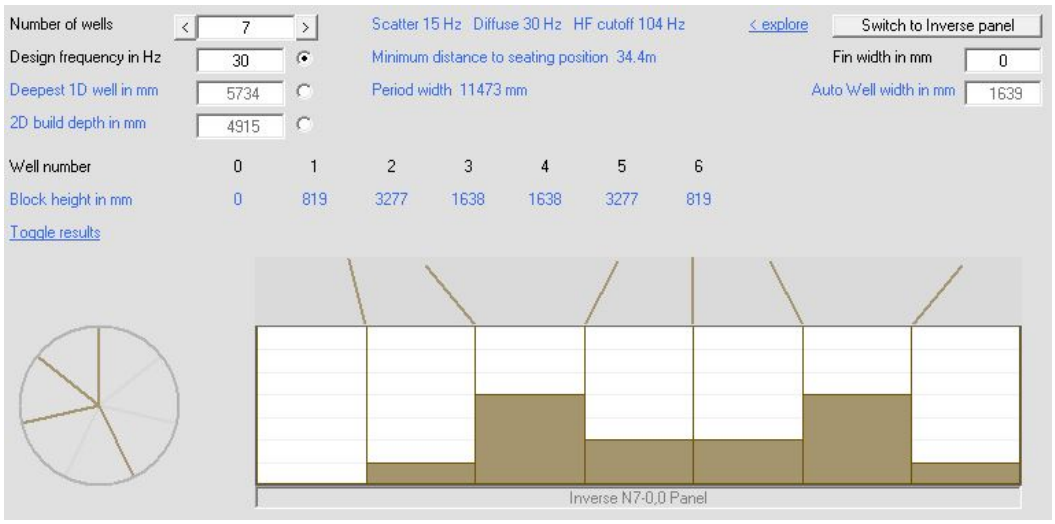

Fig. 3.10: QRDude software interface.

3.8.1 Vertical 1-D diffuser

Initially, linear blocks arrayed vertically are examined through Pachyderm for their scattering performance against frequencies up to 125 Hz. The coefficients are presented below in tables for three cases of well division, 3, 5 and 7 wells, according to the primary numbers used for Schroeder's mathematical sequence. As mentioned before, more wells increase the high frequency cutoff range above 30 Hz. However, the well width here represents the construction width of inclined façade walls that aim to be filled with types of uncompacted soil. A panel of 7 wells generates a well width of around 1.6 meters. A further division generates more complex constructions that obstruct the use of soil as the optimal implementation material.

As shown in the next sections, the period width for all elements is close to 11,4 meters, which is the necessary dimension for the design frequency of 30 Hz. Beside the width and height illustrated as a cross section, there is a perspective view of the periodic element, showing its scattering face. The scattering performance graphs are given by Pachyderm's scattering analysis tool for normal incidence (perpendicular direction). In these the scattering coefficients are shown as calculated up to 125 Hz. The software then measures the effect up to the next octave band (here 250 Hz) to compensate for errors at the higher frequencies. It should also be noticed that sometimes variations of the results occurred during simulations, which can be justified to the demanding process of the scattering directivity calculation and randomness of reflected rays.

For all three cases, results tend to fluctuate up and down in the area between 30 and 100 Hz. However, a general behavior is found similar with a drop at 0.2 between 50 to 80 Hz. The highest overall coefficients are seen at the 7-wells case with the lowest value being 0.35 at 60 Hz. In contrast with the rest, the 5-well case shows best scattering behavior at frequencies up to 40 Hz, but with a drop for the higher frequencies to a bottom of 0.2.

i. 3 wells (Inverse N3-0,0 Panel)

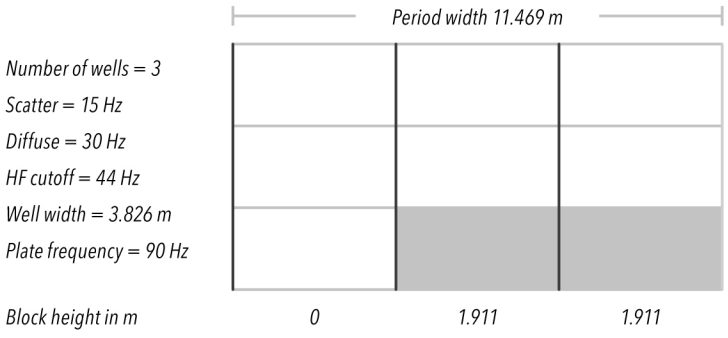

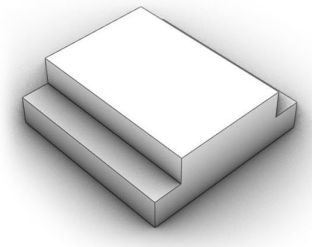

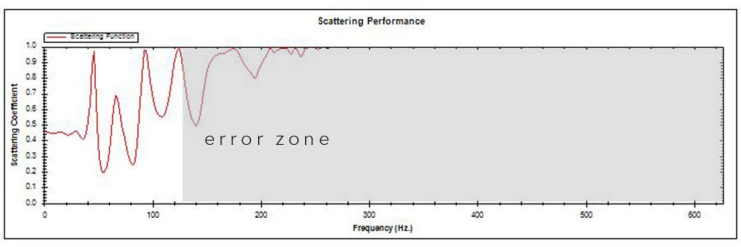

ii. 5 wells (Inverse N5-0,0 Panel)

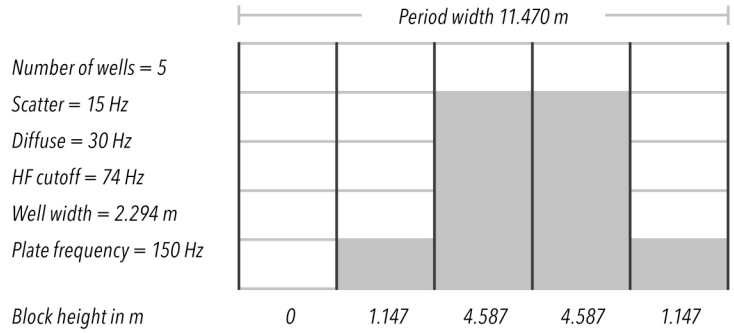

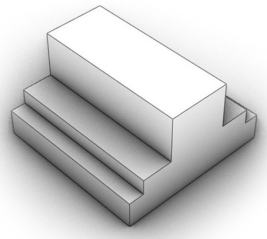

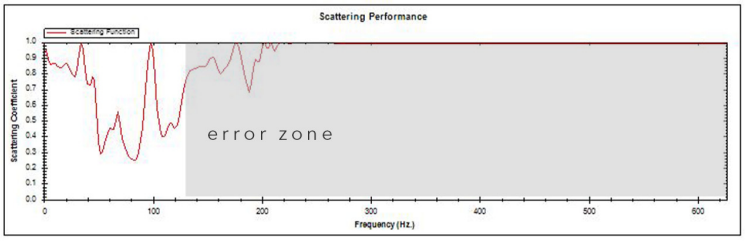

iii. 7 wells (Inverse N7-0,0 Panel)

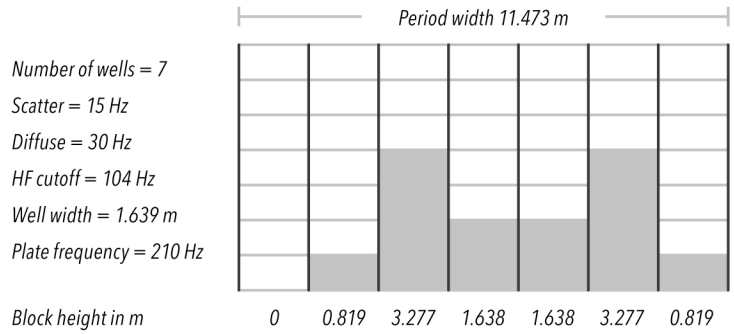

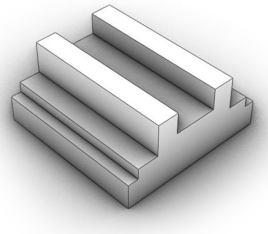

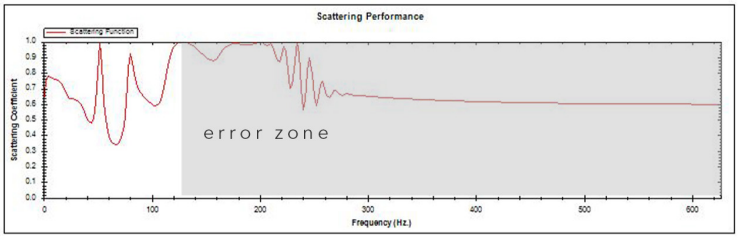

3.8.2 Inclined vertical 1-D diffuser

Similarly to the vertical geometries, the coefficients for the inclined periodic elements are calculated in Pachyderm. These options suggest the mitigation of specular reflections further away from the ground level, while creating a better geometry that can attach to the front of an embankment construction as shown before in Figure 3.9. Again, the results fluctuate in a sinewave path, but differ from the corresponding vertical cases. There is a similar deep noticed around 30 Hz for all three, while above that coefficients rise again to more than 0.5. The biggest difference is shown by the first option, where 3 inclined wells scatter frequencies lower than 40 Hz with a coefficient as high as 1. On the other hand, the same case shows the lowest dip among all at around 60 Hz.

i. *3 wells*

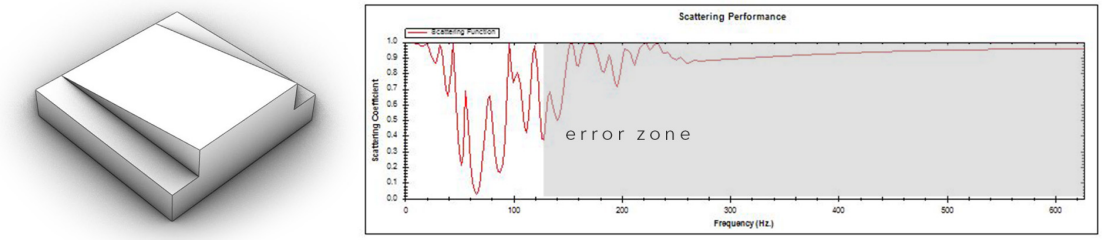

ii. *5 wells*

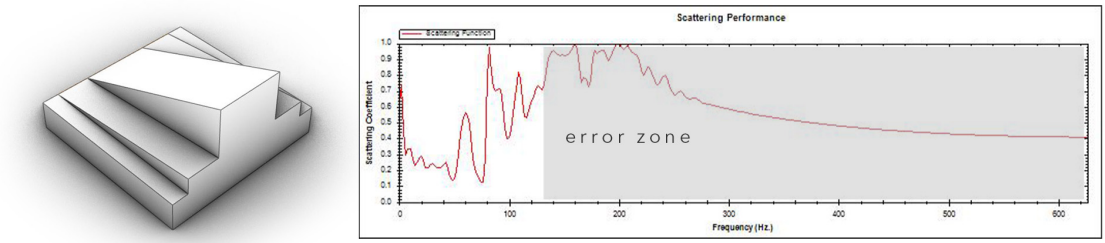

iii. *7 wells*

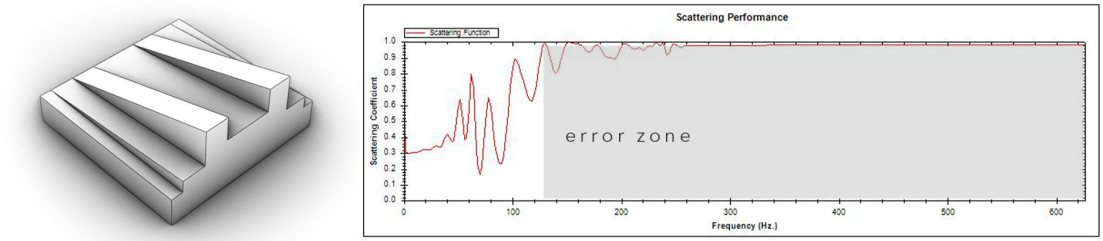

On the whole, the method is shown here to come to a further adjustment of a shielding façade that diffuses the incoming aircraft noise, if circumstances around noise-affected areas require to do so. Since the complexity of these geometries or their scattering

coefficients cannot be imported in iNoise for an acoustic analysis and a prediction of the generated urban soundscape, scattering options are not further analyzed in this design concept, apart from a comparison between scattering and non-scattering shielding faces that follows.

3.8.3 Reflected noise prediction

In order to see whether the addition of scattering surfaces has an effect in reducing the sound levels of reflections, Pachyderm was used to make a quick comparison between four cases, regarding the addition (or not) of soil absorption coefficients and scattering elements to the shielding façades, instead of a flat non-absorptive surface. Following, there are the exported simulation results as top images, alongside the section of the tested geometry, which describe the levels of sound rays exactly after bouncing from the surfaces. The values used for this test refer to the absorption of uncompacted soil (see literature) and the scattering of a 5-well inclined vertical diffuser (see previous section). As the images show concerning the peak level measured across the surface, apart from absorption, the addition of scattering to the faces contributes to a further reduction of 2dB, while rays are diffused and tend to spread more than bouncing out of a flat surface.

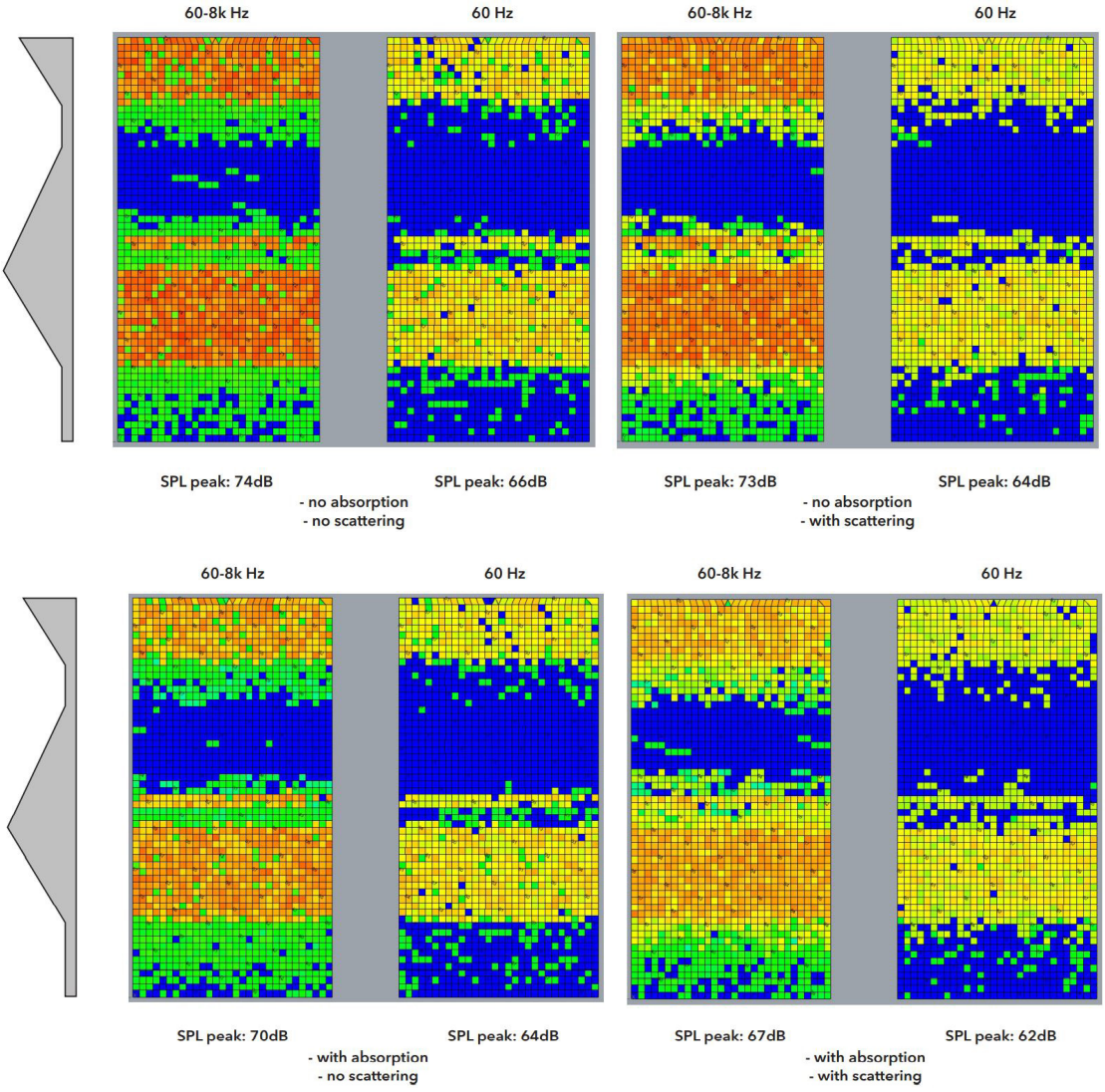

4 Design proposal

Following the results and any conclusions that were derived by the method followed, a proposal is made here about the selected study site in Rijsenhout. The design is considered simplified, as it only accounts for the volume constructed, with less detail regarding façades and constructability. In any case, it attempts to prove that the development of an acoustic analysis script related to design tools and parameterization could prove beneficial to the construction of innovative landscaping with the purpose of aircraft noise deflection.

4.1 Urban grid concept

The intention behind selecting the specific location within Rijsenhout was to consider a large unbuilt area and explore the establishment of an urban grid that covers and acoustically shields the whole building block. An array of noise mitigating elements reveals the relationship between the generated noise shadows beyond them, apart from showing the benefits of such a configuration, if designed uniformly.

As derived from the research chapter, it should be agreed that a grid that is designed parallel to the direction of a flight path shows better results in terms of material cost. Linear elements orientated parallel to the most dominant (closest) segment of the path generate maximized outdoor protected area with more significant drops in noise levels. In addition, the outer corner of a hexagonal grid has the advantage of creating more concentrated shielded areas behind its corner, something that a linear model lacks. With these in mind, it was decided to make a combination of these two options by designing a 120^0 corner against the closest position of the aircraft on its flight path and extending its edges linearly, until the site limits are reached.

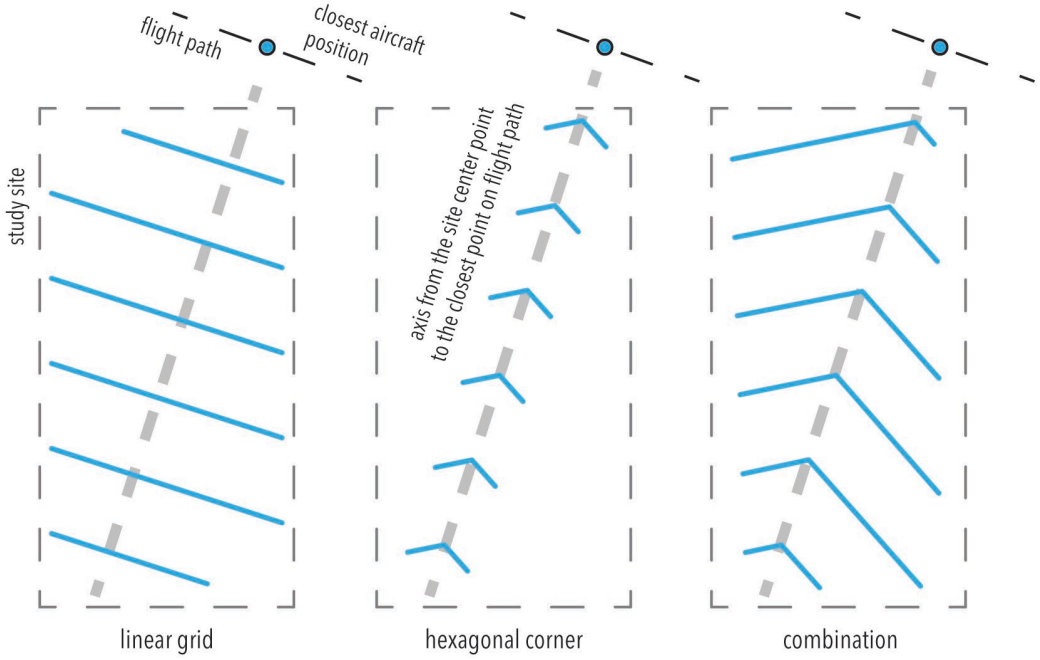

Fig. 4.1: Urban grid lines concept for the placement of noise barrier elements.

The section profile which agrees with soil constructability terms and produces a longer shadow length is selected for the embankments. In specific, an inclination of 45^0 for the shielding façade and a 35^0 tilt from the vertical axis for the back façade structure the section profile.

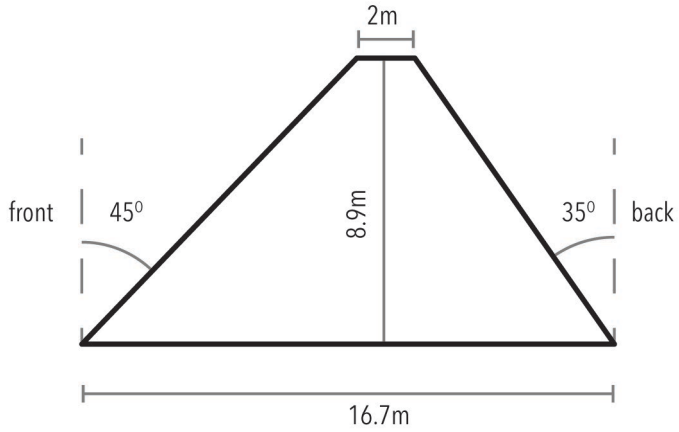

Fig. 4.2: Section profile of the soil embankments.

Then, the distance between the back to the front of the next element in the array was set to 28.5 meters, according to the length that was measured to have an outdoors noise reduction of at least 2 dB at ear height due to the embankment barriers. This way, all of the spaces with no deflected noise achieved are avoided, so that a better soundscape is created for the spaces in between. The volumetric outcome of this concept can be seen in the Figure below, including six landscape elements across the entire site. It should be noted that no further adjustments and detailing are possible at this stage, because of the limitations of the geometry that iNoise acoustics software can import as CAD drawings.

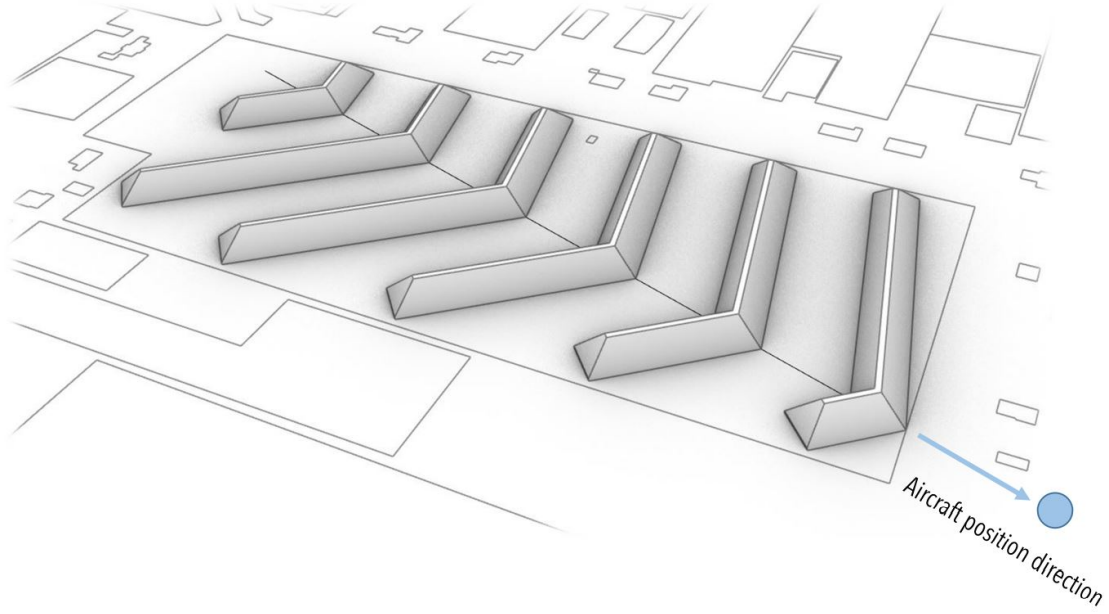

Fig. 4.3: Perspective view of the array of landscape configurations on the study site.

4.2 Acoustic analysis

After structuring the embankment volumes, the design was analyzed in iNoise with the same input data used for the testing of barrier cases, as seen in the research chapter, but this time for the whole site area. Noise maps are then produced, which are presented below. These images are important for the further treatment of outdoor ground coverage, if problematic spaces are introduced and further ground absorption is necessary, while sections act as a guide for the treatment of façades. The calculation grid was set to 0.1m height above ground and up to 20 meters high for the sections.

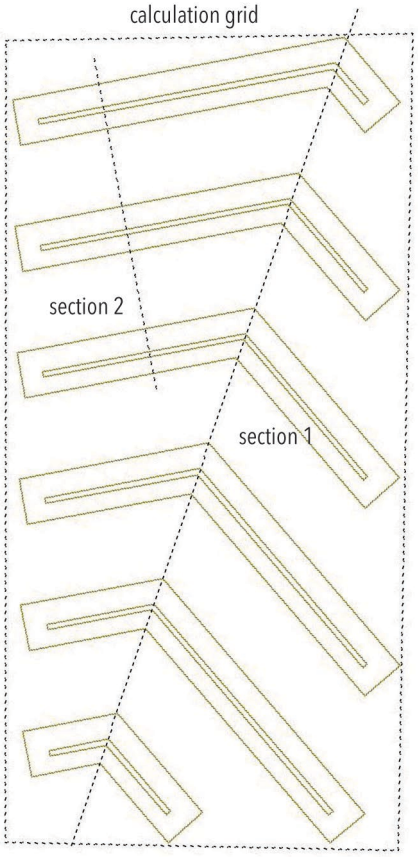

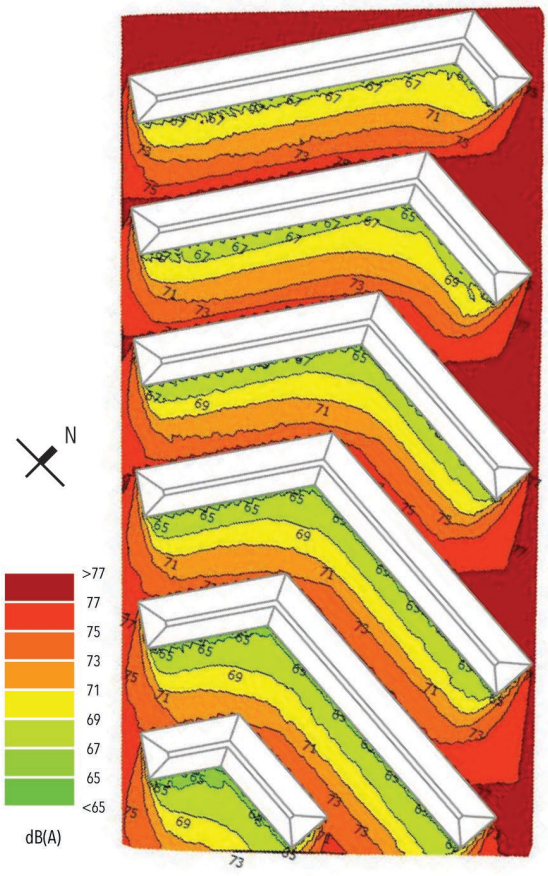

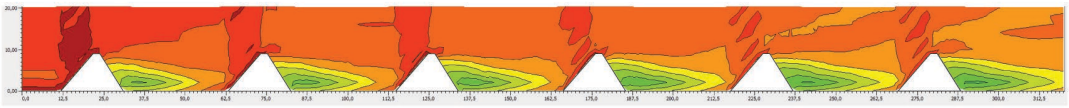

section 1

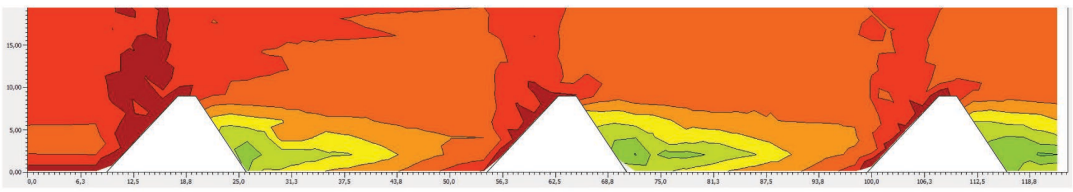

section 2

Noise maps exported as images can later be imported manually to Rhino 3D, in order to be combined into a visual understanding of noise deflections around the barriers. From that point, any designer can start making adaptations according to the prediction and finalize the construction.

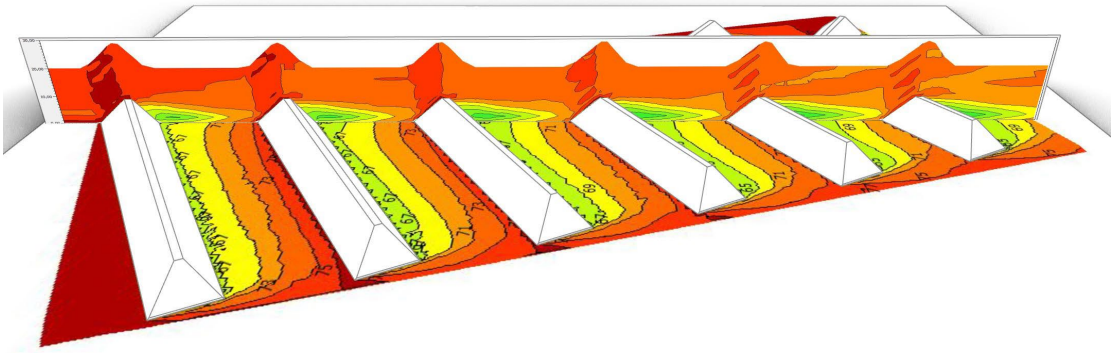

Fig. 4.4: Combination of noise maps (top view and section) from iNoise within Rhino 3D design environment.

4.3 Materialization concept

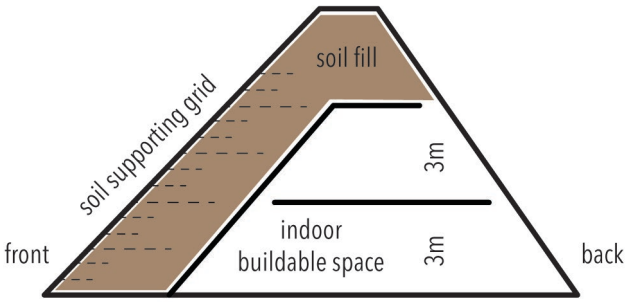

When looking on a smaller scale, it is possible to estimate the shielded façade surfaces that can be transformed into building facades. Shielded surfaces from the simulations with a reduction of 6 dB or more are considered protected from noise. In this case, the specified volume provides a habitable space of two floors. The shielding façade is filled with soil and keeps a necessary length until indoor space for the addition of soil supporting grids, according to the constructability constraints of the soil slope.

Afterwards, the prediction about the outdoor spaces can guide the adjustments of ground coverage. Spaces further away where no significant reduction is noticed should be covered with softer soil types, such as forest floor or thick moss that enhance the absorption of lower frequency noise. Likewise, depending on the protection level predicted, private yards, public spaces and pavements are added, in order to form a uniformed plan for a comfortable urban environment, both in terms of noise protection and urban connections. At this point, it is up to the designer to make choices regarding the programmed function of the construction.

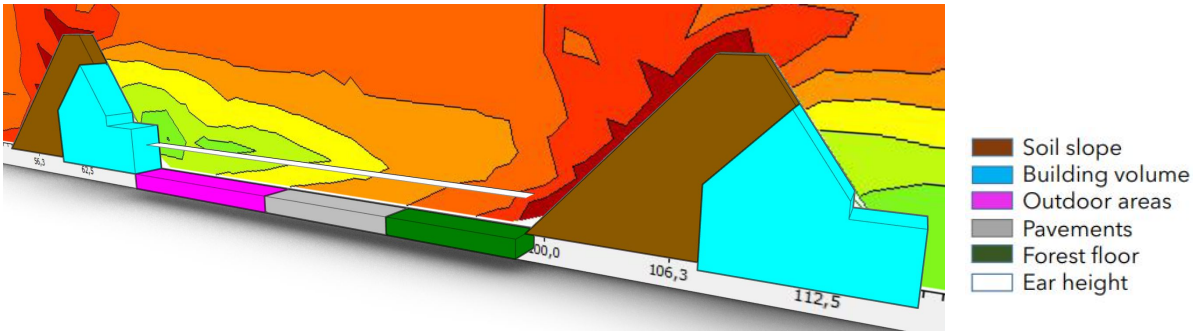

5 Conclusions & recommendations

5.1 Conclusions

The primary objective of this research was to examine the extent to which landscape configurations can improve the soundscape environment of residential areas affected by air traffic noise pollution. Later in the design chapter, the strategy of tackling the issue followed during the research chapters is described as a potential automated process within a parametric design software, which could lead to further optimization processes. In order to progress towards this goal, literature on the main factors influencing the sound propagation of a distant moving source was studied and broken down to simulation steps. In that regard, atmospheric refraction was selected as the focus on importing scripted equations that simulate the effect in a design software. In parallel, a series of simulations was conducted on test cases concerning the exclusive use of natural ground materials, in a manner of developing a sustainable noise barrier concept with less construction expenses, environmental impact and smarter urban application.

Acoustic simulations led to comparisons that could answer the research question established at the beginning. The application of soil embankments, as developed during the research process, showed that it is possible to mitigate noise and provide shielded outdoor spaces at ear height. The result is similar to the noise shadow formed by building volumes at their shielded façade (Lugten, 2018), mainly due to blocking the view of the source, with a peak noise reduction of 10dB. However, the inclination introduced for soil constructions, in combination with the low frequency absorption capabilities of uncompacted dry soil and vegetation for ground coverage, can slightly improve the result on the areas around the barrier. Lastly, the concern about the directivity of reflected soundwaves was handled by treating the shielding surfaces with the option of scattering for the low frequency ranges below 125 Hz. This addition disperses reflected noise horizontally and upwards, consequently lowering the chances of strengthened noise levels at areas in front of the barrier. Nevertheless, this effect improves the general issue slightly and should be further investigated for its benefits or alternatives.

Regarding the integration of acoustic simulations within Grasshopper, an ambitious attempt is described for representing the curvature of sound propagation due to refraction. The result cannot be considered validated at this point, since other essential sound effects should be gradually added to form a complete outdoor acoustics script that can be compared to other software. This can be feasible with the appropriate knowledge of urban acoustics and scripting development, but requires more testing and validation through recordings, scaled tests or comparison to established simulation methods. However, the understanding of the way in which geometry reacts to frequencies encourages a promising strategy for acoustical parametric design. Once the mathematical sequences behind the acoustic behavior of surfaces are understood, integrated noise mappings can be generated and designers can directly take advantage of the results. In the further purpose of aircraft noise reduction and the size of barrier constructions necessary, that ambition proves vital for confronting the issue since the earlier stage of urban arrangement.

5.2 Further research recommendations

In order to achieve the initial concept of a scripted acoustic simulation, more sound effects should be considered and structure a coded Grasshopper component. The inability of Pachyderm to handle an outdoor acoustics orientated simulation has proved that an alternative way should be developed in cases of air traffic and distances to receiver of more than 1 km. During this research, atmospheric refraction was examined so that a representation of the curved propagation path could be part of the design process. What is recommended to complete this script is the addition of diffraction, absorption, scattering and ground reflection calculations, after which validating the result would verify the level of accuracy.

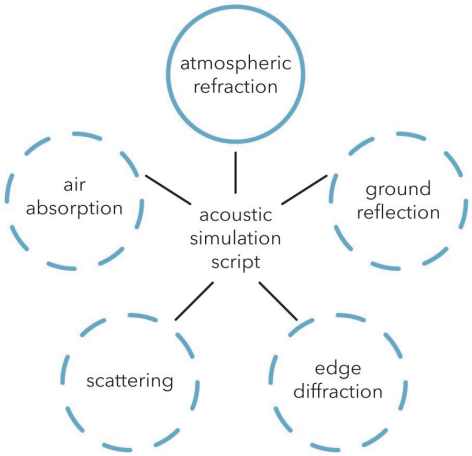

If such a script is achieved within a design software environment, further study on noise deflection can occur. Study on the acoustics beneath the embankments, what happens to the (potential) interior space, the soil depth of shielding façades with respect to structural constraints, a zoom in at the diffraction effect on the top of the pyramidal embankments are few examples of further research. Moreover, a limited amount of concepts was tested, due to the limitation of manual exchange of drawings and results between design and simulation software. A parameterization of the geometrical aspects that influence sound propagation connected to a simulation script would allow for more complex geometry tests that possibly maximize the amount of noise shadows.

Finally, the addition and examination of tree rows in scattering and absorbing noise can connect to the suggested soil embankments. This would not only help in decreasing noise levels that reach the urban area, but also contribute to a greener residential area that improves the attitude of noise-exposed inhabitants towards air traffic through psychoacoustics. Regarding scattering of reflected noise rays, in this study Schroeder-based diffusing elements were examined on necessity and adaptation to the sloped construction. The investigation of shielding façades with Helmholtz resonator cavities for absorbing low frequencies is another research study that can eliminate bulky geometries and supporting structures from being added to the barrier volumes. From that aspect, constructability of such cavities may require the use of more compacted materials than soil types, so a further investigation on how this can be achieved for low frequencies down to 30 Hz could give more refined concepts.

6 Reflection

6.1 Graduation process

The groundwork of this research is to explore the fundamentals of sound propagation in outdoor environments and develop a workflow that would suggest a potential approach on similar aircraft noise abatement issues. For the purpose of this research, the acoustical study was willingly focused on the refraction effect, which by literature should have an important impact on the sound propagation path by aircraft sources. This meant that a lot of other sound effects were omitted from this study, thus the refraction results are simplistic and should not be a rule for all cases. Equations were imported in a parametric environment so that a scripted component can adapt to various cases. The addition of other atmospheric effects and validation of scripts would compose an integration of acoustics within Grasshopper software, which would provide an immediate connection between calculations and design, consequently allowing designers to instantly observe acoustic phenomena or overwhelming results that require their attention during the design process. However, literature study did not provide similar analysis approaches on refraction and the script developed was left unverified.

In order to progress with the design of landscape noise barriers, testing elements were analyzed and compared with the use of acoustic simulation software. At first, simulations were conducted with the use of Pachyderm acoustics, which connects as a plug-in with Rhino and had the potential of immediate connection of results and design. Unfortunately, this delayed the research process by a great amount, since none of the simulations performed could handle the distant aircraft sources and could not be trusted for analysis and conclusions. The software utilizes a number of experimental tools that failed to perform fluently at outdoor acoustics studies. On the other hand, the change to iNoise simulation software did provide the necessary tools with much less assumptions regarding the set-up of cases. The goal of exporting noise maps was finally achieved and comparison of cases through a constant manual exchange of files could then be executed with confidence. Following the research by design method, a number of landscape configurations that support the initial thoughts for sustainable living and urban development led to a suggested design of urban spaces where residents can be protected, to some extent, against the disturbance of air traffic.

Strengths	Weaknesses	Opportunities	Threats
• Use of simulation software based on the Harmonoise method • Adjustments based on noise maps	• Limited tested concepts and materialization • Absence of an acoustic simulation process within the same design environment	• Gradual confirmation of most important geometric factors • Integration of equations within a design environment	• Developed refraction script without validation • Exclusion of other sound effects

6.2 Societal impact

Noise annoyance produced by aircraft flyovers affects a wide population of residents near airports. The results of this urban scale study aim to be applied in urban planning strategies, landscape designs and materialization of public spaces. From an engineering point of view, aircraft noise is a problem concerning urban acoustics principles, noise reduction methods within a built environment, as well as the sustainable way of living inside noise-exposed regions. The large scale constructions that aircraft noise reduction requires is an ethical matter to be aware of. Large configurations within a residential area has a great impact on urban connections too, so communication between the acoustician and the urban designer is crucial. For this reason, the design outcome concerns a site within Rijsenhout residential area and tries to compose a 'comfortable' urban design against aircraft noise.

As the results of the tested cases suggest, it would be possible to transform the construction of buildings, noise barriers and park environments into one greenery volume that combines it all. The addition of advanced technologies and materials on facades can further improve the situation. Nevertheless, this research aims to explore the capabilities of natural ground materials that eliminate the need for advancements, maintenance or excessive funding in general, making its application more feasible for less economically-developed regions. The design of test elements aims to use sustainable methods of engineering, in terms of material selection and preservation of natural environment towards a sustainable micro-climate, in addition to improving the soundscape quality of the area. Once the configurations are verified, the acoustically-driven design should provide forward steps towards reducing the research gap of aircraft noise prediction alongside a typology of noise abatement structures. The intention is to provide a workflow towards a configuration typology of landscape acoustical elements that can guide an architect since the process of planning. Because of that, the steps that are followed to conduct the study are kept simple in terms of engineering language. It is performed by an architectural engineer with the purpose to shorten the gap between designers and engineers. The workflow should provide acoustical performance data inside a design environment, making it more effective to communicate the complexity of contemporary architectural design choices with engineering data. And since the selected case study consists of a wider building block of residential spaces, it can be referred to architects designing shielded facades and courtyards, or landscape designers and urbanists planning public spaces within a city frame. In this way, the outcome contributes to the wider architectural research framework with an ethical concern on the sustainable prosperity of a city.

7 References

7.1 Projects

A. Re-sil(i)ence: A multifunctional noise barrier – M. Lugten (TU Delft, master thesis)

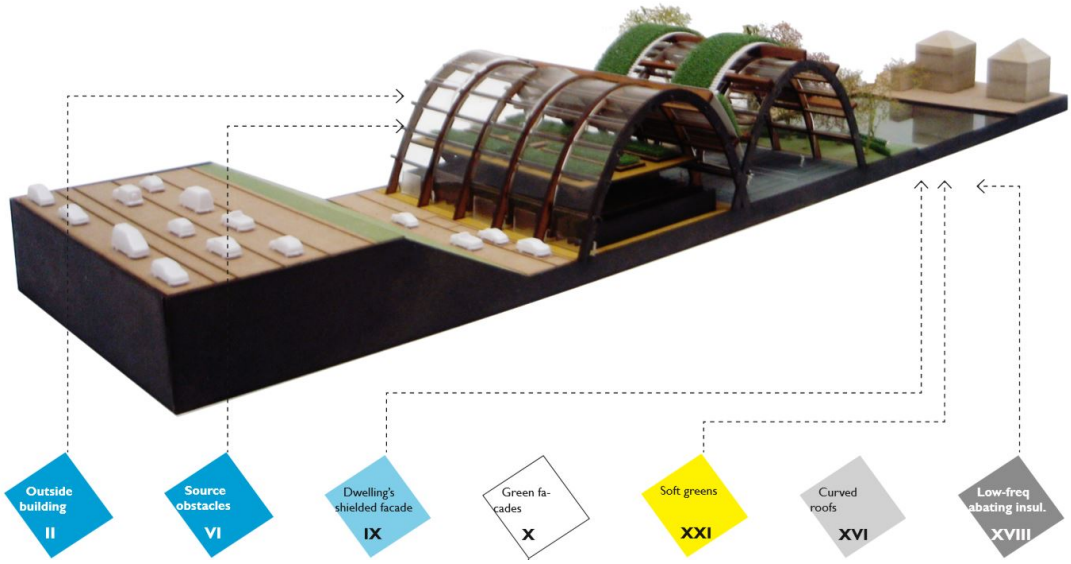

Fig. 7.1: In this proposal, "the barrier is a 50-metres wide structure which can absorb and scatter low-frequent noise. Facilities are not noise sensitive so could be exposed to sound pressure levels above legislated thresholds (>50 dB). At the barrier's rear, a noise 'shadow zone' makes it possible to store water (e.g. purified water from gravel box helophyte filters) which is sufficiently clean to be processed in greenhouses. The combination of greening and vegetation makes it possible to create a park at the banks of the pond which offer public green to residents."
Source: Re-sil(i)ence: Design patterns for an aircraft noise abating spatial environment (Lugten M., 2014: 236)

B. Buitenschot land art park – H+N+S Landscape architects, Hoofdorp

Fig. 7.2: On the authority of Schiphol a multidisciplinary team worked on a world first project: a park that exists by the grace of low frequency ground noise caused by aircraft taking off. Because of its design, the park landscape contributes to a considerable noise reduction. Measurements and calculations have shown that the ground noise is distorted and dispersed, as it were, by oblique planes.
(H+N+S Landscape architects, 2010)

C. Pavilion 21 MINI Opera space – Coop Himmenl(l)au, Munich

Fig. 7.3: "Our strategy to achieve soundscaping comprises three steps: Firstly, to realize the shielding effect between square and street, secondly, to shape the geometry of the Pavilion in such a way that the surface deflects noise, and thirdly, to design the surface of the Pavilion in such a way that it reflects and absorbs sound. In order to implement the objectives of the interior spatial acoustics, the interior wall and ceiling surfaces were fitted with a combination of perforated absorbing and smooth reflecting sandwich panels."
(Coop Himmelb(l)au, 2010)

D. Double layer structures of perforated materials – J. Krimm (TU Delft, doctoral thesis)

Fig. 7.4: The intention of this proposal was to "strengthen the effect of multiple reflections and absorption by a double layer façade structure. The irregular distribution of the holes intended a division in transparent or less transparent parts of the façade. For the second layer between the outer layer and the wall, a transparent wave formed polystyrene roof cladding was used. Distributing through the wave formed surface will reduce the direct reflected sound energy. In addition to this, extra holes in the surface were drilled in order to improve the absorption properties of the façade element".
Source: Acoustically effective façades design (Krimm, J., 2018: 173)

7.2 Literature

Aish, R. (2005). From Intuition to Precision. In Digital Design: The Quest for New Paradigms, 10-14. Lisbon: eCAADe

Arntzen, M. (2014). Aircraft noise calculation and synthesis in a non-standard atmosphere. (doctoral dissertation). Delft University of Technology, Delft, Netherlands. https://doi.org/10.4233/uuid:c56e213c-82db-423d-a5bd-503554653413

Arntzen, M., Rizzi, S. A., Visser, H. G. & Simons, D. G. (2014). Framework for Simulating Aircraft Flyover Noise Through Nonstandard Atmospheres. J. Aircr. 51, 956–966

Attenborough, K. (2007). Sound propagation in the atmosphere. in Handbook of acoustics (ed. Rossing, T.) 113–147, Springer Science+Business Media

Bartels, S., Márki, F. & Müller, U. (2015). The influence of acoustical and non-acoustical factors on short-term annoyance due to aircraft noise in the field - The COSMA study. Sci. Total Environ. 538, 834–843.

Burry, M. (2003). Between Intuition and Process: Parametric Design and Rapid Prototyping. In Architecture in the Digital Age Design and Manufacturing, Kolarevic, B. ,ed., 149-162. New York and London: Spon Press.

Connelly, M., & Hodgson, M. (2015). Experimental investigation of the sound absorption characteristics of vegetated roofs. Building and Environment, 92, 335–346. doi: 10.1016/j.buildenv.2015.04.023

Cox, T., & D'antonio, P. (2009). Acoustic absorbers and diffusers: Theory, design and application. Taylor & Francis, London

Cox, T.J., Dalenback, B.I., D'Antonio, P., Embrechts, J.J., Jeon, J.Y., Mommertz, E., Vorlander, M. (2006). A tutorial on scattering and diffusion coefficients for room acoustic surfaces, Acta Acust. United Acust. 92 (1) 1-5.

Delany, M.E., & Bazley, E. N. (1970). Acoustical properties of fibrous absorbant materials. Applied Acoustics, 3, 105-116

DELTA (2006). Nord2000. Comprehensive Outdoor Sound Propagation Model. Part 2: Propagation in an Atmosphere with Refraction. Horsholm, Denmark.

Hao, Yiying (2014). Effects of Urban Morphology on Urban Sound Environment from the Perspective of Masking Effects (doctoral dissertation). School of Architecture, The University of Sheffield.

Hörmeyer, J., Rolfes, R. (2018). Numerical Model for Prediction of Sound Propagation Emitted from Wind Turbines. Euronoise 2018 - Conference Proceedings, Crete, Greece

Hornikx, M. (2016, June 27). Ten questions concerning computational urban acoustics. Retrieved from https://www.sciencedirect.com/science/article/pii/S0360132316302359

ICAO (2016). Aircraft Noise. Available from: http://www.icao. int/environmental-protection/Pages/noise.aspx [Accessed 3 January 2020].

Jónsson, G. B., & Jacobsen, F. (2008). A Comparison of Two Engineering Models for Outdoor Sound Propagation: Harmonoise and Nord2000. Acta Acustica United with Acustica, 94(2), 282–289. doi: 10.3813/aaa.918031

Kim, Y. H., Jang, H. S., Lee, P. J., & Jeon, J. Y. (2011). Acoustical properties of vegetation including ground Surfaces for scale model reproduction. Forum Acusticum

Krimm, J. (2018). Acoustically effective façades design (doctoral dissertation). Delft University of Technology, Delft, Netherlands

Krimm, J., Knaack, U., & Techen, H. (2017). Updated urban facade design for quieter outdoor spaces. Journal of Facade Design and Engineering, 5(1), 63-75. https://doi.org/10.7480/jfde.2017.1.1422

Kuttruff, H. (2009). Room acoustics (5th ed.). Abingdon, United Kingdom: Spon Press.

Lugten, M. (2014). Re-sil(i)ence: Design patterns for an aircraft noise abating spatial environment (master thesis). Delft University of Technology, Delft, Netherlands

Lugten, M, C. (2018). Tranquillity by design (doctoral dissertation).Clare College, Cambridge, England

Maleki, K., & Hosseini, S.M. (2011). Investigation of the effects of leaves, branches and canopies of trees on noise pollution reduction.

Mpiris A., Athanasopoulos I., Aggelou A., Demiri K., Tsiraki S. (2011). Architectural and musical accompaniments. Published by Pataki, Athens, Greece.

Netjasov, F. (2012). Contemporary measures for noise reduction in airport surroundings. Appl. Acoust. 73, 1076–1085.

Nota, R., Barelds, R., van Maercke, D. (2005). Technical Report HAR32TR-040922-DGMR20: Harmonoise WP 3 Engineering method for road traffic and railway noise after validation and fine-tuning. Retrieved from the Information Sociate and Technology (IST) Programme

Oxman, R. (2008). Towards a Performance based Generation and Formation Model in Architectural Design. In IJAC International Journal of Architectural Computing Vol. 6, 1-17.

Peters, B. (2010, September 1). Integrating Sound Scattering Measurements in the Design of Complex Architectural Surfaces: Informing a parametric design strategy with acoustic measurements from rapid prototype scale models. Retrieved January 8, 2020, from https://adk.elsevierpure.com/en/publications/integrating-sound-scattering-measurements-in-the-design-of-comple.

Peters, B. (2009). Parametric Acoustic Surfaces. ACADIA. Retrieved from https://www.researchgate.net/publication/38977141_Parametric_Acoustic_Surfaces

Peters, B. (2007). The Smithsonian Courtyard Enclosure: a Case-Study of Digital Design Processes. In Expanding Bodies: Art "Cities" Environment: Proceedings of the 27th Annual Conference of the Association for Computer Aided Design in Architecture (ACADIA), 74-83. ACADIA. Halifax, Nova Scotia, Canada: Dalhousie, NSCAD & CDRN.

Salomons, E. M. (2001). Computational atmospheric acoustics. Kluwer Academic Publishers

Science Communication Unit (2017). Science for Environment Policy. Noise abatement approaches. Future Brief 17. Produced for the European Commission DG Environment by the Science Communication Unit, UWE, Bristol. Available at: http://ec.europa.eu/science-environment-policy

Siltanen, S., Tapio, L., & Savioja, L. (2010). Rays or waves? Understanding the strenght and weakn esses of computational room acoustics modeling techniques. Paper presented at the Inte rnational Symposium on Room Acoustics, Melbourne, Australia.

Thomas P., Boes, M., Van Renterghem, T., Botteldooren, D., Hornikx, M., Desmet, W., Nilsson, M. (2012). Auralisation of a car pass-by behind a low finite length vegetated noise barrier, in: Proc. of 9th European Conference on Noise Control, pp. 932e937

Tsinikas N. (2009). Architecture & Music. University Studio Press, Thessaloniki, Greece.

Vlaun, N. (2015). Sound Working Environments: Optimizing the acoustic properties of open plan workspaces using parametric models (master thesis). Delft University of Technology, Delft, Netherlands

Zaporozhets, O., Tokarev, V. & Attenborough, K. (2011). Aircraft Noise: Assessment, Prediction and Control. Taylor & Francis

Website sources

Acs.psu.edu. (2020). Refraction of Sound Waves. [online] Available at: https://www.acs.psu.edu/drussell/Demos/refract/refract.html [Accessed 19 Dec. 2019].

Aircraftnoise.com.au. (2020). Aircraft noise | aircraftnoise.com.au. [online] Available at: http://aircraftnoise.com.au/causes-of-aircraft-noise/ [Accessed 3 Jan. 2020].

Coop Himmelb(l)au. (2020). Pavilion 21 MINI Opera Space. [online] Available at: http://www.coop-himmelblau.at/architecture/projects/pavilion-21-mini-opera-space/ [Accessed 06 Nov. 2019].

Flighttracking.casper.aero. (2020). Schiphol - Flighttracking. [online] Available at: https://flighttracking.casper.aero/ams/ [Accessed 3 Jan. 2020].

Geogrid.com. (2020). Geogrid. [online] Available at: <https://www.geogrid.com/> [Accessed 18 May 2020].

Grc.nasa.gov. 2020. Speed Of Sound. [online] Available at: https://www.grc.nasa.gov/www/k-12/airplane/sound.html [Accessed 24 January 2020].

Grc.nasa.gov. (2020). Earth Atmosphere Model - Metric Units. [online] Available at: https://www.grc.nasa.gov/WWW/K-12/rocket/atmosmet.html [Accessed 20 Jan. 2020].

H+N+S Landscape architects. (2020). H+N+S Landscape architects - Land art park Buitenschot. [online] Available at: http://www.hnsland.nl/en/projects/land-art-park-buitenschot [Accessed 06 Nov. 2019].

Noiselab.casper.aero. (2020). Live noise levels. [online] Available at: http://noiselab.casper.aero/ams/#page=actual [Accessed 3 Jan. 2020].

Simanek, D. (2015). Physics Puzzles – Sound reasons. [online] Available at: https://www.lockhaven.edu/~dsimanek/puzzles/soundreasons.htm [Accessed 19 Jan. 2020].

Subwoofer-builder.com. 2020. Qrdude: Quadratic Residue Diffuser Calculator. [online] Available at: <https://www.subwoofer-builder.com/qrdude.htm> [Accessed 14 May 2020].

Titan Environmental Containment Ltd. 2020. Erosion Control Blankets - Titan Environmental Containment Ltd.. [online] Available at: <https://www.titanenviro.com/products/erosion-sediment-control/erosion-control-blankets/> [Accessed 10 June 2020].

Weather.uwyo.edu. (2020). Atmospheric Soundings. [online] Available at: http://weather.uwyo.edu/upperair/sounding.html [Accessed 21 Jan. 2020].